



UNIL | Université de Lausanne

Unicentre

CH-1015 Lausanne

<http://serval.unil.ch>

Year : 2022

An active locus coeruleus in sleep: Towards a dynamic structure of NREM sleep

Osorio Forero Alejandro

Osorio Forero Alejandro, 2022, An active locus coeruleus in sleep: Towards a dynamic structure of NREM sleep

Originally published at : Thesis, University of Lausanne

Posted at the University of Lausanne Open Archive <http://serval.unil.ch>

Document URN : urn:nbn:ch:serval-BIB_D90AD523A8D17

Droits d'auteur

L'Université de Lausanne attire expressément l'attention des utilisateurs sur le fait que tous les documents publiés dans l'Archive SERVAL sont protégés par le droit d'auteur, conformément à la loi fédérale sur le droit d'auteur et les droits voisins (LDA). A ce titre, il est indispensable d'obtenir le consentement préalable de l'auteur et/ou de l'éditeur avant toute utilisation d'une oeuvre ou d'une partie d'une oeuvre ne relevant pas d'une utilisation à des fins personnelles au sens de la LDA (art. 19, al. 1 lettre a). A défaut, tout contrevenant s'expose aux sanctions prévues par cette loi. Nous déclinons toute responsabilité en la matière.

Copyright

The University of Lausanne expressly draws the attention of users to the fact that all documents published in the SERVAL Archive are protected by copyright in accordance with federal law on copyright and similar rights (LDA). Accordingly it is indispensable to obtain prior consent from the author and/or publisher before any use of a work or part of a work for purposes other than personal use within the meaning of LDA (art. 19, para. 1 letter a). Failure to do so will expose offenders to the sanctions laid down by this law. We accept no liability in this respect.



UNIL | Université de Lausanne

Faculté de biologie
et de médecine

Département des neurosciences fondamentales, UNIL

An active locus coeruleus in sleep: Towards a dynamic structure of NREM sleep

Thèse de doctorat en Neurosciences

présentée à la

Faculté de biologie et de médecine
de l'Université de Lausanne

par

Alejandro OSORIO-FORERO

Master en ingénierie biomédicale de *la Universidad de Los Andes*, Colombie

Jury

Prof. Dr. Jean-Pierre Hornung, Président
Prof. Dr. Anita Lüthi, Directrice de thèse
Prof. Dr. Paul Franken, Expert
Prof. Dr. Antoine Adamantidis, Expert

Thèse n° 333

Lausanne
2022

***Programme doctoral interuniversitaire en Neurosciences
des Universités de Lausanne et Genève***

Imprimatur

Vu le rapport présenté par le jury d'examen, composé de

Président·e	Monsieur	Prof.	Jean-Pierre	Hornung
Directeur·trice de thèse	Madame	Prof.	Anita	Lüthi
Expert·e·s	Monsieur	Prof.	Paul	Franken
	Monsieur	Prof.	Antoine	Adamantidis

le Conseil de Faculté autorise l'impression de la thèse de

Monsieur Alejandro Osorio-Forero

Master in Biomedical engineering, Université de Los Andes, Colombie

intitulée

**An active locus coeruleus in sleep:
Towards a dynamic structure of NREM sleep**

Lausanne, le 24 juin 2022


pour Le Doyen
de la Faculté de Biologie et de Médecine

Prof. Jean-Pierre Hornung

To my family, my mentors and my friends.

Contents

A Acknowledgements	1
B Abstract	3
B.1 Abstract	3
B.2 Résumé	4
C Introduction	5
Prologue: Sleep is a continuous, dynamic process	5
1 Aims of this introduction	6
2 Definitions	6
3 Electrophysiological manifestation of the infraslow timescale during NREM sleep	9
3.1 Visual manifestations on the infraslow timescale during NREM sleep	9
3.2 Full band or direct-current variations in the EEG	12
3.3 Fluctuations in the band-limited power activity in the EEG	12
3.4 Other manifestations of the infraslow timescale during NREM sleep	14
3.5 Functional implications of infraslow fluctuations during NREM sleep	14
4 The <i>locus coeruleus</i> in sleep	15
4.1 Noradrenergic signaling in the brain	16
4.2 LC unit activity across the sleep-wake cycle	17
4.3 Other measures of LC activity across the sleep-wake cycle	19
4.4 The LC as a candidate for the generation of infraslow fluctuations in sleep spindle density during NREM sleep	21
5 Aims of the thesis	24
D Results	25
Noradrenergic circuit control of non-REM sleep substates	25
E Discussion	27
1 Scientific contributions	27
1.1 Noradrenergic LC mechanisms are causally related to the infraslow fluctuations in sigma activity during sleep	27
1.2 The noradrenergic LC system creates windows of opportunity for behavioral transitions	28
2 Technical contributions and limitations	32
2.1 Fiber photometry	32
2.2 <i>In-vivo</i> optogenetics	33

3	Broadening the view on neuromodulation during sleep	35
3.1	Other neuromodulators during NREM sleep	35
3.2	Possible regulation of noradrenergic LC fluctuations during NREM sleep	36
4	Impact and perspectives	38
4.1	General impacts and perspectives of this work	38
4.2	Implications in hyperaroused brain states	41
5	Closing remarks	42

F Article **66**

A Acknowledgements

The Ph.D. is a period of scientific and personal growth. During this period, one has the valuable opportunity to search for an answer that contributes to the understanding of nature or the advance in technology, hoping to contribute to the advance of humanity. For me, it was an incredible adventure, and it was most gratifying thanks to the people I had the honor and pleasure to share this time with. I am full of gratitude to those that made this possible.

First, I thank my current mentor and Ph.D. advisor, Prof. Anita Lüthi. She is an actual role model and source of inspiration for the people in her team in both professional and personal aspects. I acknowledge her trust and support throughout my Ph.D. She adapts to each of our characters and strengths to make the best of us and the team. She taught me, with her example, that the job of a leader is to create the optimal environment for the people he/she is responsible for. She reminded me to be excited about our scientific exercise and the precise use of techniques. I am and always will be grateful for her guidance. It has been a true honor to join her and her team in unraveling the secrets of the sleeping brain and body.

I want to thank also the valuable inputs and discussions with my jury committee. I thank Profs. Paul Franken, Antoine Adamantidis, and Jean-Pierre Hornung. I learned much about how to think about my current and future directions in science.

I thank Dr. Laura Fernández. For her support and joy in scientific activity. She has a lot of passion for sleep and its story and the people behind it. She reminded me of the importance of balance. Her talent in organization and aesthetics for communication are inspirational. Laura, together with prof. Lüthi, sets the high standards for the creativity, communication, and clarity that are at the core of our scientific style.

I thank my friends and colleagues in the Lüthi lab that encouraged me to believe in myself throughout these years. To Najma Cherrad for her unconditional friendship, strength, and character that taught me the importance of fighting for what you believe is right, with confidence and conviction, but overall, to put friends first. To Dr. Romain Cardis for his creativity to solve problems and for his critical thinking and sharp ideas that taught me to think simple (it is often the best way to solve a problem). To Dr. Gil Vantomme and his outstanding organizational skills for teaching me the importance of bringing people together in other creative and administrative activities. In the end, science is a social endeavor. To the new members in the lab, Lila Banterle and Dr. Georgios Foustoukos, for their hard and patient way of working. To Dr. Elidie Béar, Aurélie Guillaume Gentil, and Christiane Devenoges, their kindness and hard work made all this project possible in such an efficient manner. I thank the master and pre-master

students in the lab, particularly Angelo Guadagno and his love for nature and Harishini and her willingness to learn. To Zoe Nicolas for her passion for science and to change the system.

I want to thank the funding agencies that made my work possible here in Switzerland and the University of Lausanne. The Faculty of Biology and Medicine for giving me the opportunity to join such an excellent scientific environment. I thank the Life Sciences Switzerland (LS2) and the Swiss public agencies that supported some of my trips and my work in the lab. I thank the Lemanic Neuroscience Doctoral School and Dr. Ulrike Toepel for their support during the doctoral process. Likewise, I want to thank the principal investigators from the Department of Fundamental Neuroscience (DNF) at the University of Lausanne for showing me the many ways to do and think of science. To the administrative personnel at the DNF, it was a pleasure to work with you all. To the general services at the DNF that made our daily life comfortable with a clean and agreeable environment. I want to thank particularly Nholphy Solano and Jacinto Castañeda. They came to greet me at the office almost every day to remind me about the kindness of my roots. I thank the team in the animal facility; they all took outstanding care of our animals, with the relevance and ethics of such endeavor. I also thank other scientific collaborators and colleagues during my Ph.D. Especially to my friend *Dr.* Georgia Kautsoudi, we started this journey simultaneously and shared our scientific and personal growth throughout this time. To Mohit Dubey and Thijs Willems, Dr. Stephanie Holden, and Prof. Jeanne Paz, with whom I collaborated and learned a lot about the application and value of my work. I want to acknowledge my friends and colleagues in the neuroscience of sleep; they are numerous and of great personal value; I sleep glad to know I am part of such a competent and joyful community, with a hunger for knowledge and a curiosity for the mystery of sleep. It is the people there, in the lab, thinking, working long hours, that push the limits of knowledge. I additionally thank my mentors at the University of *Andes* and the University Autónoma de Manizales. Like the family during the first years of childhood, the first academic years are decisive to the scientist. I, therefore, own them the scientist I am and constantly want to become.

I want to acknowledge that friends are the family one gets to pick, and I could not be thankful enough for their support. To all of them, this work is also your work. I thank Claudia Moroni for the patience and for sharing memories I never imagined living. I am unimaginably thankful to my family; my parents and sister were always there to support and believe in me.

Finally, I want to thank all the sleep scientists that inspired me. In sleep science, we are indeed on the shoulders of giants.

B Abstract

B.1 Abstract

From the outside, sleep looks like a homogeneous and static behavioral state accompanied by disconnection from the external world and a change in consciousness. Yet sleep is heterogeneous, both in its behavioral and physiological manifestations. On the multi-minute timescale, sleep alternates between non-rapid eye movement sleep (NREM) and REM sleep. During NREM sleep, infraslow (0.1 — 0.01 Hz) fluctuations in cortical rhythms, brain temperature, heart rate, and pupil diameter emerge. My thesis is about the mechanisms underlying the temporal heterogeneity of sleep, focusing particularly on the systems responsible for the physiological and behavioral infraslow variations during NREM sleep.

This thesis asks about the role of the wake-promoting noradrenergic *locus coeruleus* (LC) system in the modulation of close-to-minute variations in brain and bodily signatures of arousability levels during NREM sleep. I used cutting-edge methods in neuroscience to monitor LC activity and its noradrenaline (NA) release in the brain. My work showed that, unexpectedly, the LC is highly active during NREM sleep and generates periodic NA release in the thalamus. This neuromodulatory output is the mechanistic basis that coordinates infraslow rhythms from the brain and the periphery during NREM. These observations are a significant step toward refining the temporal dimension of NREM sleep as a brain state for which neuromodulation is essential to regulate its physiological and behavioral features. This work builds up from a systems neuroscience approach in sleep in which the neuromodulatory dimension becomes inextricably linked to the electrophysiological characteristics of NREM sleep.

These observations advance basic insights into how sleep heterogeneity arises from its biological foundations and contribute to the neurobiological core features of sleep. As a major result, my thesis work identifies NREM sleep as a state in which monoamines play a central modulatory role with implications for understanding healthy and pathological forms of sleep. For example, in disorders where abnormal arousability levels are a defining feature, or in conditions where the LC or the thalamus are affected.

B.2 Résumé

Le sommeil est un état comportemental globalement homogène et statique en apparence, durant lequel s'opèrent un changement de conscience et une déconnexion avec le monde extérieur. Le sommeil est néanmoins un état hétérogène tant au niveau physiologique que comportemental alternant des stades de sommeil NREM (*i.e.* sans mouvements rapides des yeux) et de sommeil REM (ou paradoxal, *i.e.* avec mouvements rapides des yeux). Au sein même du sommeil NREM, il y a une hétérogénéité temporelle caractérisée par des fluctuations infra-lentes (0.1 — 0.01 Hz) des rythmes corticaux, de la fréquence cardiaque. Cette thèse explore les mécanismes de l'hétérogénéité temporelle du sommeil NREM, et en particulier ceux des variations physiologiques et comportementales infra-lentes, enrichissant les notions de neurobiologie de base sur l'organisation du sommeil.

Ma thèse explore le rôle d'un noyau noradrénergique majeur promouvant l'éveil, le *locus coeruleus* (LC), dans la modulation lente (~ 1 min) des signatures électrophysiologiques caractéristiques de la vigilance lors du sommeil NREM. J'ai utilisé des méthodes modernes de neurosciences des systèmes afin de suivre l'activité du LC et sa libération de noradrénaline (NA) dans le cerveau. J'ai obtenu des résultats inattendus qui montrent que le LC est fortement actif durant le sommeil NREM et libère la NA de manière périodique dans le thalamus. Cette variation de neuromodulation est le mécanisme essentiel pour coordonner les paramètres physiologiques entre le cerveau et la périphérie (*i.e.* le corps) et permettre une réactivité comportementale au cours du sommeil NREM. Ces résultats révisent nos principes sur le sommeil NREM: c'est un état de vigilance durant lequel la neuromodulation est cruciale pour réguler ses caractéristiques physiologiques et comportementales.

Mon travail contribue fondamentalement aux connaissances sur l'origine biologique de l'hétérogénéité du sommeil, et révèle le rôle central des monoamines pour le moduler. Les implications sont concrètes pour comprendre le sommeil sain ou pathologique, comme lors des troubles de l'éveil (insomnie, maladies liées au stress), ou lorsque le LC ou le TRN sont altérés comme dans la maladie d'Alzheimer ou la schizophrénie.

C Introduction

Prologue: Sleep is a continuous, dynamic process

“If I have seen further it is by standing on the shoulders of Giants.”

Isaac Newton [1]

It was in Autumn 2010 when Drs. Francia Restrepo and Mauricio Medina taught me how to score sleep stages in humans. I was amazed by the richness of the signals and how heterogeneous was the activity produced by the brain during a period that otherwise looks like a behaviorally quiescent state. The amount of physiologically meaningful information my mentors could gather from these waveforms was surprising. They were able to know when the subjects started falling asleep, to determine how consolidated and “normal” their slumber was, or to identify patterns that implied pathological forms of sleep. However, the most intriguing observation that caught my attention was the highly discrete method for scoring sleep states in epochs of 30 s-duration. It was evident that these artificial windows were not appropriate to capture the heterogeneous dynamics of the data. For instance, a 30-s window could contain features of two different sleep states. Also, within an individual window, one could observe multiple divergent features, depending on the brain areas. Still, this approach has been the gold standard for decades in understanding sleep, diagnosing patients, or even following up on treatments for multiple disorders. Little I imagined at the time that over a decade later, I was going to write this thesis on the mechanisms that regulate the temporal properties in the sleeping brain and body that looks at sleep as a continuum generated by the interaction of multiple systems. Here, I will not focus on the typical questions of *why do we sleep?* or *what are the functions of sleep?*. With the work I present here, instead, I will try to shed some light on the question *how do we sleep?* by focusing on one mechanism that contributes to making sleep heterogeneous in its electrophysiological and physiological features in time. I will argue that this work made a decisive step forward in the neural bases of sleep function and behavior that are defining sleep, yet that has never been looked at through the neuroscientist’s eyes.

1 Aims of this introduction

Sleep is part of the continuum of alternations between natural behavioral states that range from alert wakefulness to deep sleep with dramatic changes in physiological activity [2]. During sleep, temporal heterogeneity arises on multiple timescales. For instance, changes between two different sleep stages appear within minutes, forming a sequence or cycle that constitutes the macro-architecture of sleep. These are the non-rapid-eye-movement (NREM) and REM sleep. Within these two principal states of sleep, multiple physiological processes vary on a multi-second to sub-second timescale and create what is known as the micro-architecture of sleep. Of particular interest are “infraslow” oscillations that refer to changes on the 10 — 100 s (0.1 — 0.01 Hz) range. Within the infraslow timescale, second and sub-second physiological activity patterns are organized [3, 4]. Thus, they have been linked to the crucial restorative [5] and memory consolidation [6, 7] functions of sleep. In this work, I will focus on the infraslow changes happening during NREM sleep.

Interestingly, these micro-architectural features are also related to fluctuations in the arousal levels during sleep [2], reflecting windows of opportunity where sensory vigilance is promoted [4]. These behavioral correlates of infraslow changes within NREM sleep have linked them to fluctuations in the arousal systems. Among them, the noradrenergic *locus coeruleus* (LC) activity is a strong candidate underlying these fluctuations in brain and body dynamics during sleep.

In the introduction of the thesis, I will cover the fundamentals of the macro- and microarchitecture of sleep. Next, I will summarize the study of infraslow fluctuations that take place during NREM sleep from an electrophysiologist’s point of view. Finally, from the neurophysiologist’s perspective, I will review some key points in the literature on the LC, and the reasons for which this brain area is exceptionally placed to play a role in the infraslow manifestations of NREM sleep’s micro-architecture.

2 Definitions

Continuous changes in behavioral states happen on multiple timescales. Among them, sleep is a reversible state of behavioral quiescence with reduced levels of responsiveness to external stimuli. In its most “conventional” form, animals entering this state present a stereotypical recumbent posture with decreased muscle tone and closed eyes. Sleep is also accompanied by changes in physiological processes that are typically monitored with a combination of electrophysiological techniques referred to as polysomnography, which encompasses the recording of the brain and body signals that include, but are not limited to, the electroencephalogram (EEG), electromyogram (EMG), electrooculogram (EOG), electrocardiogram (ECG).

Two states are usually recognized within sleep in mammals, defined by different physiological features. Among these, rapid eye movements were a distinctive characteristic of these stages at the moment of their first descriptions in humans [8] and cats [9]. Thus, REM sleep (also known as paradoxical sleep) is described as a stage in which the animals enter muscle atonia, evident from the behavioral point of view, and the reduced EMG. From the EEG standpoint, this state is accompanied by fast, low-voltage activity in the cortex and hippocampal theta (6 — 10 Hz) activity in rodents and cats [9, 10]. The recurrent movements of the eyes are also a defining parameter of this stage as well as the increase in the heart rate (see example in Figure 1A). A second state referred to as non-REM (NREM) sleep, in opposition to REM sleep, represents the majority of the sleep time in most mammals (75 — 80 % of the total sleep time [11, 12]). This sleep stage is rich in electrophysiological patterns in the EEG. For instance, high-amplitude and low-frequency waves appear across multiple cortical areas, a reason why large portions of NREM sleep are also known as slow-wave sleep (SWS). Additionally, during this period, waxing and whining graphoelements elements with frequencies between 10 and 15 Hz are observed across multiple cortical areas, but mainly in the somatosensory cortex in mice [13] (see example traces in Figure 1A). These electrophysiological patterns are called sleep spindles and they are known to reflect the interaction of reticular and relay cells of the thalamus [14]. Compared to wakefulness, this sleep stage also shows a reduction in EMG activity and a lower heart rate. These two states (NREM and REM sleep) alternate across the resting period of most mammals and create a structure or macro-architecture that is depicted across time in a so-called hypnogram (See example Figure 1B).

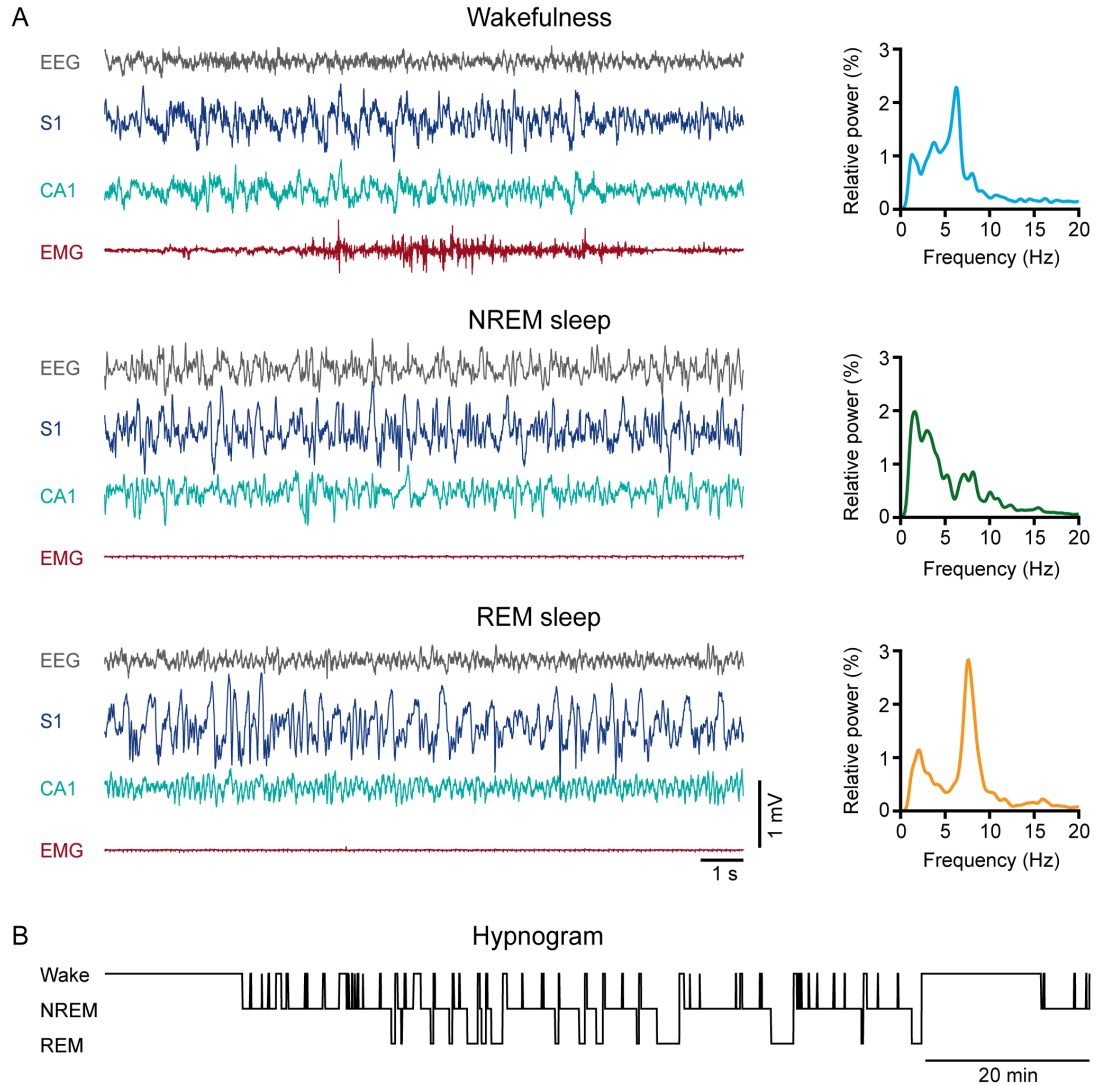


Figure 1: Electrophysiological features of vigilant states in mice. (A) Characteristic traces showing the EEG, local field potential (LFP) of primary somatosensory cortex (S1) and CA1 area of the hippocampus, and EMG for wakefulness, NREM sleep, and REM sleep (Left) and the respective power spectral density from the EEG traces (Right). (B) Representative 2 hr hypnogram (From ZT2) of a mouse depicting the changes in behavioral states across time, including wakefulness (Wake), NREM sleep, and REM sleep.

Another way to differentiate these states is by the particular signature of the Fast Fourier Transform (FFT) from the EEG signal. The EEG's FFT during NREM sleep highlights the relative presence of different frequency bands. The power spectrum of NREM sleep shows a narrow increased activity in the 0 — 4 Hz frequency range. On the other hand, in rodents and cats, the spectral density of REM sleep exhibits a prominent

peak in the 6 — 10 Hz range known as theta band, which is thought to be mainly imposed by the hippocampal activity [4]. During wakefulness, a low-amplitude and mixed-frequency activity appear together with relative increases in faster bands (> 20 Hz), so-called beta and gamma bands.

In summary, different oscillations in the brain create the electrophysiological fingerprints of each behavioral state. However, depending on the timescale, infraslow and ultrafast frequencies may emerge [15]. In this work, I propose that the arousal-modulating-noradrenergic-LC system plays fundamental mechanistic roles in the infraslow fluctuations of brain and body parameters during NREM sleep.

3 Electrophysiological manifestation of the infraslow timescale during NREM sleep

Infraslow fluctuations can be observed during wakefulness and sleep in humans and other animals [16]. In this chapter, I will focus on the infraslow fluctuations happening in NREM sleep. I will start by summarizing visually defined episodes of stereotypical brain activity that emerge distinctively from the one in the background. Then, I will mention infraslow oscillations in voltage within the full-band EEG. Next, I will review the variations in band-limited EEG and body signals. Finally, I will comment on other manifestations of these infraslow timescales and their possible functional implications (see examples in Figure 2).

3.1 Visual manifestations on the infraslow timescale during NREM sleep

As for the visually defined infraslow hallmarks of NREM sleep, specific blocks of characteristic electrophysiological activity in the brain and the body have been reported since the earliest days of sleep monitoring. These include the “*Phases d’Activation Transitoire*” [2, 17], “Cyclic Alternating Patterns” (CAP) [18], “small-amplitude irregular activity” (SIA) [19, 20], “Low Activity Microstates” or LOW [21], among others. All of them have particular electrophysiological properties and theoretical implications in the practice of sleep research. This section will summarize some of the classical frames of reference used to study the temporal heterogeneity of NREM sleep from its evident visual manifestations.

The PATs [2, 17] are defined as recurrent arousal events characterized by a shift of the EEG spectrum towards high frequencies accompanied by an increase in EMG activity, changes in posture or body movements, and a transitory rise in heart rate. These events can last for multiple seconds, and they can emerge spontaneously or as a result of sensory stimulation [2, 22]. Although the mechanisms underlying these events remained unclear,

the reticular activating system is thought to play a role [23].

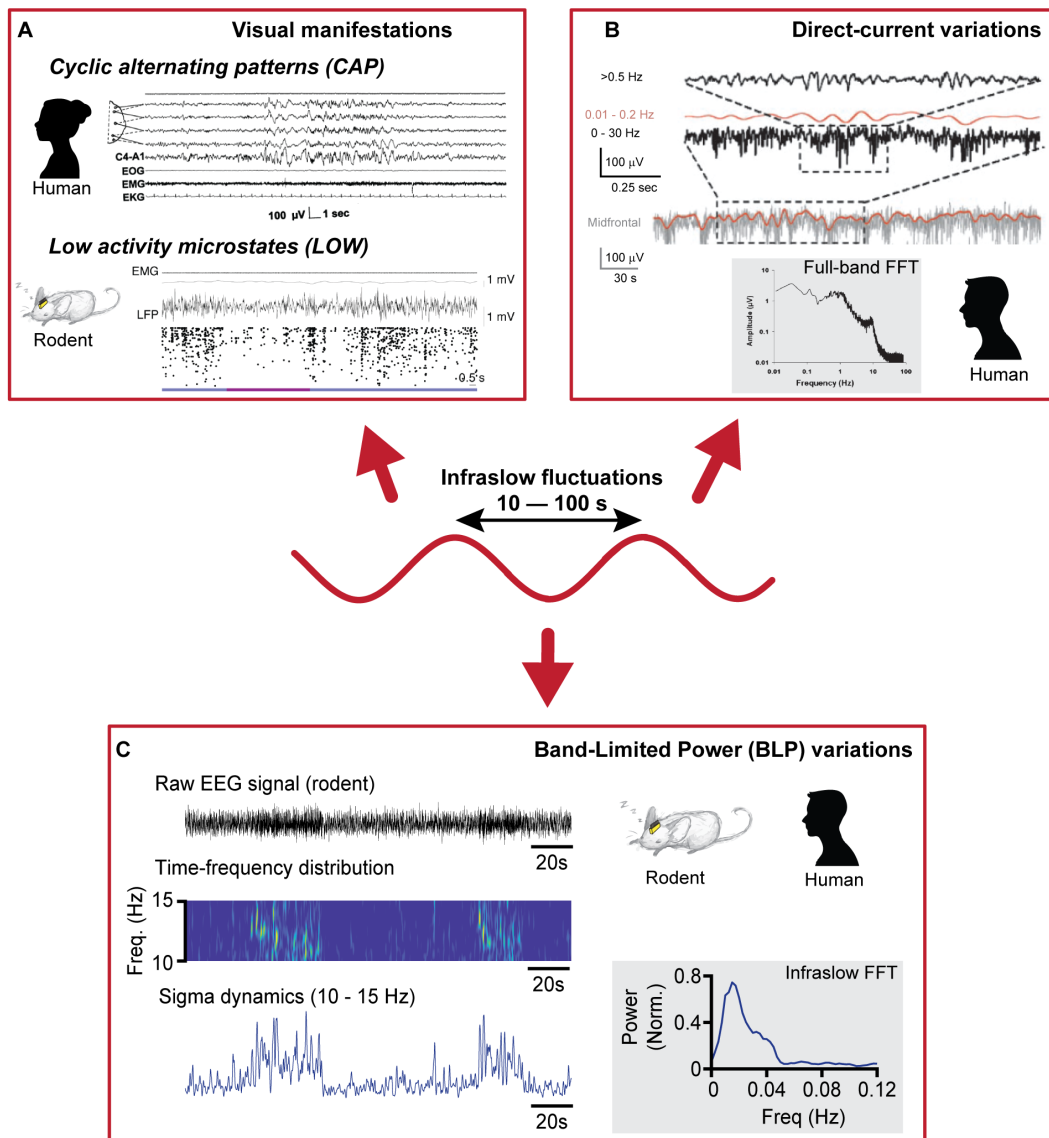


Figure 2: Scheme Showing three different ways to study infraslow timescale during NREM sleep. (A) Discrete visual manifestations of characteristic electrophysiological activity showing an example of the "cyclic alternating patterns" (CAP) in humans showing a "Phase A" in the center of the recording (example from [18]) and the "Low Activity Microstates" (LOW) in rodents highlighted in purple (example from [21]). (B) Direct-current or full band variations (example from [24]). (C) Band-Limited Power (BLP) variations in faster frequency bands. The example shows the infraslow fluctuations in sigma activity during NREM sleep.

The group of Mario Terzano et al. [18] first described the CAPs as spontaneous and stereotypical transient EEG activity with variable periodicity ranging from 20 —

40 s (See example in Figure 2A). These patterns are expressed as alternations in brain rhythms [25] and variations of autonomic signals such as heart rate and respiration [26]. This periodic activity encompasses two phases of activity that alternate. The first one includes high amplitude slow frequency activity known as **phase A**. This period can also contain bursts of delta or alpha (9 — 13 Hz in humans) waves, and other types of EEG graphoelements called K-complexes. Phase A is then followed by low amplitude mixed activity, named **phase B**. In these studies, sleep spindles have not been explicitly considered as a particular marker of any of the two phases, other than being present at the beginning or the end of Phase A [3]. CAPs have been related to sleep instability or disturbances as they are increased in some sleep disorders [25, 26]. However, CAPs have also been considered part of healthy sleep. For instance, phase A has been proposed to reflect an active process involved in sleep maintenance [2]. Like the PAT, the biological origins of CAPs are unknown. Still, the reticular activating system comes out again as a possible candidate for the generation of these events [2].

The research on PATs and CAPs has been conducted mainly in the human [2, 16]. However, animal studies have also observed evidence for an infraslow organization of NREM sleep. For instance, Cornelius Vanderwolf *et al.* [19, 27] described a local decrease in the hippocampal activity of rodents that lasted from seconds to minutes during the natural waking behavior of rodents and called them SIA. This reduced amplitude activity was also observed during NREM sleep and has been referred to as S-SIA [28]. These events last tens of seconds, represent around 33% of NREM time, and never come just before REM sleep. Additionally, Jarosiewicz and Skaggs [20] found that auditory stimuli during NREM sleep can induce S-SIA episodes. The origins of these hippocampal-activity-defined episodes are unknown. Instead, the mechanistic research focus has been on the hippocampal unit activity during these periods. For example, firing patterns of hippocampal place-cells during S-SIA periods recapitulated the memory of a context rather than the immediate visual information around the animal [29].

Similar to the SIA, low EEG activity or “LOW” states were recently described by Miyawaki *et al.* [21]. These were defined as periods of diminished slow-wave and spindle activity across multiple areas in the cortex during NREM sleep that last for multiple seconds (See example in Figure 2A). A usual feature of LOW is the “rebound” of oscillatory NREM sleep patterns following the episode. Moreover, low-amplitude, fast frequency EEG with a concomitant increase in EMG transient events called microarousals (MA) are more prevalent during LOW states. Compared to the original SIA periods described by Vanderwolf [19] in wakefulness, LOW episodes have higher delta and theta activity. However, these authors suggest that S-SIA and LOW could share similar mechanisms and that they might represent the same “sleep state” where diminished

neuronal spiking could promote possible restorative functions in the cells [21]. Both LOW and SIA periods, even discrete events by definition, have been suggested to “*represent the sleep and waking extremes of a continuum of microarousals*” [16] citing ([5, 30]).

3.2 Full band or direct-current variations in the EEG

Compared to the visually defined spontaneous transients of brain activity, another way to look at EEG changes on the infraslow timescale is to directly measure voltage fluctuations within the full-band EEG signal (See example in Figure 2B). However, this represents a challenge for most of the acquisition systems used in electrophysiology because they operate under alternating current amplifiers and filter out low-frequency components in the signals to eliminate artifacts produced by the high impedance between the electrodes and the tissue. However, DC amplifiers and non-polarizable electrodes allow the stable recording of electrophysiological fluctuations for long periods.

This approach has allowed the description of infraslow fluctuations in the brain during wakefulness [24]. Additionally, Picchioni et al. [31] performed a simultaneous recording of full-band EEG while measuring Blood Oxygenation Level-Dependent (BOLD) activity with functional magnetic resonance imaging (fMRI) during sleep. They found that infraslow oscillations in the EEG voltage in the 0.05 — 0.099 Hz frequency range were positively correlated with subcortical variations in BOLD activity. At the same time, the cortical areas showed a negative correlation with these signals. Furthermore, another study [32] found that fluctuations in EEG in the range of 0.02 — 0.2 Hz during human sleep were associated with interictal activity in epileptic patients, hence, supporting the idea of a functional implication of these oscillations in the regulation of physiological (or in this case pathological) brain activity.

3.3 Fluctuations in the band-limited power activity in the EEG

Another approach to look at infraslow oscillations during sleep is to measure fluctuations in faster activity patterns, *i.e.*, measuring the dynamics of specific frequency bands (examples of the method used in this project is shown in Figures 2C and 3). This approach, here referred to as band-limited power (BLP) activity, was first applied by Gert Pfurtscheller in 1976 to follow changes in the alpha (7 — 13 Hz) band during a cognitive task [33]. Comparable methods revealed multi-second fluctuations in different frequency bands during quiet wakefulness [34–36].

Using a similar approach during NREM sleep, Achermann and Borbely [37] showed that slow-wave activity (< 4.5 Hz) fluctuated with a periodicity of ~ 20 s (0.047 Hz). In comparison, sigma activity showed a period of ~ 4 s (0.22 Hz) in humans. However,

this study used a 64 s moving window (20 s shifts), limiting the frequency resolution for possible slower components. The authors hypothesize that delta activity fluctuations could be related to variations in cerebral blood flow. Similarly, intracranial recordings in the human auditory cortex [38] showed that gamma (40 — 100 Hz) activity fluctuates on infraslow timescales (<0.1 Hz) during NREM sleep.

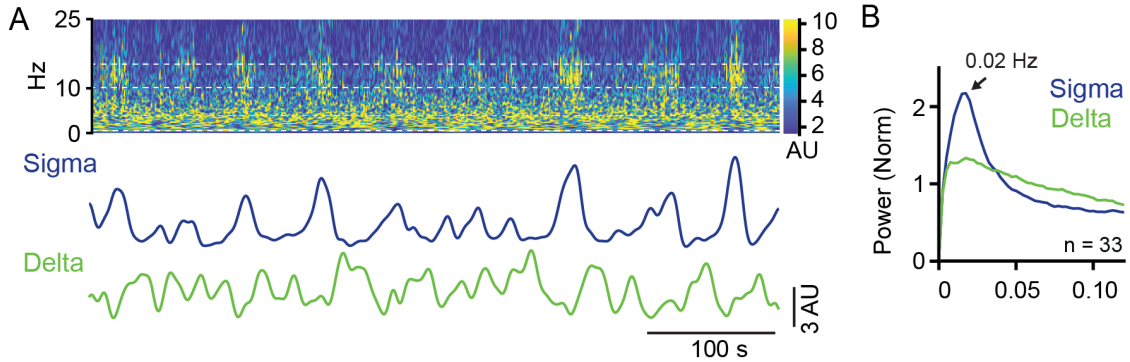


Figure 3: Representation of the typical approach for band-limited power activity measures. (A) From top to bottom: time-frequency distribution depicting the spectral changes in 0 — 25 Hz activity from the local field potential in the somatosensory cortex of a mouse. Sigma (Blue) and delta (Green) activity from the distribution constructed by collapsing the frequency dimension in the 10 — 15 Hz and 1.5 — 4 Hz, respectively. (B) Power spectral density of the respective signals from (A). Modified from Figure 1 in [39].

Interestingly, a strong, well-defined 0.02 Hz fluctuation in sigma activity emerges during human and mouse NREM sleep [6] (See example in Figure 3). This brain rhythm is well known to be associated with electroencephalographic graphoelements known as sleep spindles, which reflect the recurrent bursting activity of thalamocortical networks [4]. Furthermore, this infraslow organization of sigma was phased locked with the fluctuations in hippocampal ripple activity [6] thought closely related to memory consolidation processes during NREM sleep. The observation of infraslow changes in the sigma activity and/or spindle density has been independently observed by other groups. For instance, sigma activity and the clustering of sleep spindles fluctuated on an infraslow timescale that peaks around 0.015 to 0.02 Hz in humans [40]. Consistent with the results from Lecci et al. [6], the fluctuating pattern was maximal during N2 compared to the N3 stage of NREM sleep. Further topological analysis of these fluctuations showed a maximal representation in central, parietal, and occipital regions.

Moreover, with a combination of EEG and magnetoencephalography, Weber et al. [41] showed that fast sigma (12 — 16 Hz) and low gamma (30 — 40 Hz) activity fluctuated over a ~ 40 s period in human NREM sleep. These authors proposed that cortical

spindle activity helps synchronize local gamma activity with possible implications in sleep-dependent memory consolidation processes. In line with these observations, at least at the level of the sleep spindles, auditory-cue reactivation of memory traces during moments of high spindle activity in deep NREM sleep facilitated memory consolidation [7]. On the contrary, cue presentation during spindle-refractory periods failed to produce the same effect. The authors proposed that possible alternations between high and low spindle activity have beneficial effects on cue memory reactivation.

3.4 Other manifestations of the infraslow timescale during NREM sleep

Functional imaging studies propose that specialized networks in the brain are confined in functionally defined modules [42], *i.e.*, brain regions that show correlated BOLD activity. Independent infraslow fluctuations of these modules' activity were increased during NREM sleep [43]. Supporting this observations, Fukunaga et al. [44] described a marked 0.01 — 0.05 Hz fluctuation in BOLD activity in the visual cortex. Still, the authors mentioned that these fluctuations appear across independent cortical and subcortical areas during quiet wakefulness and sleep. Furthermore, these fluctuations were stronger during sleep compared to quiet wakefulness, with maximum power at ~ 0.02 Hz.

A ~ 50 s periodicity was reported for variations in the heart rate [6] and pupil diameter [45] during NREM. These variations in autonomic bodily parameters were strongly correlated to the infraslow fluctuations in sigma activity in the brain, suggesting a possible shared mechanism that modulates central and peripheral physiological processes.

3.5 Functional implications of infraslow fluctuations during NREM sleep

Functional implications of infraslow changes in the brain and the body during NREM sleep were described. For instance, infraslow fluctuations in sigma activity, the heart rate, and the pupil diameter were related to sleep fragility and memory consolidation. Auditory [6] or direct visual [45] stimulation during NREM sleep at periods of high levels of sigma activity, low heart rate, and reduced pupil diameter were associated with reduced behavioral changes in mice. *Au contraire*, the same sensory stimuli during the alternative period within this fluctuation (*i.e.*, low sigma, elevated heart rate, and increased pupil diameter) resulted in sensory-evoked arousals in the animals. These responses were evident by increases in the muscle tone and the desynchronization of the EEG. Thus, the authors proposed that not only physiological changes happen at this ~ 50 s timescale but also fluctuations in sleep fragility. Supporting this hypothesis, we recently showed that not only evoked arousals but also spontaneous MA happen in a phase-locked manner within the infraslow fluctuations in sigma [46] during this sleep period. Possible thalamic

gating mechanisms could underlie such variations in sensory arousability during NREM sleep. Potential additional implications of these fluctuations, particularly those associated with the LC, are further mentioned in the discussion session of the thesis.

Finally, periodic organization of sleep spindles such as the ones suggested by Lecci et al. [6] was proposed to serve a purpose in consolidating NREM sleep-dependent memories [47]. Supporting this hypothesis, in a declarative memory task, the magnitude of the 0.02 Hz fluctuation in sigma during the post-learning sleep predicted the sleep-benefit in episodic memory correlates in humans [6]. Furthermore, auditory cue reactivation of declarative memories during spindles increased consolidation of the memory traces but not during spindle-refractory periods [7]. Therefore, possible convergent mechanisms could be associated with the physiological fluctuations during NREM sleep and their behavioral outcomes.

4 The *locus coeruleus* in sleep

The *locus coeruleus* or LC, first described by Johann Christian Reil (or Felix Vicq-Azur, depending on the source) and named as such by the brothers Joseph and Karl Wenzel [48] are a pair of nuclei located at the sides of the four ventricles in the rostral and dorsal pontine tegmentum [49–51]. This nucleus contains a dense cluster of noradrenergic cells with wide projections to both the forebrain and hindbrain [52–54], with complex interactions organized in spatial and temporal ensembles [55–57] and it is the major source of NA in the mammalian forebrain [57]. The synthesis of NA in these neurons produces neuromelanine as a by-product, giving this area the dark color responsible for its name (from the Latin “sky-blue region”). The LC contains around 1,000-to-2,000 cells in the rodent [58–60] and $\sim 20,000$ -50,000 cells in humans [61, 62]; with significantly higher numbers in comparison to other primates [50]. Noradrenergic neurons in the brainstem show rich and heterogeneous genetic [63] and phylogenetic [64] profiles in which the LC encompasses the A4 and particularly A6 neuronal groups from the catecholamine groups described by Hökfelt et al. [65]. Additionally, the LC is among the most divergent neuromodulatory systems concerning sex differences, with over 100 genes differentially expressed [66].

Functionally, the LC activity has been long related to “*stimuli, both environmental and physiological, that represent a challenge to the organism*” [67]. However, a wide variety of other functions have been directly related to the noradrenergic LC system [68] ranging from the modulation of attention [69], stress [70], mood [71], pain [68] and memory consolidation [72], to optimization and orientation of task-related decision and sensory tuning processes [73–78]. However, from early studies of electrophysiological unit

recordings and pharmacological approaches, the modulation of the sleep-wake behavior has been of great interest [79].

4.1 Noradrenergic signaling in the brain

NA acts on adrenergic receptors or adrenoceptors (AR), which are commonly classified into three groups: $\alpha 1$, $\alpha 2$, and β AR. These groups are divided into subgroups (*i.e.*, $\alpha 1a$, $\alpha 1b$ and $\alpha 1d$, $\alpha 2a$, $\alpha 2$ and $\alpha 2c$, and $\beta 1$, $\beta 2$ and $\beta 3$) [80]. These receptors are part of the G protein-coupled receptors. Each group of AR are preferentially linked to a particular family of guanine nucleotide-binding regulatory protein (known as G proteins). $\alpha 1$ AR are mainly linked to Gq proteins which are known to mobilize Ca^{2+} and activate Ca^{2+} influx in the cells [81, 82]; likewise, these receptors have been related to the activation of Na^+/H^+ exchangers and the modulation of K^+ channels [80]. $\alpha 2$ AR are primarily associated with Gi proteins. These proteins inhibit adenylyl cyclase (AC) and decrease cyclic adenosine monophosphate (cAMP) generation. It has been suggested that $\alpha 2$ can also couple to Gs and Gq proteins; however, the coupling to Gi is approximately 1000 times bigger [83]. Finally, β AR are associated with Gs protein pathways that activate AC and therefore increase levels of cAMP, which results in activation of cAMP-gated ion channels [80]. It is important to understand these different signaling pathways on a cell-by-cell basis since they determine the electrophysiological and biochemical consequences of receptor activation.

Accordingly, the distribution of the AR groups and subgroups within the mammalian brain has been studied since the 90s [84–88]. In this paragraph, I summarize the distribution of some of these receptors in areas related to the generation of the spindles and the control of sleep from studies mostly using *in situ* hybridization to quantify AR mRNA in the rat; for a complete description of these distributions, I refer to the original publications. $\alpha 1$ AR are high in areas such as the reticular nucleus of the thalamus (TRN; particularly $\alpha 1a$ and $\alpha 1d$), the central group of the thalamus (such as the rhomboid, $\alpha 1b$), the dorsal raphe (DR; particularly $\alpha 1b$) the pineal gland and the dorsolateral amygdala ($\alpha 1a$ and $\alpha 1b$) [84, 85, 88]. $\alpha 2a$ AR are high in the LC, the parabrachial nucleus, the dorsal motor nucleus of the vagus, the nucleus of the solitary tract, and pontine and tegmental nuclei, the lateral and posterior hypothalamic area [87]. $\alpha 2b$ AR are highly expressed in central thalamic nuclei and the amygdala [85]. Then, $\alpha 2c$ AR are primarily expressed in cortical and basal nuclei. Finally, β AR are mainly located in the “principal” or “relay” nuclei in the thalamus (central nuclei $\beta 2$ and $\beta 1$ in the primary sensory ones) but not in the TRN [86].

These molecular data show that noradrenergic signaling is broad and specific across brain areas that control the sleep-wake cycle and in areas essential in the generation

of sleep-related cortical rhythms. Nonetheless, scrutiny of the published results showed significant discrepancies between studies. Therefore, *in-vitro* assessment of the region and cell-specific responses to noradrenaline (NA) exposition could be considered a suitable alternative or addition in studying the distribution of AR across the brain; I cover such responses in a latter introductory section (Introduction Chapter 4.4).

4.2 LC unit activity across the sleep-wake cycle

Initially, the noradrenergic LC cells were considered a group of densely packed neurons [89] working homogeneously as a group [90] to regulate NA across the brain 4. Early studies of unit activity in the '70s were mainly performed on the cat. These studies concluded: First, LC activity was not significantly different between quiet wakefulness (qW) and slow-wave or NREM sleep and exceptionally high during active wakefulness (aW) and paradoxical (REM) sleep [91]. Second, the LC is represented by a large and dispersed population of noradrenergic cells interspersed among a large population of non-noradrenergic neurons [89]. Third, LC activity shows two types of cell groups, one preferentially active during REM sleep and a second one showing a different activity pattern, being high in wake, partially low during NREM, and almost silent during REM sleep [92].

In the '80s, a refined analysis of the shape of the action potential of noradrenergic cells and the inclusion of other species with more compact and neurochemically homogeneous LC showed that noradrenergic LC neurons present an activity profile such that $aW > qW > NREM > REM$ [67, 90, 93], within this decade the idea that LC is a functionally homogeneous group of cells gained popularity. At the time, noradrenergic LC activity was associated with particular sleep patterns such as sleep spindles [90] or a permissive role in the generation of REM sleep [67]. In the '90s, however, LC research focused more on the activity patterns emerging from these noradrenergic neurons during wakefulness. For example, some authors suggested that LC activity is highly tonic during behavioral agitation, whereas overall resting states were associated with a reduced LC tonic activity [94]. In contrast, others proposed a phasic activity pattern in response to sensory stimuli or stressful situations [95]. These ideas were further refined in the last 20 years [76, 78].

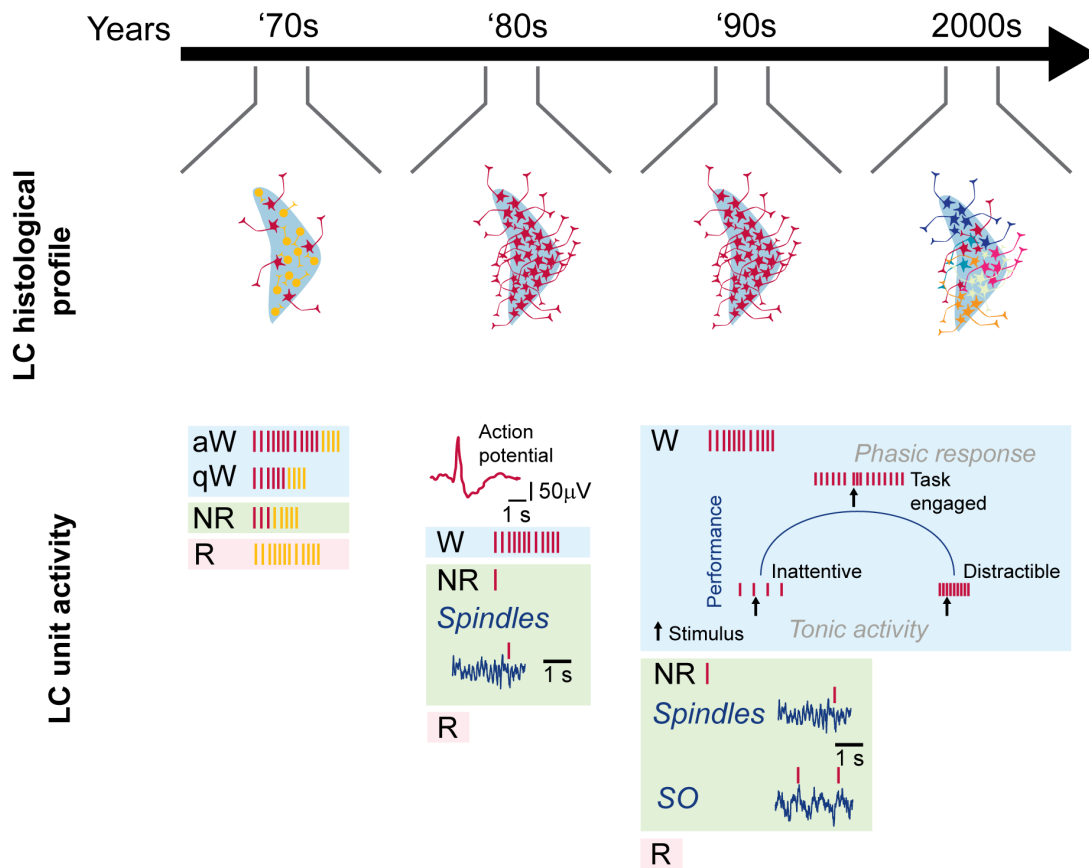


Figure 4: Timeline schematizing the overall view of the cellular populations of the Locus coeruleus (LC) as described in the introductory section 4.2. In the '70s, the LC units show two cell populations with different activity patterns (shown in red and yellow) in active and quiet wake (aW and qW), NREM sleep (NR), and REM (R) sleep. In the '80s, the representative shape of the action potential of noradrenergic cells and the study of species with a more compact noradrenergic population showed high activity during wake (W), low in NREM sleep, and silent during REM sleep. In the '90s, studies of LC activity described phasic and tonic activities during wakefulness. In the '2000s, studies showed the complexity of the noradrenergic LC system with anatomical and functional ensembles; studies focused mainly in the LC activity patterns during wakefulness. Some studies related to the LC unit activity during across the sleep-wake cycle also challenged the dogma of a quiescent LC during NREM sleep.

Finally, the new century came along with a refreshed and open perspective about the role of the LC across behavioral states. Remarkably, this period challenged the “*dogma*” about the quiescence of these neurons during NREM sleep [96, 97]. Indeed, these authors proposed that LC units occasionally fire in a highly synchronized burst during NREM sleep. Moreover, they further discovered that noradrenergic LC neurons increase their

firing on a learning-depending basis during NREM sleep to levels as high as the ones observed during aW. Interestingly, optogenetic activation of LC neurons during NREM sleep altered memory consolidation in the rat [98]. Furthermore, noradrenergic LC activity was related to oscillatory patterns during NREM sleep, such as slow oscillations in the cortex [97] or spindles in the hippocampus [98].

4.3 Other measures of LC activity across the sleep-wake cycle

Naturally, other methods can be used to study noradrenergic or LC activity in the brain during the sleep-wake cycle. This section deals with some of the significant findings related to *in-vivo* electrochemical voltammetry, microdialysis, and structural and functional imaging techniques.

Electrochemical measurements: Among the methods for detecting free NA levels in the brain, some use the electrochemical properties of catecholamines. Amperometry and voltammetry use controlled changes in current or voltage, respectively, applied to miniature carbon electrodes to account for the differences in the waveform produced by the oxidation of the molecules in the sample. A so-called “fingerprint” is created depending on the amount of a given solute present in the sample [99, 100]. Pioneering works with these techniques in the context of neuroscience happen in the 70s with Ralph Adams *et al.*, [100–102]; These techniques have been primarily used to record the NA release in response to electrical stimulation of the LC or LC fibers [103–105] during anesthesia. Moreover, this method has been used to measure the noradrenergic response to sensory stimuli during anesthesia [106]. Among the advantages of this technique is the high time resolution. However, the major limitation of these methods is the difficulty of distinguishing between monoamines, particularly dopamine and NA, because so far, they show similar fingerprints in the voltammograms [99, 103, 107]. Moreover, *in-vivo* voltammetry measures relative instead of absolute concentrations, which reduces the flexibility of its use across the sleep-wake cycle [108]. Novel approaches such as different types of electrode materials [109] or different waveforms [110] to overcome these limitations are a matter of current investigation.

Microdialysis: A second important technique to measure the concentration of free levels of a substance in the brain is to take a sample of the cerebrospinal fluid (CSF). Microdialysis uses the same principle of dialysis to perform such endeavors. From as early as 1966 [111], this technique uses a flow of artificial CSF throughout a miniature dialysis probe to collect samples of the surrounding CSF and its content. With these samples, multiple other methods, such as High-Performance Liquid Chromatography, can be used to quantify the amount of substances contained in the sample, such as NA. Microdialysis has been widely used to study noradrenergic LC response upon electrical

stimulation [108, 112] or pharmacological [113] manipulations during anesthesia or the co-release properties of these cells [114].

In the context of the sleep-wake cycle, *in-vivo* microdialysis studies have measured NA levels in the brain in multiple species [115]. These studies mostly showed that NA levels were high during wakefulness, intermediate during NREM sleep, and low during REM sleep. However, already de Saint Hilaire et al. [116] showed that noradrenergic levels in wakefulness could be lower than those observed during NREM sleep in rats. Additionally, when distinctions between active and quiet wakefulness were made, the differences between these two states usually were higher than those between qW and NREM, which generally did not differ significantly [117, 118]. Moreover, differences in NA levels across behavioral states seemed to depend on the sampling region, for instance, whether it is cortical or subcortical [119, 120]. Moreover, some studies do not differentiate between NREM and REM ([117], more examples in [115]).

Most importantly for the study of behavioral states, microdialysis has significantly low sampling rates ranging from 5 to 30 min [118–121]; additionally, in the cases where a “high” time resolution (<15 min) is used, the flow rates are not compatible with all species and manipulations. Also, all solutes capable of crossing the probe membrane used in the dialysis process are depleted from the sampling area, which can have a substantial effect on the system being studied [122]. The latter could have possible implications in the sleep-wake-regulation research.

These limitations of microdialysis make it unrealistic to report the real-time dynamics of these molecules within the sleep-wake cycle or their relation to specific electrophysiological features during sleep. Instead, this technique is best suitable to study absolute NA levels in the brain and correlate them with the majority of the behavioral state, the light/dark cycle [115], or overall response to manipulations such as sleep deprivation [121] during the sampling period.

Imaging techniques: Similarly, imaging techniques can also study LC structure, integrity, and function during different behaviors. In the case of MRI, protocols that allow the visualization of neuromelanin permit the segmentation of regions containing such molecules, as is the case for the LC [123], also known as “neuromelanin-sensitive” imaging [124]. Although it is still at its early stage, with the anatomical segmentation of the LC, MRI functional approaches such as BOLD or more refined anatomical profiling, such as diffusion tensor imaging, are feasible for future studies with the noradrenergic system. Moreover, current Positron Emission tomography (PET) in humans [125] or microPET in rodents [126, 127] makes it possible to image NA transporter density by using noradrenergic related radioligands such as [^{11}C]MeNER.

The use of these techniques in the study of the LC gained further appreciation for its

direct application in humans [128, 129] and its relevance in the context of LC structural or functional changes in neurodegenerative disorders [125, 128, 130] and major depression. Additionally, imaging studies in rodents while manipulating LC activity can also raise awareness of the function of this noradrenergic system. For example, Zerbi et al. [131] showed that chemogenetic stimulation of noradrenergic LC neurons resulted in increased activity in salience and fear processing networks during anesthesia supporting the LC role in regulating large-scale arousal networks.

In the context of sleep, the study of the LC is relatively new in the imaging field. However, some studies shed some light in this direction in the healthy and pathological brain. For instance, one study [49] showed that the BOLD activity in dorsal brainstem areas encompassing the LC reflects relatively increased activity patterns during NREM sleep together with slow (< 1 Hz) waves but not with delta (1 — 4 Hz) waves during NREM sleep. Similar to the previous observation in noradrenergic LC unit activity associated with cortical slow-oscillations in rodents [97], this result also challenged the idea of general low LC activity during NREM sleep [132].

Concerning structural studies in neurodegenerative disorders and their related sleep changes, Doppler et al. [125] found that the density of NA transporter in arousal-promoting and propagating areas were anticorrelated to CAP rate during NREM sleep. This result was particularly significant in Parkinson’s disease (PD) patients suggesting alterations in sleep instability associated with noradrenergic dysfunction in this population. The authors conclude that alterations in noradrenergic signaling in PD patients could lead to altered arousability and response to arousal stimuli. CAP has been previously associated with sleep stability and not only with the intrusion of wakefulness during NREM sleep [2]. Another study [133], using high resolution (7 T) imaging, found that reduction in the anatomical LC intensity, usually related to the structural integrity of this nucleus, was correlated with higher self-reported awakenings assessed using sleep quality questionnaires. This result was mainly observed in subjects with high tau protein in plasma. Most of these studies mentioned the necessity of including additional electrophysiological data to further decipher the possible roles of LC integrity and activity during sleep.

4.4 The LC as a candidate for the generation of infraslow fluctuations in sleep spindle density during NREM sleep

This chapter summarizes evidence that the noradrenergic LC activity is a strong candidate to play potential roles in infraslow electrophysiological manifestations during NREM sleep. The focus is principally on the clustering of sleep spindle density on a 50 s timescale and the accompanying heart rate variations observed in the mouse.

Fluctuations in LC electrophysiological and BOLD activity: Infralow fluctuations in the wide-band field potentials have been described for multiple areas in the brain [134]. Similarly, Filippov et al. [135] showed changes in the infralow range in the LC and the serotonergic dorsal raphe (DR), with a peak around 0.02 — 0.04 Hz in freely moving rats. Likewise, these areas also exhibited variations in even slower frequencies in the order of minutes (< 0.002 Hz). This study departed from previous observations from the same group [136] where they described infralow fluctuations in areas related to visual processing (lateral geniculate nucleus and visual cortex) under different optical environmental contexts. In similar experimental conditions, including freely moving behavior and during different types of visual stimuli, the field potential in both the LC and DR vary at similar infralow frequencies. However, in these studies, the animal’s behavioral state was not included in the analysis; given the described experimental conditions, most probable, these recordings represent the activity during waking behavior. Still, sleep-related variations in LC activity may continue during NREM sleep. Supporting this hypothesis, Dang-Vu et al. [49] found increases in the BOLD signal within the pontine tegmentum, an area that includes the LC associated with slow-waves during sleep.

The LC as a gate for sensory evoked arousals during NREM sleep: An important observation related to the infralow fluctuations in the physiological brain and body activity during NREM sleep is their correlation to sensory-evoked [6, 45] or spontaneous [46] arousal events. These studies found that fragility periods during NREM sleep were associated with low sigma activity, which is congruent with lower sleep spindles. At these moments, the probability of arousal events was increased. These results are consistent with pioneering ideas supporting a role of thalamic-generated spindle activity in sensory gating [137–139].

Recently, a hallmark study [140] showed a direct link between the levels of LC activity and the threshold of sensory-evoked arousability during NREM sleep. In this work, background unit activity levels of noradrenergic LC neurons were anticorrelated to arousal-threshold levels upon auditory stimulation in rats. For instance, optogenetic or pharmacologic activation of noradrenergic LC neurons reduced the arousal threshold. The opposite manipulations, *i.e.*, the inhibition of these cells, resulted in an increased arousal threshold and a reduction of the waking probability after the same type of stimuli. These results support a permissive role for the noradrenergic LC system in sensory gating during NREM sleep and set a strong argument related to noradrenergic LC signaling with the infralow changes in sleep fragility.

A role of the LC in the modulation the autonomic nervous system: As mentioned in the introduction chapter 3.4, in addition to the fluctuations in sigma activity, the heart rate and the pupil diameter vary on an infralow close-to-minute timescale during NREM

sleep [6, 45]. These correlative observations suggest that there could be shared or associated mechanisms between central and autonomic circuits during this behavioral state. The LC plays a critical role in the modulation of heart rate (for a review, see [141]), possibly acting on both sympathetic and parasympathetic systems. In fact, given the strong anatomical projections from and to sympathetic areas, as is the case with the nucleus paragigantocellularis, the LC has been considered a key element in this system, including (but not limited to) the control of the heart rate [141]. For instance, LC activity is engaged in stressful situations, including those directly related to cardiovascular control, such as during hypotensive stress. Furthermore, because noradrenergic LC neurons also respond to particularly high prefrontal activity, it has been proposed that the LC supply a cognitive value to sympathetic response [142]. Or play a critical role in orienting resources to maintain arousal and cognitive flexibility [74].

Similarly, the LC is heavily connected to parasympathetic networks [143], and it plays a critical role in inhibiting this system [141]. Optogenetic stimulation of LC neurons increased GABAergic transmission in cardiac vagal neurons throughout α 1- and β 1 AR. Interestingly, modulation of parasympathetic activity, such as activating the dorsal vagal complex or vagal nerve stimulation, resulted in increased LC activity as shown by increases in c-Fos [144, 145] or *in-vivo* Ca^{2+} transients in noradrenergic LC neurons [146]. Given the prominent role of the LC in modulating sympathetic and parasympathetic activity, the noradrenergic LC system has been implicated in the regulation and integration of autonomic responses in emotional activation [71].

As in the case of the heart rate modulation, the sympathetic and parasympathetic role of the LC has been involved in the regulation of the pupil diameter in a top-down manner [147–149]. Interestingly, direct electrical stimulation of the vagal nerve increased pupil diameter in the rat [150]. Likewise, transcutaneous electrical stimulation of the vagus nerve increased the pupil diameter in humans [151]. These authors associated these observations with the recruitment of noradrenergic LC activity upon these manipulations. In the context of sleep, infraslow fluctuations in the pupil diameter were reduced by pharmacological inhibition of direct parasympathetic but not sympathetic signaling in the eye [45].

Altogether, the essential role of the LC in the modulation of heart rate and pupil diameter and the tightly coherent fluctuations of these two autonomic signals during NREM sleep is an additional argument to support the study of the noradrenergic LC system in this context.

Noradrenergic modulation of thalamic activity: The noradrenergic LC system is known to tune thalamic activity [75] in a manner capable of suppressing cellular spindle patterns via α 1 and β AR [152]. The cellular mechanisms responsible for this interaction have been

intensely studied by the group of David McCormick. For instance, neurons in the dorsal lateral geniculate nucleus of cats and guinea pigs showed an α 1- [153] and β -dependent depolarization [153–155] mediated by I_h currents and activation of AC. In the same species, thalamic reticular neurons were depolarized in response to NA [156]. Cells from most thalamic nuclei exhibited a depolarization upon NA exposure [157]. Furthermore, neurons in the LGN and the reticular/perigeniculate nucleus of ferrets depolarized when exposed to NA, a response that was dependent on β - and α 1-AR, respectively [158]. These observations are congruent with possible infraslow changes in noradrenergic signaling in the thalamus in a way that could regulate the periodic spindles-free periods during NREM sleep.

5 Aims of the thesis

This thesis aimed to explore possible neuronal mechanisms responsible for the infraslow variations in sleep spindle density observed in mouse NREM sleep. For the reasons provided in the introduction, I hypothesized that the LC would be an ideal candidate to pursue these mechanisms. To investigate this possibility, I used cutting-edge neuroscience methods to characterize NA's infraslow dynamics in the thalamus, a master generator of the spindle activity that is well represented within the sigma band during NREM sleep. Furthermore, I optogenetically activated and inhibited noradrenergic cells within the LC to test for the sufficiency and necessity of this system in the fluctuation in the brain and its possible role in the coordination of these changes and the ones observed in the heart rate. I additionally used *in-vivo* pharmacology and *in-vitro* electrophysiological techniques to study the cellular mechanisms involved in the thalamic response to NA release from the LC. I discuss how the experimental observations argue for a causal role of the noradrenergic LC system in the modulation of these infraslow changes and coordinate NREM sleep substates that possibly favor fundamental physiological processes in this vigilance state. The results could have crucial implications for understanding sleep physiology in health and disease.

D Results

Noradrenergic circuit control of non-REM sleep substates

Alejandro Osorio-Forero, Romain Cardis, Gil Vantomme, Aurelie Guillaume-Gentil, Georgia Katsioudi, Christiane Devenoges, Laura M.J. Fernandez, and Anita Lüthi

<https://doi.org/10.1016/j.cub.2021.09.041>

At first sight, sleep might seem like a homogeneous state. During this period, goal-directed behaviors and responses to external stimuli are drastically reduced. However, a total and persistent disconnection from the environment is a suboptimal solution for an organism's survival because it would make it vulnerable to potential external dangers. Recent observations highlight fluctuations in brain and body hallmarks of arousability during non-rapid-eye-movement (NREM) sleep that complement this state with recurrent fluctuations in sensory vigilance levels [6, 45, 46]. These include fluctuations in the sigma power and hippocampal ripple activity in the brain, variations in the heart rate, and pupil diameter changes that create NREM substates with different levels of sensory vigilance. Before this study, the mechanisms underlying such fluctuations were not clear. Nevertheless, among the best candidates for such wide brain and bodily modulation was the noradrenergic *locus coeruleus* (LC) system. The LC is a nucleus commonly associated with stress and high attention periods during wakefulness. However, the noradrenergic LC cells are still active during NREM sleep and can mediate sensory responsiveness during this vigilance state [140]. Furthermore, during wakefulness, the LC tunes sensory processes throughout modulation of thalamic activity [75], a key area for the generation of sleep spindles and sigma activity. Additionally, the LC is a crucial part of the autonomic nervous system and can regulate variations in both the heart rate [159] and pupil diameter [147, 148]. In this study, I aimed to investigate the role of the noradrenergic LC system in regulating brain and body hallmarks of vigilance during NREM sleep.

In this study, I combined polysomnographic recordings and local field potentials (LFP) in S1 with pharmacological, optogenetic, or fiber photometry approaches in freely moving mice and *in-vitro* patch-clamp recordings in ventral posteromedial (VPM) and reticular thalamic nucleus (TRN) neurons to study pursue this objective. I showed that mean NA levels in the thalamus were high and varied on a close-to-minute timescale during NREM sleep. Additionally, I demonstrated that these fluctuations were necessary and sufficient to regulate variations in sigma activity and the clustering of spindles during NREM sleep. Furthermore, I found that the LC activity was most likely temporally organized in a close-to-minute timescale. I further described the network and cellular mechanisms underlying these observations. I showed that noradrenergic LC activity in the thalamus rather than in the cortex was relevant for the organization of the spindles and that it does so by a long-

lasting depolarization of VPM and TRN neurons mediated by β - and α 1-AR, respectively. Finally, the experiments also pointed out that noradrenergic LC could be able to modulate the coordination between the heart rate variations and the fluctuations in sigma activity during NREM sleep. Altogether, these experiments established the LC as a protagonist in the generation of NREM substates with different physiological features, states previously related to sensory arousability.

This project is the principal work of my doctoral thesis. Here, I carried out all the *in-vivo* experiments and analysis. I designed the experiments and protocols for the pharmacology, optogenetic, and fiber photometry with the guidance and support of Profs. Anita Lüthi and Dr. Laura Fernandez. Dr. Romain Cardis developed the closed-loop algorithms that I later adapted for my particular questions and context. In this project, I also contributed to the recollection of the data for the *in-vitro* recordings in which Prof. Anita Lüthi, and particularly Dr. Gil Vantomme, who did most of the recollection. I analyzed all the data in this project for the *in-vivo* and *in-vitro* experiments.

E Discussion

1 Scientific contributions

1.1 Noradrenergic LC mechanisms are causally related to the infraslow fluctuations in sigma activity during sleep

The noradrenergic LC system has long been associated with playing a critical role in regulating states of wakefulness [68, 69, 74]. With the experiments carried out in this project, we showed that NA levels in the thalamus were high and fluctuated on a close-to-minute (~ 0.02 Hz) infraslow timescale. These fluctuations in neurotransmitter levels at a specific brain site, the sensory thalamus, underlay fluctuations in the power of sigma (10 — 15 Hz) activity measured electroencephalographically. Mechanistically, this is explained by the cellular effects of NA on sleep-spindle generating thalamic circuits [39]. We established the mechanistic link between LC's thalamic projections sites and electroencephalographic sleep rhythms primarily by precisely timed optogenetic interrogation of LC neurons during NREM sleep. Activation of these cells reduced sleep spindles and sigma activity and disrupted the fluctuations in this frequency band. Instead, inhibition of these neurons increased the spindles and sigma, disrupting their periodic pattern. These observations confirmed the sufficiency and necessity of this system in the infraslow modulation of sleep spindles and sigma activity that were related to NREM sleep substates with different levels of arousability [6]. We further showed that, mechanistically, these results were consistent with slow depolarizations from relay-sensory and reticular neurons in the thalamus as a response to NA release from LC terminals depending on β or α AR, respectively. Critical to the success of my Ph.D. project was the timing of optogenetic manipulation of LC neurons to specific time points determined by online monitoring and analysis of sleep, followed by closed-loop feedback to the optogenetic stimulation device. The implementation of closed-loop techniques has been essential in the real-time probing of the electrical activity patterns of the LC. The results showed that activation of LC cells targeting sigma's rising phase or inhibition during the descending phase of this signal reduced its fluctuations by suppressing or maintaining high levels of this activity and the generation of sleep spindles, respectively. Interestingly, the opposite manipulation (activation during descending and inhibition at ascending phases of sigma activity) entrained and organized these fluctuations. These results are best explained by a periodic activation of noradrenergic LC neurons on the infraslow timescale. In line with these observations, LC calcium activity was measured during NREM sleep, and the described dynamics support this hypothesis [160]. Given the recurrent raising patterns of Ca^{2+} , these authors proposed that these cells fire in a recurrent phasic instead of a low

tonic manner during NREM sleep.

I see these observations as my principal scientific contribution because it brings forward that natural activity patterns of a brain area sculpt the temporal heterogeneity of sleep. At the same time, I emphasize that it is essential to keep in mind that my work is a step towards a neuromodulatory description of sleep microarchitecture that likely concerns many brain areas. The LC itself projects profusely throughout the brain and interacts with other monoaminergic brain areas, such as the serotonergic dorsal raphe (for review, see [161]). Therefore, my work is a scientific contribution to the systems neuroscience of sleep neuromodulation and its behavioral correlates.

1.2 The noradrenergic LC system creates windows of opportunity for behavioral transitions

Since the 80s, the French researcher Claude Gottesmann and his team focused on the transitions between NREM and REM sleep in mammals [162]. He proposed the term “intermediate” stage (IS) for the 20 — 50 second period before the REM onset characterized by increased sigma activity and sleep spindles density predominately in the anterior cortex, together with elevated hippocampal theta in rats [162] and latter in cats [163], and mice [164] (See example in Figure 5A). Interestingly, this period resembled the brain state of animals that underwent an intercollicular midbrain transection [162, 165] which allowed him to suggest that probably *“activatory ascending influences from the brainstem, which modulate waking processes, gradually decrease during slow sleep and are the lowest during the intermediate stage, when the influences for paradoxical sleep are still negligible”*. Furthermore, since these early years, they hypothesize that given the similarities between this *“cerveau isolé”* preparation and the IS, the arousal threshold should be higher during this period compared to other moments during NREM sleep.

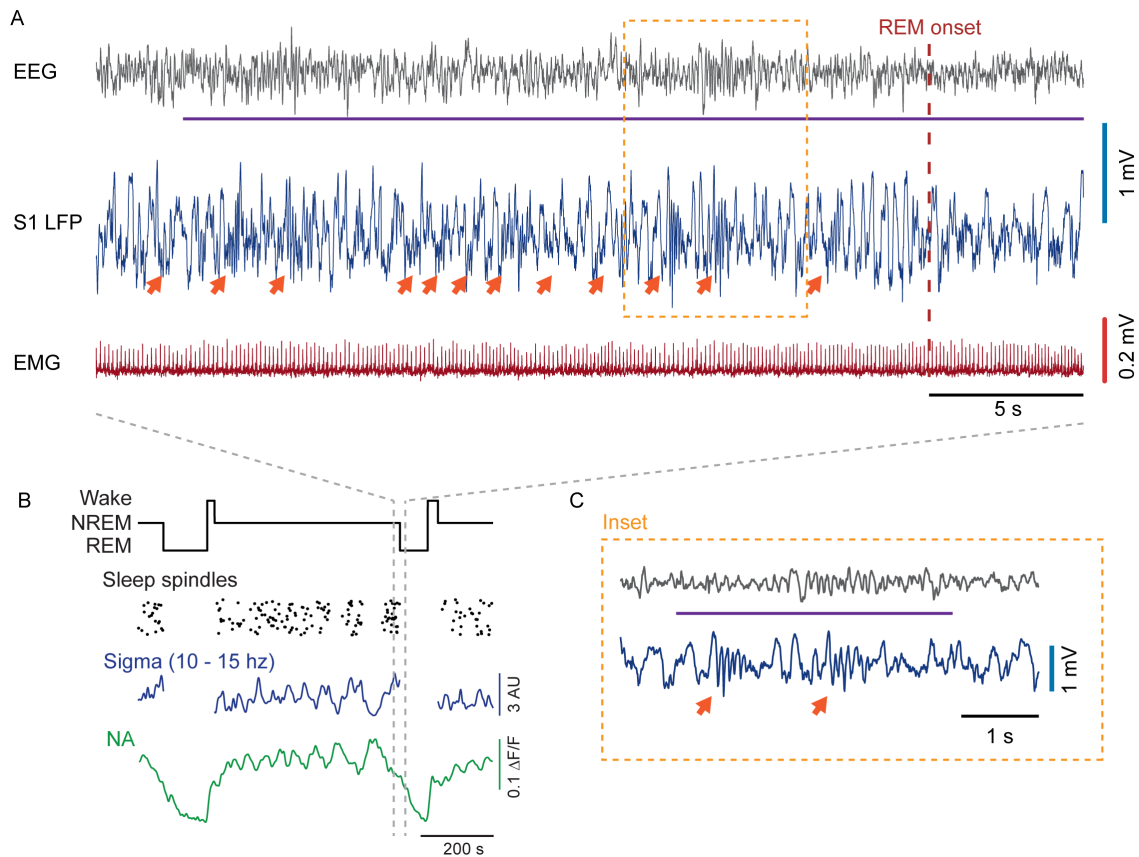


Figure 5: Intermediate sleep in mice. (A) An example of the intermediate stage in mice. Note the increase in sleep spindles in the local field potential (LFP) in the somatosensory cortex (S1) marked with the arrows and the increase of theta activity in the frontoparietal EEG highlighted with the horizontal purple line. The visually scored REM transition is marked with a vertical discontinuous line. The area denoted by the dotted square is expanded in (C). (B) From top to bottom: Hypnogram depicting the alternations between wake, NREM sleep, and REM sleep. Clustering of automatically detected sleep spindles depicted as scattered dots in time. Sigma (10 — 15 Hz) activity during NREM sleep. Relative fluorescence from a genetically encoded NA biosensor in the thalamus using fiber photometry. (C) Inset of the marked area in (A) showing an inset of the EEG and S1-LFP activity during intermediate sleep. The arrows point to sleep spindles in S1, and the purple vertical line indicates theta activity in the EEG.

Our experiments validated these observations. NREM-to-REM transitions are periods of high sigma and spindle activity. We further showed that these periods are causally associated with decreased NA levels in the thalamus that started to decay before REM onset in the same time-frame described for IS (Figure 5B). Furthermore, recurrent moments of low NA levels in the thalamus that creates periods of high spindle density were associated with increased arousability threshold during auditory stimulation [6] or

spontaneous MA [46]. A direct link between the noradrenergic LC unit activity and sensory-evoked awakenings during NREM sleep was causally confirmed by Hayat et al. [140]. Thus, the higher spindle density and arousability thresholds described by Gottesman *et al.* during IS are most probably related to the reduced NA levels in the thalamus here described. Other possible mechanisms might play a role in promoting the additional features of IS, such as the increase of theta activity. The latter was previously associated to hypothalamic [166, 167], and cholinergic activity [168]. Indeed, the activity of putative cholinergic neurons in tegmental nuclei is known to increase previous and during REM sleep [169, 170]

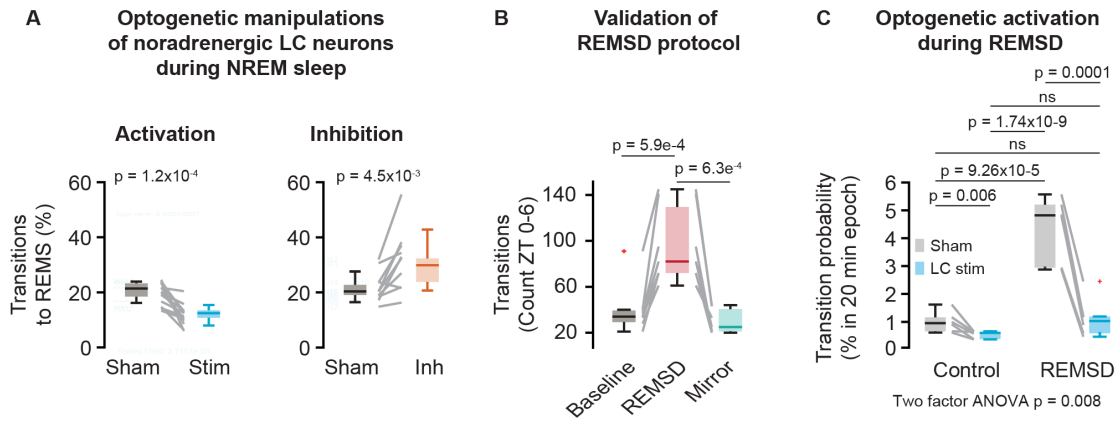


Figure 6: Modulating NREM-to-REM transitions. (A) Optogenetic activation (Left) or inhibition (Right) of noradrenergic LC neurons using a closed-loop targeting NREM sleep as in [39]. (B) NREM-to-REM transition count in the ZT0-6 light period for the validation of a REM sleep deprivation (REMSD) protocol. For this purpose, a DC-micromotor in the recording implant of the animals was activated after 10 s of automatic detection of REM sleep (based on EMG and EEG θ/δ ratio). (C) NREM-to-REM transition probability during REMSD or control condition (no REMSD) with concomitant optogenetic activation of noradrenergic LC neurons or sham stimulation (*ceteris paribus* with the stimulating LED off). Each 20 min stimulation period took place every 40 min in the ZT1-9 light period.

Furthermore, the noradrenergic LC system has been long related to playing a permissive function for REM sleep generation [90]. Consistent with this observation, optogenetic activation of noradrenergic LC neurons during NREM sleep, drastically reduced the NREM-to-REM transitions, and the opposite effect (increased transitions) was true for optogenetic inhibition of these cells during NREM sleep (Figure 6). Further experiments showed that the suppressing effect of optogenetic LC activation during NREM sleep holds under conditions of high REM sleep pressure (Figure 6B and 6C). In

these experiments, we increased REM sleep pressure by closed-loop-mediated REM sleep deprivation (REMSD) together with optogenetic stimulation of noradrenergic LC neurons during NREM sleep (Figure 6C). Activation of LC neurons during REMSD reduced the NREM-to-REM transitions to levels similar to those observed in the deprivation protocol. In line with these observations, electrical stimulation of the LC at low frequency (2 Hz) and intensity (200 μ A) reduced REM sleep [171]. These results suggest that the LC actively suppresses transitions into REM sleep so that solely LC activation could be enough to perform REMSD.

The regulation of NREM-to-REM transitions is a complex problem that involves multiple systems. Our results support the idea of a permissive role of the noradrenergic LC system in the NREM-to-REM transition. How the real-time dynamics of the noradrenergic LC system interact with other REM promoting, permissive, or suppressing regions to finally produce the transition is still unclear. Still, pharmacology experiments showed that noradrenergic signaling suppressed the activity of REM-promoting regions [172, 173]. Additionally, Franz Weber *et al.*, propose that ventral lateral Periaqueductal gray (vlPAG) GABAergic neurons play a critical role in the regulation of these transitions [174, 175]. By a series of experiments measuring and modulating these REM-off neurons [176], they showed that: 1. their activity was high after each REM sleep episode, correlated to the length of the previous REM bout. 2. optogenetic stimulation of these neurons suppressed REM sleep while their inhibition precipitated these transitions, similar to our observations with the noradrenergic LC neurons. 3. activity of GABAergic vlPAG neurons started high after REM sleeps and decayed during the following NREM sleep period until it reached values that facilitated REM sleep transition. Moreover, the period of high GABAergic vlPAG activity was also consistent with moments of low probability for NREM-to-REM transitions [175]. As a result, these authors proposed that GABAergic vlPAG neurons might reflect the emancipation of REM sleep pressure that also seemed to play an active role in regulating sleep cycles. If the activity of these neurons fluctuates during NREM sleep, or how they interact with the noradrenergic LC system is an open question. However, projections between these regions have been described. Thus, as a working hypothesis for future directions, fluctuations in noradrenergic LC activity might serve as a gate that allows transitions to REM sleep while keeping sensory vigilance during NREM sleep independent of GABAergic vlPAG activity. However, when the activity of this second population falls under a threshold **and** noradrenergic LC activity is reduced, REM promoting regions take over and initiate the transition to REM sleep, and possible further inhibition of noradrenergic LC neurons takes place (see Figure ??).

2 Technical contributions and limitations

2.1 Fiber photometry

As part of my Ph.D. process, I set up the *in-vivo* fiber photometry technique to monitor the real-time dynamics of NA in the thalamus across the sleep-wake cycle. To do that, I virally expressed a newly developed G-protein-coupled-receptor-activation-based NA (GRAB_{NE}) sensor in the cells of the dorsal thalamus. I used the basic principles of the technique to set up the control and acquisition of the fluorescent signal directly with the same system as for the other electrophysiological recordings, allowing direct synchronization throughout all registered signals. However, it is crucial to consider that this technology is recent and still emerging and interpreting the results should be taken with care. For instance, the measurements obtained by the photodetector are relative to the NA levels in the recorded area, and the measures might depend on the physical characteristics of the sampling region; therefore, absolute values of NA are unknown. Furthermore, intrinsic properties of the tissue or the sensor kinetics could generate fluorescent responses that are not specific to the levels of NA; therefore, different controls using non-noradrenergic responsive sensors or utilizing isosbestic light stimulation of the sensor, or replicating the experiment with a control virus, are recommended for future experiments. So far, in our lab, current control experiments using a similar fiber photometry approach, but with isosbestic light stimulation, fail to show fluctuations in the fluorescence during NREM sleep (See Figure 7). However, during REM sleep, a minor and not significant change is recorded, suggesting that possible features in the tissue might still produce artifacts in the recording.

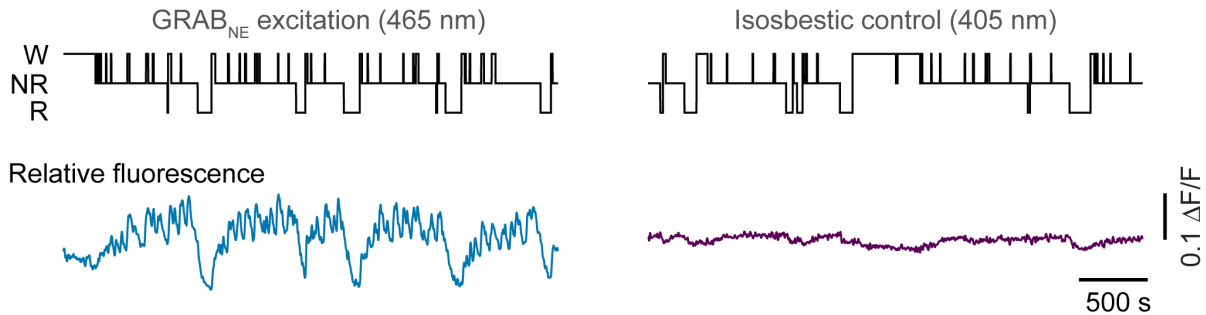


Figure 7: Example of relative fluorescence using a LED within the excitation band of the GRAB_{NE} biosensor (Right) or a LED with an Isosbestic bandwidth (Left) to control for non-noradrenergic related fluorescence. Note the lack of significant variations in the control experiment with the Isosbestic stimulation. Recordings from Najma Cherrad.

Additionally, the measure of NA levels in the thalamus does not necessarily reflect LC activity as NA can also be released in the forebrain from other noradrenergic brainstem

areas [63]. However, recently, Kjaerby et al. [160] measured concomitant Ca^{2+} from putative noradrenergic LC neurons and NA levels in the mPFC (Figure 8). Similar to our findings, these experiments showed recurrent increases in forebrain NA levels during NREM sleep that follows an increase in Ca^{2+} transients in LC neurons. Subsequently, relative silent periods of LC activity generated the infraslow fluctuating patterns of NA. In contrast to the idea of the low tonic activity of these cells during NREM sleep based on electrophysiological approaches [90, 93], the authors proposed that recurrent phasic activity of the noradrenergic LC population is responsible for the periodic release of NA.

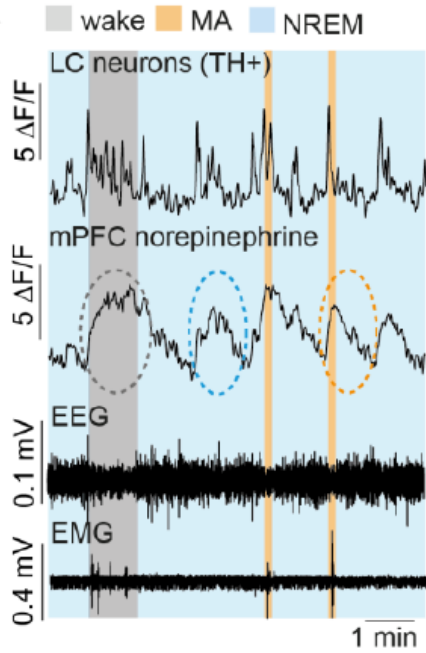


Figure 8: Representative traces depicting concomitant Ca^{2+} activity of tyrosine hydroxylase positive neurons (TH+) in the LC measured by fiber photometry followed by the relative fluorescence from a GRAB_{NE} sensor in the medial prefrontal cortex (mPFC). EEG and EMG activity was measured to assess the animal’s behavioral state. Note the increase of Ca^{2+} transients in LC neurons followed by the increases in NA. Figure 1C in [160].

2.2 *In-vivo* optogenetics

Among the most challenging yet stimulating techniques I learned and mastered during my Ph.D. project was the optogenetic and chemogenetic manipulation of genetically defined neuronal populations in specific brain areas. In this section, I will concentrate on the major observations and limitations of the optogenetic interrogation of noradrenergic LC activity during sleep. Here, I refined the surgical and manipulation procedures and designed the experiments. Additionally, I used closed-loop algorithms developed by Dr. Romain Cardis for different purposes and adapted them to my particular questions.

Optogenetic specific activation of noradrenergic LC neurons during NREM sleep using frequencies >5 Hz results in an immediate transition to wakefulness [98, 177, 178]. This effect depended on NA as genetic disruption of DBH in these neurons did not produce sleep-to-wake transitions upon similar optogenetic stimulation [178]. Moreover,

the probability of behavioral arrest with these manipulations highly depends on the stimulation parameters [177]. However, even at low frequencies, optogenetic stimulation of noradrenergic LC cells altered hippocampal delta and sigma activities during NREM sleep, disrupting the coupling between sleep spindles and hippocampal ripples [98]. Similar to this noradrenergic effect, Oikonomou et al. [179] showed that optogenetic “burst” (10 s of 25 Hz) activation of serotonergic DR cells reduces sleep time. However, tonic (12.5 min of 3 Hz) activation of the same population reduced REM sleep while increasing NREM sleep. In our work, direct optogenetic activation of noradrenergic LC neurons at 1 Hz, specifically during NREM sleep, consolidated this sleep state at the expense of both wakefulness and REM sleep.

Nonetheless, it is important to mention that artificial manipulation of cell populations does not necessarily recapitulate their natural activity. This concern is particularly relevant for the effect of optogenetic activation of LC neurons in the coordination of cortical sigma activity and heart rate. We showed that activation during NREM sleep disrupted the phase relation of these two signals while stimulation during low sigma activity entrained and increased the anticorrelation. The effect in the first scenario did not seem to increase the heart rate, while the second one produced this effect. This result suggests that alternative or complementary compensatory mechanisms could be involved in this outcome. Still, peripheral manipulation of heart rate through pharmacological agents acting on the parasympathetic or the sympathetic cardiac output did not seem to affect sigma fluctuations. Thus, “top-down” rather than “bottom-up” cardiac mechanisms are more likely to play a role in this coordination.

Concerning the effect of the noradrenergic modulation on spindle clustering, the results from the pharmacological and time-locked optogenetic manipulation to different levels of sigma activity are best explained by a periodic increase in noradrenergic LC neuronal activity on an infraslow timescale that releases NA in the thalamus. Consistent with this observation, Kjaerby et al. [160] described recurrent increases of putative noradrenergic LC Ca^{2+} activity followed by silent periods of these neurons that alternate on a multi-second timescale during NREM sleep.

Finally, optogenetic inhibition of noradrenergic LC neurons during NREM sleep disrupted the fluctuations in sigma activity and increased spindle density. When performed at moments of ascending sigma activity using a closed-loop algorithm, the inhibition regularized and maintained the fluctuations in sigma activity in the somatosensory cortex resembling the observations of optogenetic activation of these neurons during the descending phase of sigma. One possibility for this result is that the cessation of inhibition could result in a rebound released of NA that imposes the fluctuation. Ramp-like termination of the optogenetic manipulations has been proposed

as a possible alternative for this problem in LC populations [52]. Thus, future experiments should take this into account to confirm these observations. Still, taking into account the Ca^{2+} activity pattern of noradrenergic LC neurons [160], it is still possible that in natural conditions, infralow fluctuations in forebrain NA might represent the release of inhibition upon LC neurons.

3 Broadening the view on neuromodulation during sleep

Naturally, alternative or complementary mechanisms could also be involved in regulating infralow changes in physiological and electrophysiological activity during NREM sleep. Furthermore, additional top-down, bottom-up, or autoregulatory mechanisms could interact with or modulate LC activity to produce these fluctuations. In this chapter, I outline some of these possibilities.

3.1 Other neuromodulators during NREM sleep

Other monoamines have been previously linked to the regulation of the sleep-wake cycle [10, 180–182]. Additionally, the activity of other monoaminergic neurons might fluctuate on infralow timescales. For example, Oikonomou et al. [179] showed that Ca^{2+} transients of serotonergic DR neurons seem to fluctuate on an infralow timescale. Furthermore, the dynamics of serotonin levels in the forebrain and hindbrain also exhibited an infralow oscillatory patterns within NREM sleep when measured using a similar approach to the present study [183]. Reciprocal interconnections between the DR and the LC have been previously described [184]. Moreover, serotonin was sufficient to reduce spindle generating activity in the thalamus [158], and fluctuation in DR Ca^{2+} were correlated to different levels of arousal in mice. How these serotonergic and noradrenergic systems interact to produce the observations we report in this work is still an open question. However, the results from the specific *in-vivo* pharmacology and the optogenetic manipulations suggest that, at least for the clustering of the sleep spindles and the fluctuation in sigma, NA is a decisive protagonist.

Genetically encoding sensors for other monoamines and other sleep-modulating molecules such as dopamine [185], acetylcholine [186], or oxytocin [187] have been developed, and novel versions of these biosensors, including those for NA, are being created. These advances will expand the range sensitivity of the sensors to monitor these molecules with different kinetic resolutions, an essential condition for the real-time resolution required to study their dynamics in sleep. Worth mentioning in this context is the recent finding from Hasegawa et al. [188] relating dopamine levels in the amygdala as a crucial element in the REM sleep transition. Further studies recording one or multiple

molecules at different sites will help elucidate the real-time neuromodulatory mechanisms of sleep regulation.

3.2 Possible regulation of noradrenergic LC fluctuations during NREM sleep

Fluctuations in LC activity can arise from different interactions with other systems in the forebrain, the hindbrain, or other parameters in the body. For instance, “top-down” regulation of LC activity has been suggested to play a critical role in engaging vigilance during wakefulness [142]. During NREM sleep, sleep spindles have been proposed to engage LC activity [90, 98] presumably in a top-down manner throughout fronto-cerulean pathways. Additionally, the optogenetic activation of thalamic reticular neurons increased sleep spindles and promoted NREM-to-REM sleep transitions [189]. Although the termination of individual sleep spindles seems a rather improbable possibility, given the time-course of action of NA in the thalamus, the recruitment of noradrenergic LC neurons could indeed respond to forebrain activity in a manner that does regulate the infraslow organization of sleep spindles in the cortex. Furthermore, in addition to engaging this noradrenergic system, these top-down mechanisms could also recruit REM-promoting regions that facilitate transitions to this sleep state. Further research in this direction, such as optogenetic modulation of cortico-cerulean terminals during NREM sleep, could address these questions directly.

Similarly, “bottom-up” mechanisms can modulate the activity of noradrenergic LC neurons [190, 191] and produce widespread activation of the cortex [146]. Although peripheral pharmacological modulation of the autonomic tone did not seem to affect infraslow fluctuations in the sigma power in the brain [39], increases in NA in the cortex and hippocampus were observed upon electrical stimulation of vagal nerve afferents [192]. Thus, peripheral changes in bodily activity should not be discarded as a possible complementary mechanism in the electrophysiological close-to-minute variations of LC activity during NREM sleep. Moreover, changes in the infraslow components of the full band EEG in anesthetized cats have been related to variations in inhaled CO₂ [193]. The LC is widely known for its chemosensing properties [194]. Small changes in pH can strongly modulate LC firing activity [195]. This effect has mainly been related to the LC role in respiration [196]. However, variations in respiration during NREM sleep can also interact with the ongoing LC activity in the multi-second timescale.

Other mechanisms could also be involved in the infraslow organization of NREM sleep. For instance, spontaneous infraslow oscillations in the membrane potential of thalamic [197], cortical [136], DR and LC [135] cells have been previously described and been associated to regulatory mechanisms in health and disease. Likewise, infraslow fluctuations in extracellular ATP [198] –thought to be regulated by multi-second

brain and body parameters on these timescales is an open question.

4 Impact and perspectives

This chapter summarizes how my thesis could influence future experimentation in the field (some of them summarized in Figure 10). The first part will give an overview of the possible role of the noradrenergic LC system during NREM sleep in sleep-related memory consolidation and the modulation of general arousability and sensory processing during sleep. Then, I will discuss the possibility that the natural fluctuations in NA during NREM sleep could regulate neurovascular coupling in health and its possible relation with neurodegenerative disorders. Finally, in a different sub-chapter, I will discuss the potential implications of my work in conditions where abnormal arousability levels are a defining feature, such as insomnia or stress-related disorders. Further comprehensive considerations are covered in [161].

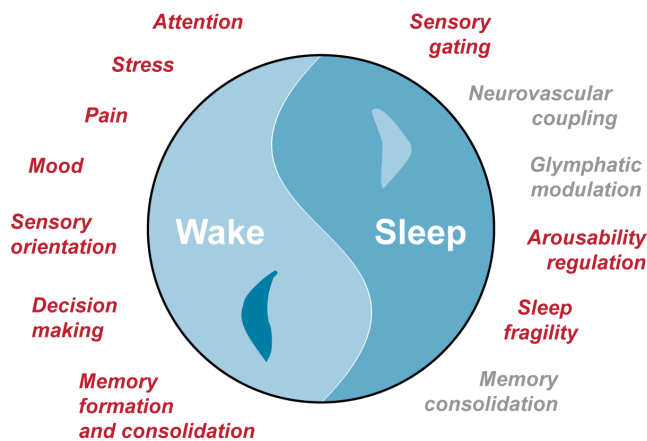


Figure 10: Scheme summarizing current (red) and yet-to-test (gray) functions of the noradrenergic LC system in wake and sleep.

4.1 General impacts and perspectives of this work

Sensory gating and arousability: A defining feature of sleep is that it is “easily” reversible. This is a distinctive behavioral feature compared to coma or anesthesia. Furthermore, the fact that sleeping animals still respond to external stimuli adds an adaptive element to this behavioral state because the organism reacts to environmental changes that can represent a danger. Still, continuity of sleep is essential for its beneficial and restorative effects [202–204]. From its initial descriptions, the coordinated infraslow fluctuations in sigma activity, heart rate, and pupil diameter during NREM sleep were related to a higher probability of evoked [6, 45] or spontaneous [46] arousal events. Interestingly, an independent study [140] also showed that the probability of provoking awakenings upon short (1 s) auditory stimulation was sensitive to the natural or artificially-modulated activity of LC neurons.

This is consistent with previous studies linking the LC unit activity to sleep-to-wake transitions [205]. NA production was directly associated with maintaining arousal states, even when the animals were exposed to salient stressful stimuli [178].

The observations from my thesis work demonstrated that periodic increases in LC activity render NREM sleep to recurrent states that facilitate vigilance. This suggests the existence of NREM sleep substates with differential brain information processing properties. Consistent with these results, Seibt et al. [206] showed that Ca^{2+} activity in cortical dendrites increased during spindle periods during mouse NREM sleep. Moreover, the cortico-cortical transmission of auditory sensory information measured by the strength of the response to acoustic stimulation differs between distinct behavioral states [207].

Given the different behavioral outcomes associated with the NA fluctuations in the thalamus, future studies should focus on the differential subcortical and cortical responses to sensory stimuli across the LC-activity-defined substates described here. In a first pilot in this direction, I analyzed the evoked response to short auditory tones (10 ms; pure-tone stimulation) in the primary auditory and somatosensory cortices (Figure 11). The amplitude of the evoked potentials changed not only between NREM and wake but also between high and low levels of sigma activity. Further analysis of the evoked potentials to tones and to different types of stimuli could give a further mechanistic understanding of the possible role of noradrenergic signaling in sensory processing during sleep.

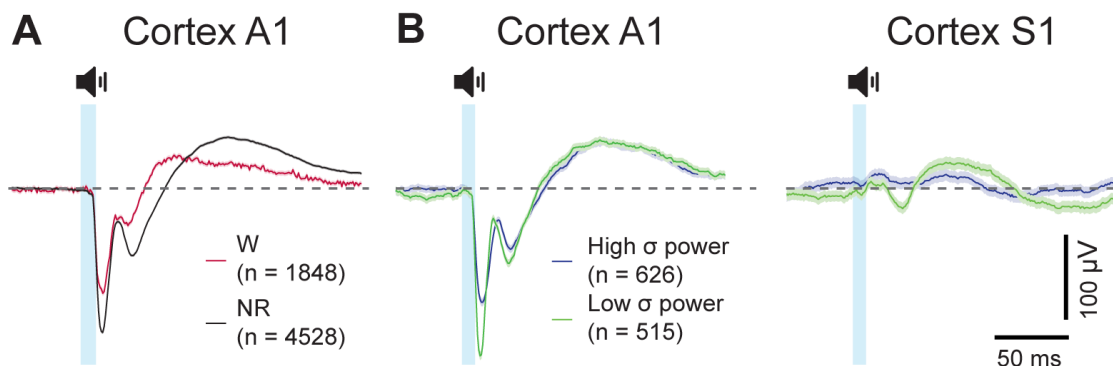


Figure 11: Auditory evoked response during wakefulness and NREM sleep. (A) Auditory evoked related potentials of primary auditory cortex (A1) to 10 ms pure-tone stimulation (Light blue shaded area) during wakefulness (W) and NREM sleep (NR). (B) Auditory evoked response from A1 and primary somatosensory (S1) areas in periods of high and low sigma (σ) power during NREM sleep. The traces summarize multiple sessions of a single animal ($n = 1$).

Memory consolidation: The LC activity has proven to be crucial in forming memories [208]. The manipulation of LC activity across multiple hippocampal regions has shown

the sufficiency and necessity of this neuromodulatory system in creating and maintaining memories [209–211].

The release or co-release of dopamine from the LC in the hippocampus and its role in the stability of hippocampal-dependent memories [209] further increase the interest in LC activity during NREM sleep and is a possible role in memory consolidation. Additionally, other types of co-release mechanisms from the LC have been related to different learning processes. For instance, Yang et al. [212] showed that glutamate and NA co-release in the parabrachial nucleus is essential for the modulation of amygdala signaling in this area to code for behavioral adaptations mediated by fearful memories.

Interestingly, the stimulation of LC activity during post-learning sleep was detrimental to sleep-dependent memory consolidation processes [98, 213]. However, these manipulations occurred across NREM sleep episodes without considering the infraslow variations in LC activity within this heightened state. As proposed by Antony et al. [7] for the case of auditory cue reactivation in relation to the sleep spindles, alternations between spindle dense and free periods could be equally crucial for different sleep-dependent memory consolidation processes.

Neurovascular coupling and neurodegenerative disorders: Possibly, one of the most promising impacts of these observations is related to the noradrenergic modulation of the neurovascular coupling and its possible role in the elimination of noxious aggregates in the brain during sleep. NA is a major regulator of microvasculature in the brain [214]. Also, it has been proposed to play a crucial role in coordinating different cell types to increase and regulate brain processes such as plasticity and inflammatory response [215]. In addition, the glymphatic system that consists of the perivascular space created by astrocytes and vascular endfeet is thought to facilitate the clearing of harmful molecules and aggregates during NREM sleep [216]. Consistent with these observations, infraslow fluctuations in BOLD activity and cerebrospinal fluid flux were correlated to variations in slow-wave activity in human NREM sleep [217]. Therefore, alternations in LC activity during this period might regulate the coordination of neuronal and neurovascular processes during this sleep state.

The role of the LC in modulating the neurovascular system and the possible association to “brain clearing” was proposed to play critical roles in Alzheimer’s disease (AD) pathophysiology [214]. Moreover, the LC is among the first areas that show hyperphosphorylated- τ -protein aggregation in AD patients far before the clinical appearance of symptoms [218]. Therefore, the structural integrity of LC was suggested as an early marker for the prompt diagnosis of this disorder [219]. Interestingly, sleep alterations were noticed parallel to LC deterioration but previous to the cognitive decline in AD [220, 221]. It is unknown whether LC alterations predispose AD or if

another pathophysiological feature of the disorder precedes the integrity decline of this noradrenergic system. However, stimulation of LC activity alone can rescue learning deficits in murine AD models [222].

As part of my thesis, I relate infraslow fluctuations in electrophysiological sleep rhythms and heart rate variations to noradrenergic LC activity in the brain. These markers can be measured in a non-invasive manner and have been described in humans. Therefore, the study of infraslow fluctuations during sleep in AD patients and animal models of AD could represent a niche of study for potential diagnosis criteria in the early detection of this neurodegenerative disorder.

4.2 Implications in hyperaroused brain states

Arousal, as the physiological and psychological state of being awake or responsive to external stimuli, is modulated by multiple systems that include, but are not limited to, the serotonergic, dopaminergic, cholinergic, and noradrenergic brainstem systems, the histamine and orexinergic systems in the hypothalamus and thalamocortical circuits [223]. All of them define particular features of arousal. In this chapter, I focus on the noradrenergic LC system in the regulation of arousal during NREM sleep. Interestingly, NA has been related to arousal since the beginning of the neurobiological characterization of the state in 1949 [224]. However, it was not until 1955 when the publication that made the LC highly recognizable came along [225], and more than twenty years had to pass before the noradrenergic nature of LC neurons was discovered [226–228].

We can think of arousal as a continuum rather than a discrete state. *i.e.* there are levels of arousal rather than a dichotomy between being or not aroused. Among the high levels of this continuum, there is stress which is the physiological response to stimuli that represents an unpredictable and uncontrollable challenge to the organism [229]. This response, when excessive, is related to a hyperactivity of the LC noradrenergic system that exhibits particular sleep signatures that includes a reduction of deep slow-wave sleep and increased phasic REM density (for review, see [230] and Figure 12A). During these REM periods, increased noradrenergic LC signaling is thought to produce abnormal potentiation of aversive memories compared to healthy sleep, where periods of LC silence allow for depotentiation of these negative memory traces. Similar alterations in REM sleep were described for hyperarousal-related sleep disorders like insomnia, where the name of “restless REM” has been proposed [231] (see Figure 12B). Other particular features of the LC are interesting to understanding pathological forms of arousal during sleep. For instance, the sex-specific genomic footprint in the LC is among the highest in the brain, with over 100 genes differentially expressed between males and females [66], making it an excellent candidate for understanding biological differences in psychiatric disorders

such as anxiety or insomnia where a predisposition for these conditions is significantly higher in women [232].

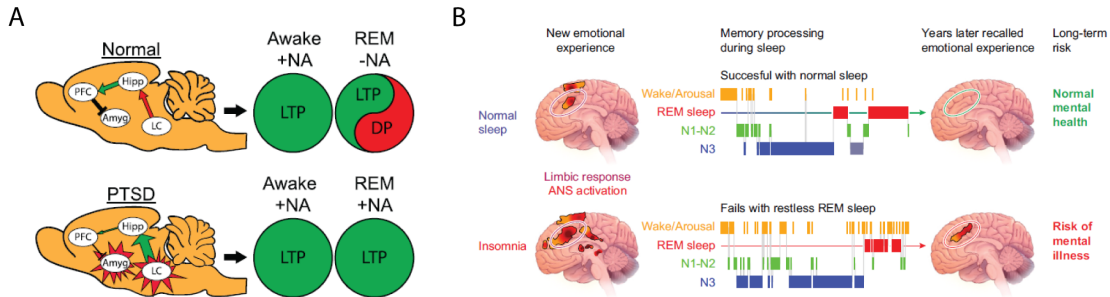


Figure 12: The locus coeruleus (LC) and hyperarousal brain states. (A) Representative model comparing LC activity in healthy sleep and in patients (or models) of post-traumatic stress disorder (PTSD). Figure 1 in [230]. (B) Graphical abstract in [231] representing the association between restless REM sleep and insomnia.

The decline of noradrenergic LC signaling during REM sleep has been suggested to be a prerequisite for emotional discharge in limbic circuits [231]. In this context, the LC activity during sleep has been hypothesized to serve as a mechanism of dissociation between the declarative or semantic elements of an experience and its related arousal or emotional correlates. The new evidence regarding the dynamics of NA signaling in the forebrain during the sleep-wake cycle advocates for a bidirectional role of the LC in this process. High and fluctuating levels of NA in NREM sleep may support semantic memory consolidation processes. In contrast, the low levels during REM sleep could promote synaptic depotentiation and downscaling negative memory traces. Thus, aberrant noradrenergic activity during REM sleep in subjects with insomnia may contribute to maladaptive representations of emotional experiences. These observations align with classic results from other neurological disorders related to emotional unbalance. For instance, both humans and rodents significantly improved depressive symptoms after multiple days of REM sleep deprivation [233] (for review see [234]). Surprisingly, subjects that did not respond to this treatment also did not improve with antidepressant drugs that reduced REM sleep [233]. Hence, one mechanism for which antidepressant drugs are thought to help resolve depressive symptoms is their impact on REM sleep, particularly long REM sleep bouts with a significant reduction of NA levels in the forebrain.

5 Closing remarks

We sleep with the same brain that we use when we are awake. Behavioral states emerge from the complex interaction between multiple systems, among which neuromodulation

has always played critical roles [235]. NREM sleep is defined by its behavioral, electrophysiological, and physiological features. Among them, reversibility and response to external (or internal) stimuli are defining behavioral attributes, and the appearance of sleep spindles and delta activity is at the core of the electrophysiological ones. The experiments performed in this thesis advance the understanding of how these features are organized across time during NREM sleep. In my thesis, I brought an engineering perspective to the questions here addressed and adopted a systems neuroscience approach, used tools in electrophysiology and neurobiology to conclude that the noradrenergic LC system, a system previously associated almost exclusively with wakefulness, is part of the foundations of temporal heterogeneity in behavioral and electrophysiological characteristics of NREM sleep.

My work is, then, one step toward understanding the real-time dynamics and function of neuromodulation in the sleeping brain. It is a mechanistic attempt to refine the ideas of the scientists that inspired me into the field with a dynamic and continuous eye [2]. This work has possible important implications in the fields of cognitive and sensory processes during sleep and in the understanding of the pathophysiology of disorders where altered arousability levels are a defining feature, such as in the case of excessive stress or insomnia. Likewise, these results can be used in conditions where the LC integrity is affected, like in the case of neurodegenerative disorders, particularly AD.

Publication list

- G. Katsioudi, **A. Osorio-Forero**, F. Sinturel, C. Hagedorn, F. Kreppel, U. Schibler, and D. Gatfield. Recording of Diurnal Gene Expression in Peripheral Organs of Mice Using the RT-Biolumicorder. *In Circadian Regulation*. Pages 217-242. Humana, New York, NY, 2022
- **A. Osorio-Forero**, N. Cherrad, L. Banterle, L.M.J. Fernandez, and A. Lüthi. When the locus coeruleus speaks up in sleep: recent insights, emerging perspectives. *Int. J. Mol. Sci*, 23(9): 5028, 2022.
- **A. Osorio-Forero**, R. Cardis, G. Vantomme, A. Guillaume-Gentil, G. Katsioudi, C. Devenoges, L.M.J. Fernandez, A. Lüthi. Noradrenergic circuit control of non-REM sleep substates. *Curr. Biol.*, 31(22): 5009-5023, 2021.
- S.S. Holden, f.f. Grandi, O. Aboubakr, B. Higashikubo, F.S. Cho, A.H. Chang, **A. Osorio-Forero**, A.R. Morningstar, v. Mathur, L.J. Kuhn, ... J. Paz. Complement factor C1q mediates sleep spindle loss and epileptic spikes after mild brain injury. *Science*, 373(6560): p.eabj2685, 2021.
- R. Cardis, S. Lecci, L.M.J. Fernandez, **A. Osorio-Forero**, P. Chu Sin Chung, S. Fulda, I. Decosterd, and A. Lüthi. Corticoautonomic local arousals and heightened somatosensory arousability during nrems of mice in neuropathic pain. *Elife*, 10:e65835, 2021.
- G. Vantomme G, **A. Osorio-Forero**, A. Lüthi, L.M. Fernandez. Regulation of local sleep by the thalamic reticular nucleus. *Frontiers in Neuroscience*. 13:576. 2019.
- L.M.J. Fernandez, G. Vantomme, **A. Osorio-Forero**, R. Cardis, E. Beard, and A. Lüthi. Thalamic reticular control of local sleep in mouse sensory cortex. *Elife*, 7:e39111, 2018.

References

- [1] I. Newton. Isaac newton letter to robert hooke, 1675. *Simon Gratz collection. Digital Library. Retrieved from <https://digitallibrary.hsp.org/index.php/Detail/objects/9792>*, 2019.
- [2] P Halasz and R Bodizs. *Dynamic structure of NREM sleep*. Springer Science & Business Media, 2012.
- [3] M.G. Terzano and L. Parrino. Origin and significance of the cyclic alternating pattern (cap). *Sleep Med. Rev.*, 4(1):101–123, 2000.
- [4] L.M.J. Fernandez and A. Lüthi. Sleep spindles: mechanisms and functions. *Physiol. Rev.*, 100(2):805–868, 2020.
- [5] P. Halász, M. Terzano, L. Parrino, and R. Bódizs. The nature of arousal in sleep. *J. Sleep Res.*, 13(1):1–23, 2004.
- [6] S. Lecci, L.M.J. Fernandez, F.D. Weber, R. Cardis, J. Chatton, J. Born, and A. Lüthi. Coordinated infraslow neural and cardiac oscillations mark fragility and offline periods in mammalian sleep. *Sci. Adv.*, 3(2):e1602026, 2017.
- [7] J.W. Antony, L. Piloto, M. Wang, P. Pacheco, K. A Norman, and K.A. Paller. Sleep spindle refractoriness segregates periods of memory reactivation. *Curr. Biol.*, 28(11):1736–1743, 2018.
- [8] E. Aserinsky and N. Kleitman. Regularly occurring periods of eye motility, and concomitant phenomena, during sleep. *Science*, 118(3062):273–274, 1953.
- [9] M. Jouvet. Paradoxical sleep—a study of its nature and mechanisms. *Prog. Brain Res.*, 18:20–62, 1965.
- [10] M. Jouvet. Sleep and serotonin: an unfinished story. *Neuropsychopharmacology*, 21(2):24S–27S, 1999.
- [11] S. Chokroverty. An overview of sleep. *Sleep Med.*, pages 7–16, 1994.
- [12] D.R. Samson and C.L. Nunn. Sleep intensity and the evolution of human cognition. *Evol. Anthropol.*, 24(6):225–237, 2015.
- [13] L.M.J. Fernandez, G. Vantomme, A. Osorio-Forero, E. Cardis, R. and Béard, and A. Lüthi. Thalamic reticular control of local sleep in mouse sensory cortex. *Elife*, 7:e39111, 2018.

- [14] M. Steriade. Grouping of brain rhythms in corticothalamic systems. *Neuroscience*, 137(4):1087–1106, 2006.
- [15] G Buzsaki. *Rhythms of the Brain*. Oxford university press, 2006.
- [16] B.O Watson. Cognitive and physiologic impacts of the infraslow oscillation. *Front. Syst. Neurosci.*, page 44, 2018.
- [17] J.P. Schieber, A. Muzet, and P.J. Ferriere. Phases of spontaneous transitory activation during normal sleep in humans. *Arch. Sci. Physiol.*, 25(4):443–465, 1971.
- [18] M. Terzano, D. Mancina, M.R. Salati, G. Costani, A. Decembrino, and L. Parrino. The cyclic alternating pattern as a physiologic component of normal nrem sleep. *Sleep*, 8(2):137–145, 1985.
- [19] C Vanderwolf. Limbic-diencephalic mechanisms of voluntary movement. *Psychol. Rev.*, 78(2):83, 1971.
- [20] B. Jarosiewicz and W.E. Skaggs. Level of arousal during the small irregular activity state in the rat hippocampal eeg. *J. Neurophysiol.*, 91(6):2649–2657, 2004.
- [21] H. Miyawaki, Y.N. Billeh, and K. Diba. Low activity microstates during sleep. *Sleep*, 40(6), 2017.
- [22] J Ehrhart and A Muzet. Frequency and duration of transitory activation phases during normal or disturbed sleep in man. *Arch. Sci. Physiol.*, 28(3):213–260, 1974.
- [23] P. Halász. The microstructure of sleep. *Suppl Clin Neurophysiol.*, 57:521–533, 2004.
- [24] S. Vanhatalo, J. Voipio, and K. Kaila. Full-band eeg (fbeeg): an emerging standard in electroencephalography. *Clin. Neurophysiol.*, 116(1):1–8, 2005.
- [25] M.G. Terzano, L. Parrino, . Smerieri, R. Chervin, S. Chokroverty, C. Guilleminault, M. Hirshkowitz, M. Mahowald, H. Moldofsky, A. Rosa, et al. Atlas, rules, and recording techniques for the scoring of cyclic alternating pattern (cap) in human sleep. *Sleep Med.*, 3(2):187–199, 2002.
- [26] L. Parrino, R. Ferri, O. Bruni, and M.G. Terzano. Cyclic alternating pattern (cap): the marker of sleep instability. *Sleep Med. Rev.*, 16(1):27–45, 2012.
- [27] I.Q. Whishaw and C. Vanderwolf. Hippocampal eeg and behavior: change in amplitude and frequency of rsa (theta rhythm) associated with spontaneous and learned movement patterns in rats and cats. *Behav. Biol.*, 8(4):461–484, 1973.

- [28] B. Jarosiewicz, B.L. McNaughton, and W.E. Skaggs. Hippocampal population activity during the small-amplitude irregular activity state in the rat. *J. Neurosci. Res.*, 22(4):1373–1384, 2002.
- [29] B. Jarosiewicz and W.E. Skaggs. Hippocampal place cells are not controlled by visual input during the small irregular activity state in the rat. *J. Neurosci. Res.*, 24(21):5070–5077, 2004.
- [30] B.O. Watson, D. Levenstein, J.P. Greene, J.N. Gelinias, and G. Buzsáki. Network homeostasis and state dynamics of neocortical sleep. *Neuron*, 90(4):839–852, 2016.
- [31] D. Picchioni, S.G. Horowitz, M. Fukunaga, W.S. Carr, J.A. Meltzer, T.J. Balkin, J.H. Duyn, and A.R. Braun. Infralow eeg oscillations organize large-scale cortical–subcortical interactions during sleep: a combined eeg/fmri study. *Brain Res.*, 1374:63–72, 2011.
- [32] S. Vanhatalo, J. M. Palva, M.D. Holmes, J.W. Miller, J. Voipio, and K. Kaila. Infralow oscillations modulate excitability and interictal epileptic activity in the human cortex during sleep. *PNAS*, 101(14):5053–5057, 2004.
- [33] G. Pfurtscheller. Ultralangsame schwankungen innerhalb der rhythmischen aktivität im alpha-band und deren mögliche ursachen. *Pflügers. Archiv.*, 367(1):55–66, 1976.
- [34] D.A. Leopold, Y. Murayama, and N.K. Logothetis. Very slow activity fluctuations in monkey visual cortex: implications for functional brain imaging. *Cereb. Cortex* ., 13(4):422–433, 2003.
- [35] K. Linkenkaer-Hansen, V.V. Nikouline, J.M. Palva, and R.J. Ilmoniemi. Long-range temporal correlations and scaling behavior in human brain oscillations. *J. Neurosci. Res.*, 21(4):1370–1377, 2001.
- [36] A.L. Ko, F. Darvas, A. Poliakov, J. Ojemann, and L.B. Sorensen. Quasi-periodic fluctuations in default mode network electrophysiology. *J. Neurosci. Res.*, 31(32):11728–11732, 2011.
- [37] P. Achermann and A.A. Borbely. Low-frequency (≤ 1 hz) oscillations in the human sleep electroencephalogram. *Neuroscience*, 81(1):213–222, 1997.
- [38] Y. Nir, R. Mukamel, I. Dinstein, E. Privman, M. Harel, L. Fisch, H. Gelbard-Sagiv, S. Kipervasser, F. Andelman, M. Y Neufeld, et al. Interhemispheric correlations of slow spontaneous neuronal fluctuations revealed in human sensory cortex. *Nat. Neurosci.*, 11(9):1100–1108, 2008.

- [39] A. Osorio-Forero, R. Cardis, G. Vantomme, A. Guillaume-Gentil, G. Katsioudi, C. Devenoges, L.M.J. Fernandez, and A. Lüthi. Noradrenergic circuit control of non-rem sleep substates. *Curr. Biol.*, 31(22):5009–5023, 2021.
- [40] Z.I. Lázár, D.J. Dijk, and A.S. Lázár. Infralow oscillations in human sleep spindle activity. *J. Neurosci. Res. methods*, 316:22–34, 2019.
- [41] F.D. Weber, G.G. Supp, J.G. Klinzing, M. Mölle, A.K. Engel, and J. Born. Coupling of gamma band activity to sleep spindle oscillations—a combined eeg/meg study. *NeuroImage*, 224:117452, 2021.
- [42] M. De Luca, C.F Beckmann, N De Stefano, P.M. Matthews, and SM Smith. fmri resting state networks define distinct modes of long-distance interactions in the human brain. *Neuroimage*, 29(4):1359–1367, 2006.
- [43] M. Boly, V. Perlberg, G. Marrelec, M. Schabus, S. Laureys, J. Doyon, M. Pélégrini-Issac, P. Maquet, and H. Benali. Hierarchical clustering of brain activity during human nonrapid eye movement sleep. *PNAS*, 109(15):5856–5861, 2012.
- [44] M. Fukunaga, S.G. Horovitz, P. van Gelderen, J.A. Zwart, J.M. Jansma, V.N. Ikonomidou, R. Chu, R.H.R. Deckers, D.A. Leopold, and J.H. Duyn. Large-amplitude, spatially correlated fluctuations in bold fmri signals during extended rest and early sleep stages. *Magn. Res. Imag.*, 24(8):979–992, 2006.
- [45] Ö. Yüzgeç, M. Prsa, R. Zimmermann, and D. Huber. Pupil size coupling to cortical states protects the stability of deep sleep via parasympathetic modulation. *Curr. Biol.*, 28(3):392–400, 2018.
- [46] S. Cardis, R. and Lecci, L.M.J Fernandez, A. Osorio-Forero, P.C.S. Chung, S. Fulda, I. Decosterd, and A. Lüthi. Cortico-autonomic local arousals and heightened somatosensory arousability during nrems of mice in neuropathic pain. *Elife*, 10:e65835, 2021.
- [47] A. Boutin and J. Doyon. A sleep spindle framework for motor memory consolidation. *Philos. Trans. R. Soc. B*, 375(1799):20190232, 2020.
- [48] T. Maeda. The locus coeruleus: history. *J. Chem. Neuroanat.*, 18(1-2):57–64, 2000.
- [49] T.T. Dang-Vu, M. Schabus, M. Desseilles, G. Albouy, M. Boly, A. Darsaud, S. Gais, G. Rauchs, V. Sterpenich, G. Vandewalle, et al. Spontaneous neural activity during human slow wave sleep. *Proc. Natl. Acad. Sci. USA*, 105(39):15160–15165, 2008.

- [50] Y. Sharma, T. Xu, W.M. Graf, A. Fobbs, C.C. Sherwood, P.R. Hof, J.M. Allman, and K.F. Manaye. Comparative anatomy of the locus coeruleus in humans and nonhuman primates. *J. Comp. Neurol.*, 518(7):963–971, 2010.
- [51] V. Chan-Palay and E. Asan. Quantitation of catecholamine neurons in the locus coeruleus in human brains of normal young and older adults and in depression. *J. Comp. Neurol.*, 287(3):357–372, 1989.
- [52] V. Breton-Provencher and M. Sur. Active control of arousal by a locus coeruleus gabaergic circuit. *Nat. Neurosci.*, 22(2):218–228, 2019.
- [53] V. Breton-Provencher, G.T. Drummond, and M. Sur. Locus coeruleus norepinephrine in learned behavior: anatomical modularity and spatiotemporal integration in targets. *Front. Neural Circuits*, 15, 2021.
- [54] S.E. Loughlin, S.L. Foote, and F.E. Bloom. Efferent projections of nucleus locus coeruleus: topographic organization of cells of origin demonstrated by three-dimensional reconstruction. *Neuroscience*, 18(2):291–306, 1986.
- [55] N.K. Totah, Ricardo M Neves, and N.K. and Eschenko O. Panzeri, Stefano and Logothetis. The locus coeruleus is a complex and differentiated neuromodulatory system. *Neuron*, 99(5):1055–1068, 2018.
- [56] N.K.B Totah, N.K. Logothetis, and O. Eschenko. Noradrenergic ensemble-based modulation of cognition over multiple timescales. *Brain Res.*, 1709:50–66, 2019.
- [57] P.R. Manger and O. Eschenko. The mammalian locus coeruleus complex—consistencies and variances in nuclear organization. *Brain Sci.*, 11(11):1486, 2021.
- [58] G. Goldman and P.D. Coleman. Neuron numbers in locus coeruleus do not change with age in fisher 344 rat. *Neurobiol. Aging*, 2(1):33–36, 1981.
- [59] R.R. Sturrock and K.A. Rao. A quantitative histological study of neuronal loss from the locus coeruleus of ageing mice. *Neuropathol. Appl. Neurobiol.*, 11(1):55–60, 1985.
- [60] R. Von C, B. Thomas, J.M. Savitt, K.L. Lim, M. Sasaki, E.J. Hess, V.L. Dawson, and T.M. Dawson. Loss of locus coeruleus neurons and reduced startle in parkin null mice. *PNAS*, 101(29):10744–10749, 2004.
- [61] P.R. Mouton, B. Pakkenberg, H.J.G. Gundersen, and D.L Price. Absolute number and size of pigmented locus coeruleus neurons in young and aged individuals. *J. Chem. Neuroanat.*, 7(3):185–190, 1994.

- [62] K.F. Manaye, D.D. McIntire, D.M.A. Mann, and D.C. German. Locus coeruleus cell loss in the aging human brain: A non-random process. *J. Comp. Neurol.*, 358(1):79–87, 1995.
- [63] S.D. Robertson, N.W. Plummer, J. De Marchena, and P. Jensen. Developmental origins of central norepinephrine neuron diversity. *Nat. Neurosci.*, 16(8):1016–1023, 2013.
- [64] D.A. Steindler and B.K. Trosko. Two types of locus coeruleus neurons born on different embryonic days in the mouse. *Anat. Embryol.*, 179(5):423–434, 1989.
- [65] T. Hökfelt, R. Martensson, A. Björklund, S. Kleinau, and M. Goldstein. *Distributional maps of tyrosine-hydroxylase-immunoreactive neurons in the rat brain*, pages 55–122. Elsevier, Amsterdam, Netherlands, 1984.
- [66] B. Mulvey, D.L. Bhatti, S. Gyawali, A.M. Lake, S. Kriaucionis, C.P. Ford, M.R. Bruchas, N. Heintz, and J.D. Dougherty. Molecular and functional sex differences of noradrenergic neurons in the mouse locus coeruleus. *Cell Rep.*, 23(8):2225–2235, 2018.
- [67] D.A. Rasmussen, K. Morilak and B.L. Jacobs. Single unit activity of locus coeruleus neurons in the freely moving cat: I. during naturalistic behaviors and in response to simple and complex stimuli. *Brain Res.*, 371(2):324–334, 1986.
- [68] G.R. Poe, S. Foote, O. Eschenko, J.P. Johansen, S. Bouret, G. Aston-Jones, C.W. Harley, D. Manahan-Vaughan, D. Weinshenker, R. Valentino, et al. Locus coeruleus: a new look at the blue spot. *Nat. Rev. Neurosci.*, 21(11):644–659, 2020.
- [69] G. Aston-Jones, M. Iba, E. Clayton, J. Rajkowski, and J. Cohen. The locus coeruleus and regulation of behavioral flexibility and attention: clinical implications. 2007.
- [70] R.J. Valentino and E. Van Bockstaele. Convergent regulation of locus coeruleus activity as an adaptive response to stress. *Eur. J. Pharmacol.*, 583(2-3):194–203, 2008.
- [71] G. Aston-Jones, J. Rajkowski, P. Kubiak, R.J. Valentino, and M.T. Shipley. Role of the locus coeruleus in emotional activation. *Prog. Brain Res.*, 107:379–402, 1996.
- [72] S.J. Sara. Locus coeruleus in time with the making of memories. *Curr. Opin. Neurobiol.*, 35:87–94, 2015.

- [73] G. Aston-Jones and J.D. Cohen. Adaptive gain and the role of the locus coeruleus–norepinephrine system in optimal performance. *J. of Comp. Neurol.*, 493(1):99–110, 2005.
- [74] S.J. Sara and S. Bouret. Orienting and reorienting: the locus coeruleus mediates cognition through arousal. *Neuron*, 76(1):130–141, 2012.
- [75] D.M. Devilbiss and B.D. Waterhouse. The effects of tonic locus ceruleus output on sensory-evoked responses of ventral posterior medial thalamic and barrel field cortical neurons in the awake rat. *J. Neurosci.*, 24(48):10773–10785, 2004.
- [76] D.M. Devilbiss, Michelle E Page, and B.D. Waterhouse. Locus ceruleus regulates sensory encoding by neurons and networks in waking animals. *J. Neurosci. Res.*, 26(39):9860–9872, 2006.
- [77] D.M. Devilbiss and B.D. Waterhouse. Phasic and tonic patterns of locus coeruleus output differentially modulate sensory network function in the awake rat. *J. Neurophysiol.*, 105(1):69–87, 2011.
- [78] D.M. Devilbiss. Consequences of tuning network function by tonic and phasic locus coeruleus output and stress: regulating detection and discrimination of peripheral stimuli. *Brain Res.*, 1709:16–27, 2019.
- [79] Barbara E.J. Sleep–wake state regulation by noradrenaline and serotonin. 2009.
- [80] D.M Perez. *The adrenergic receptors: in the 21st century*. Springer Science & Business Media, 2006.
- [81] Robert M Graham, Dianne M Perez, John Hwa, and Michael T Piascik. α 1-adrenergic receptor subtypes: molecular structure, function, and signaling. *Circulation research*, 78(5):737–749, 1996.
- [82] Hongying Zhong and Kenneth P Minneman. α 1-adrenoceptor subtypes. *Eur. J. Pharmacol.*, 375(1-3):261–276, 1999.
- [83] Olivier Chabre, Bruce R Conklin, Suzanne Brandon, Henry R Bourne, and Lee E Limbird. Coupling of the alpha 2a-adrenergic receptor to multiple g-proteins. a simple approach for estimating receptor-g-protein coupling efficiency in a transient expression system. *Journal of Biological Chemistry*, 269(8):5730–5734, 1994.
- [84] H.E.W. Day, S. Campeau, S.J. Watson Jr, and H. Akil. Distribution of α 1a-, α 1b- and α 1d-adrenergic receptor mrna in the rat brain and spinal cord. *J. Chem. Neuroanat.*, 13(2):115–139, 1997.

- [85] S.K. McCune, M.M. Voigt, and J.M. Hill. Expression of multiple alpha adrenergic receptor subtype messenger rnas in the adult rat brain. *Neuroscience*, 57(1):143–151, 1993.
- [86] A.P. Nicholas, V.A. Pieribone, and T. Hökfelt. Cellular localization of messenger rna for beta-1 and beta-2 adrenergic receptors in rat brain: an in situ hybridization study. *Neuroscience*, 56(4):1023–1039, 1993.
- [87] M. Scheinin, J.W. Lomasney, D.M. Hayden-Hixson, U.B. Schambra, M.G. Caron, R.J. Lefkowitz, and R.T. Fremeau Jr. Distribution of α 2-adrenergic receptor subtype gene expression in rat brain. *Mol. Brain Res.*, 21(1-2):133–149, 1994.
- [88] V.A. Pieribone, A.P. Nicholas, A. Dagerlind, and T. Hokfelt. Distribution of alpha 1 adrenoceptors in rat brain revealed by in situ hybridization experiments utilizing subtype-specific probes. *J. Neurosci. Res.*, 14(7):4252–4268, 1994.
- [89] B.E. Jones and R.Y. Moore. Catecholamine-containing neurons of the nucleus locus coeruleus in the cat. *J. Comp. Neurol.*, 157(1):43–51, 1974.
- [90] G. Aston-Jones and F. Bloom. Activity of norepinephrine-containing locus coeruleus neurons in behaving rats anticipates fluctuations in the sleep-waking cycle. *J. Neurosci.*, 1(8):876–886, 1981.
- [91] N. Chu and F.E. Bloom. Activity patterns of catecholamine-containing pontine neurons in the dorso-lateral tegmentum of unrestrained cats. *J. Neurobiol.*, 5(6):527–544, 1974.
- [92] J.A. Hobson, R.W. McCarley, and P.W. Wyzinski. Sleep cycle oscillation: reciprocal discharge by two brainstem neuronal groups. *Science*, 189(4196):55–58, 1975.
- [93] S.L. Foote, G. Aston-Jones, and F.E. Bloom. Impulse activity of locus coeruleus neurons in awake rats and monkeys is a function of sensory stimulation and arousal. *Proc. Natl. Acad. Sci. USA*, 77(5):3033–3037, 1980.
- [94] J Rajkowski, P Kubiak, and G Aston-Jones. Locus coeruleus activity in monkey: phasic and tonic changes are associated with altered vigilance. *Brain Res. Bull.*, 35(5-6):607–616, 1994.
- [95] B.D. Waterhouse, H.C. Moises, and D.J. Woodward. Phasic activation of the locus coeruleus enhances responses of primary sensory cortical neurons to peripheral receptive field stimulation. *Brain Res.*, 790(1-2):33–44, 1998.

- [96] O. Eschenko and S.J. Sara. Learning-dependent, transient increase of activity in noradrenergic neurons of locus coeruleus during slow wave sleep in the rat: Brain stem–cortex interplay for memory consolidation? *Cerebr. Cort.*, 18(11):2596–2603, 2008.
- [97] O. Eschenko, C. Magri, S. Panzeri, and S.J. Sara. Noradrenergic neurons of the locus coeruleus are phase locked to cortical up-down states during sleep. *Cerebr. Cort.*, 22(2):426–435, 2012.
- [98] K.M. Swift, B.A. Gross, M.A. Frazer, D.S. Bauer, K.J.D. Clark, E.M. Vazey, G. Aston-Jones, Y. Li, A.E. Pickering, S.J. Sara, et al. Abnormal locus coeruleus sleep activity alters sleep signatures of memory consolidation and impairs place cell stability and spatial memory. *Curr. Biol.*, 28(22):3599–3609, 2018.
- [99] A.G. Teschemacher. Real-time measurements of noradrenaline release in periphery and central nervous system. *Auton Neurosci*, 117(1):1–8, 2005.
- [100] J. Park, R.V. Bhimani, and C.E. Bass. In vivo electrochemical measurements of norepinephrine in the brain: Current status and remaining challenges. *J. Electrochem. Soc.*, 165(12):G3051, 2018.
- [101] P.T. Kissinger, J.B. Hart, and R.N. Adams. Voltammetry in brain tissue—a new neurophysiological measurement. *Brain Res.*, 55(1):209–213, 1973.
- [102] R.N. Adams. Probing brain chemistry with electroanalytical techniques. *Anal. Chem.*, 48(14):1126A–1138A, 1976.
- [103] L. Yavich, P. Jäkälä, and H. Tanila. Noradrenaline overflow in mouse dentate gyrus following locus coeruleus and natural stimulation: Real-time monitoring by in vivo voltammetry. *J. Neurochem.*, 95(3):641–650, 2005.
- [104] J. Park, B.M. Kile, and R. Mark Wightman. In vivo voltammetric monitoring of norepinephrine release in the rat ventral bed nucleus of the stria terminalis and anteroventral thalamic nucleus. *European J. Neurosci. Res.*, 30(11):2121–2133, 2009.
- [105] C. Dugast, R. Cespuglio, and M.F. Suaud-Chagny. In vivo monitoring of evoked noradrenaline release in the rat anteroventral thalamic nucleus by continuous amperometry. *J. Neurochem.*, 82(3):529–537, 2002.
- [106] P. Brun, M.F. Suaud-Chagny, F. Gonon, and M. Buda. Differential effects of desipramine on direct-and sensory-evoked noradrenaline release in thalamic locus coeruleus terminals. *Eur. J. Pharmacol.*, 235(2-3):205–210, 1993.

- [107] J. Feng, C. Zhang, J.E. Lischinsky, M. Jing, J. Zhou, H. Wang, Y. Zhang, A. Dong, Z. Wu, H. Wu, et al. A genetically encoded fluorescent sensor for rapid and specific in vivo detection of norepinephrine. *Neuron*, 102(4):745–761, 2019.
- [108] C.W. Berridge and E.D. Abercrombie. Relationship between locus coeruleus discharge rates and rates of norepinephrine release within neocortex as assessed by in vivo microdialysis. *Neuroscience*, 93(4):1263–1270, 1999.
- [109] J. Park, V. Quaiserova-Mocko, K. Peckova, J. Galligan, G. Fink, and G. Swain. Fabrication, characterization, and application of a diamond microelectrode for electrochemical measurement of norepinephrine release from the sympathetic nervous system. *Diam. Relat. Mater.*, 15(4-8):761–772, 2006.
- [110] T. Jo, K. Yoshimi, T. Takahashi, G. Oyama, and N. Hattori. Dual use of rectangular and triangular waveforms in voltammetry using a carbon fiber microelectrode to differentiate norepinephrine from dopamine. *Journal of ElectroAnal. Chem.*, 802: 1–7, 2017.
- [111] L. Bito, H. Davson, E. Levin, M. Murray, and N. Snider. The concentrations of free amino acids and other electrolytes in cerebrospinal fluid, in vivo dialysate of brain, and blood plasma of the dog. *J. Neurochem.*, 13(11):1057–1067, 1966.
- [112] S.M. Florin-Lechner, J.P. Druhan, G. Aston-Jones, and R.J. Valentino. Enhanced norepinephrine release in prefrontal cortex with burst stimulation of the locus coeruleus. *Brain Res.*, 742(1-2):89–97, 1996.
- [113] H. Kawahara, Y. Kawahara, and B.H.C. Westerink. The noradrenaline–dopamine interaction in the rat medial prefrontal cortex studied by multi-probe microdialysis. *Eur. J. Pharmacol.*, 418(3):177–186, 2001.
- [114] P. Devoto, G. Flore, P. Saba, M. Fa, and G.L. Gessa. Stimulation of the locus coeruleus elicits noradrenaline and dopamine release in the medial prefrontal and parietal cortex. *J. Neurochem.*, 92(2):368–374, 2005.
- [115] J.M.L. Menon, C. Nolten, E.J.M. Achterberg, R.N.J.M.A. Joosten, M. Dematteis, M.G.P. Feenstra, et al. Brain microdialysate monoamines in relation to circadian rhythms, sleep, and sleep deprivation—a systematic review, network meta-analysis, and new primary data. *J. Circ. Rhythms*, 17, 2019.
- [116] Z. de Saint Hilaire, M. Orosco, C. Rouch, A. Python, and S. Nicolaidis. Neuromodulation of the prefrontal cortex during sleep: a microdialysis study in rats. *Neuroreport*, 11(8):1619–1624, 2000.

- [117] P. Kalén, E. Rosegren, O. Lindvall, and A. Björklund. Hippocampal noradrenaline and serotonin release over 24 hours as measured by the dialysis technique in freely moving rats: correlation to behavioural activity state, effect of handling and tail-pinch. *European J. Neurosci. Res.*, 1(3):181–188, 1989.
- [118] S.P. Park. In vivo microdialysis measures of extracellular norepinephrine in the rat amygdala during sleep-wakefulness. *J Korean Med Sci*, 17(3):395–399, 2002.
- [119] M.N. Shouse, R.J. Staba, S.F. Saquib, and P.R. Farber. Monoamines and sleep: microdialysis findings in pons and amygdala. *Brain Res.*, 860(1-2):181–189, 2000.
- [120] O.I. Lyamin, J.L. Lapierre, P.O. Kosenko, T. Kodama, A. Bhagwandin, S. M Korneva, J.H. Peever, L.M. Mukhametov, and J.M. Siegel. Monoamine release during unihemispheric sleep and unihemispheric waking in the fur seal. *Sleep*, 39(3):625–636, 2016.
- [121] M. Bellesi, G. Tononi, C. Cirelli, and P. Serra. Region-specific dissociation between cortical noradrenaline levels and the sleep/wake cycle. *Sleep*, 39(1):143–154, 2016.
- [122] V.I. Chefer, A.C. Thompson, A. Zapata, and T.S. Shippenberg. Overview of brain microdialysis. *Curr. Protoc. Neurosci.*, 47(1):7–1, 2009.
- [123] M. Sasaki, E. Shibata, K. Tohyama, J. Takahashi, K. Otsuka, K. Tsuchiya, S. Takahashi, S. Ehara, Y. Terayama, and A. Sakai. Neuromelanin magnetic resonance imaging of locus ceruleus and substantia nigra in parkinson’s disease. *Neuroreport*, 17(11):1215–1218, 2006.
- [124] K.Y. Liu, J. Acosta-Cabronero, A. Cardenas-Blanco, C. Loane, A.J. Berry, M.J. Betts, R.A. Kievit, R.N. Henson, E. Düzel, R. Howard, et al. In vivo visualization of age-related differences in the locus coeruleus. *Neurobiol. Aging*, 74:101–111, 2019.
- [125] C.E.J. Doppler, J.A.M. Smit, M. Hommelsen, A. Seger, J. Horsager, M.B. Kinnerup, A.K. Hansen, T.D. Fedorova, K. Knudsen, M. Otto, et al. Microsleep disturbances are associated with noradrenergic dysfunction in parkinson’s disease. *Sleep*, 44(8):zsab040, 2021.
- [126] F.R. López-Picón, A.K. Kirjavainen, S. Forsback, J.S. Takkinen, D. Peters, M. Haaparanta-Solin, and O. Solin. In vivo characterization of a novel norepinephrine transporter pet tracer [18f] ns12137 in adult and immature sprague-dawley rats. *Theranostics*, 9(1):11, 2019.

- [127] A.K. Kirjavainen, S. Forsback, F.R. Lopez-Picon, P. Marjamäki, J. Takkinen, M. Haaparanta-Solin, D. Peters, and O. Solin. 18f-labeled norepinephrine transporter tracer [18f] ns12137: radiosynthesis and preclinical evaluation. *Nucl. Med. Biol.*, 56:39–46, 2018.
- [128] M. Kelberman, S. Keilholz, and D. Weinshenker. What’s that (blue) spot on my mri? multimodal neuroimaging of the locus coeruleus in neurodegenerative disease. *Front. Neurosci.*, page 1069, 2020.
- [129] N.I. Keren, C.T. Lozar, K.C. Harris, P.S. Morgan, and M.A. Eckert. In vivo mapping of the human locus coeruleus. *Neuroimage*, 47(4):1261–1267, 2009.
- [130] K.Y. Liu, F. Marijatta, D. Hämmerer, J. Acosta-Cabronero, E. Düzel, and R.J. Howard. Magnetic resonance imaging of the human locus coeruleus: a systematic review. *Neurosci Biobehav Rev.*, 83:325–355, 2017.
- [131] V. Zerbi, A. Floriou-Servou, M. Markicevic, Y. Vermeiren, O. Sturman, M. Privitera, L. von Ziegler, K.D. Ferrari, B. Weber, P.P. De Deyn, et al. Rapid reconfiguration of the functional connectome after chemogenetic locus coeruleus activation. *Neuron*, 103(4):702–718, 2019.
- [132] T.T. Dang-Vu. Neuronal oscillations in sleep: insights from functional neuroimaging. *Neuromol. Med.*, 14(3):154–167, 2012.
- [133] M. Van Egroo, R.W.E. Van Hooren, and H.I.L. Jacobs. Associations between locus coeruleus integrity and nocturnal awakenings in the context of alzheimer’s disease plasma biomarkers: a 7t mri study. *Alzheimer’s Res. Ther.*, 13(1):1–10, 2021.
- [134] J.A. Onton, D.Y. Kang, and T.P. Coleman. Visualization of whole-night sleep eeg from 2-channel mobile recording device reveals distinct deep sleep stages with differential electrodermal activity. *Frontiers in human neuroscience*, 10:605, 2016.
- [135] I.V. Filippov, W.C. Williams, and V.A. Frolov. Very slow potential oscillations in locus coeruleus and dorsal raphe nucleus under different illumination in freely moving rats. *Neurosci. Lett.*, 363(1):89–93, 2004.
- [136] I.V. Filippov and V.A. Frolov. Very slow potentials in the lateral geniculate complex and primary visual cortex during different illumination changes in freely moving rats. *Neurosci. Lett.*, 373(1):51–56, 2004.
- [137] T. McCormick, D.A. and Bal. Sensory gating mechanisms of the thalamus. *Curr. Opin. Neurobiol.*, 4(4):550–556, 1994.

- [138] A. Lüthi. Sleep spindles: where they come from, what they do. *The Neuroscientist*, 20(3):243–256, 2014.
- [139] B. Plihal and C. Gottesmann. The reticular arousal threshold during the transition from slow wave sleep to paradoxical sleep in the rat. *Physiol. Behav.*, 58(1):199–202, 1995.
- [140] H. Hayat, N. Regev, N. Matosevich, A. Sales, E. Paredes-Rodriguez, A.J. Krom, L. Bergman, Y. Li, M. Lavigne, E.J. Kremer, et al. Locus coeruleus norepinephrine activity mediates sensory-evoked awakenings from sleep. *Sci. Adv.*, 6(15):eaaz4232, 2020.
- [141] S.K. Wood and R.J. Valentino. The brain norepinephrine system, stress and cardiovascular vulnerability. *Neurosci. & Biobehav. Rev.*, 74:393–400, 2017.
- [142] G. Aston-Jones, C. Chiang, and T. Alexinsky. Discharge of noradrenergic locus coeruleus neurons in behaving rats and monkeys suggests a role in vigilance. *Prog. Brain Res.*, 88:501–520, 1991.
- [143] L.T. Lopes, L.G.A. Patrone, K. Li, A.N. Imber, C.D. Graham, L.H. Gargaglioni, and R.W. Putnam. Anatomical and functional connections between the locus coeruleus and the nucleus tractus solitarius in neonatal rats. *Neuroscience*, 324:446–468, 2016.
- [144] Z.J. Gieroba and W.W. Blessing. Fos-containing neurons in medulla and pons after unilateral stimulation of the afferent abdominal vagus in conscious rabbits. *Neuroscience*, 59(4):851–858, 1994.
- [145] D.K. Naritoku, W.J. Terry, and R.H. Helfert. Regional induction of fos immunoreactivity in the brain by anticonvulsant stimulation of the vagus nerve. *Epilepsy Res.*, 22(1):53–62, 1995.
- [146] L. Collins, L. Boddington, P.J. Steffan, and D.A. McCormick. Vagus nerve stimulation induces widespread cortical and behavioral activation. *Curr. Biol.*, 31(10):2088–2098, 2021.
- [147] S. Joshi, Y. Li, R.M. Kalwani, and J.I. Gold. Relationships between pupil diameter and neuronal activity in the locus coeruleus, colliculi, and cingulate cortex. *Neuron*, 89(1):221–234, 2016.
- [148] J. Reimer, M.J. McGinley, Y. Liu, C. Rodenkirch, Q. Wang, D.A. McCormick, and A.S. Tolias. Pupil fluctuations track rapid changes in adrenergic and cholinergic activity in cortex. *Nat. Commun.*, 7(1):1–7, 2016.

- [149] H. Gelbard-Sagiv, E. Magidov, H. Sharon, T. Hendler, and Y. Nir. Noradrenaline modulates visual perception and late visually evoked activity. *Curr. Biol.*, 28(14): 2239–2249, 2018.
- [150] R. Bianca and B.R. Komisaruk. Pupil dilatation in response to vagal afferent electrical stimulation is mediated by inhibition of parasympathetic outflow in the rat. *Brain Res.*, 1177:29–36, 2007.
- [151] O. Sharon, F. Fahoum, and Y. Nir. Transcutaneous vagus nerve stimulation in humans induces pupil dilation and attenuates alpha oscillations. *J. Neurosci.*, 41(2):320–330, 2021.
- [152] K.H. Lee and D.A. McCormick. Modulation of spindle oscillations by acetylcholine, cholecystokinin and 1s, 3r-acpd in the ferret lateral geniculate and perigeniculate nuclei in vitro. *Neuroscience*, 77(2):335–350, 1997.
- [153] D.A. McCormick. Cellular mechanisms underlying cholinergic and noradrenergic modulation of neuronal firing mode in the cat and guinea pig dorsal lateral geniculate nucleus. *J. Neurosci. Res.*, 12(1):278–289, 1992.
- [154] H.C. Pape and D.A. McCormick. Noradrenaline and serotonin selectively modulate thalamic burst firing by enhancing a hyperpolarization-activated cation current. *Nature*, 340(6236):715–718, 1989.
- [155] H.C. McCormick, D.A. and Pape. Noradrenergic and serotonergic modulation of a hyperpolarization-activated cation current in thalamic relay neurones. *Physiol. J.*, 431(1):319–342, 1990.
- [156] T. Bal and D.A. McCormick. Mechanisms of oscillatory activity in guinea-pig nucleus reticularis thalami in vitro: a mammalian pacemaker. *Physiol. J.*, 468(1):669–691, 1993.
- [157] D.A. McCormick, D.A. and Prince. Noradrenergic modulation of firing pattern in guinea pig and cat thalamic neurons, in vitro. *J. Neurophysiol.*, 59(3):978–996, 1988.
- [158] K.H. Lee and D.A. McCormick. Abolition of spindle oscillations by serotonin and norepinephrine in the ferret lateral geniculate and perigeniculate nuclei in vitro. *Neuron*, 17(2):309–321, 1996.
- [159] X. Wang, R.A. Piñol, P. Byrne, and D. Mendelowitz. Optogenetic stimulation of locus ceruleus neurons augments inhibitory transmission to parasympathetic cardiac

- vagal neurons via activation of brainstem $\alpha 1$ and $\beta 1$ receptors. *J. Neurosci. Res.*, 34(18):6182–6189, 2014.
- [160] C. Kjaerby, M. Andersen, N.L. Hauglund, F. Ding, W. Wang, Q. Xu, S. Deng, N. Kang, S. Peng, Q. Sun, et al. Dynamic fluctuations of the locus coeruleus-norepinephrine system underlie sleep state transitions. *Biorxiv*, 2020.09.01.274977, 2020.
- [161] Alejandro Osorio-Forero, Najma Cherrad, Lila Banterle, Laura MJ Fernandez, and Anita Lüthi. When the locus coeruleus speaks up in sleep: Recent insights, emerging perspectives. *International Journal of Molecular Sciences*, 23(9):5028, 2022.
- [162] P. User, H. Gioanni, and C. Gottesmann. Intermediate stage of sleep and acute cerveau isole preparation in the rat. *Acta Neurobiol. Exp*, 40:521–525, 1980.
- [163] C Gottesmann, G Gandolfo, and B Zernicki. Intermediate stage of sleep in the cat. *J. de PPhysiol.*, 79(5):365–372, 1984.
- [164] L. Glin, C. Arnaud, D. Berracochea, D. Galey, R. Jaffard, and C. Gottesmann. The intermediate stage of sleep in mice. *Physiol. & Behav.*, 50(5):951–953, 1991.
- [165] C. Gottesmann, P. User, and H. Gioanni. Sleep: a physiological” cerveau isolé” stage? *Waking Sleeping*, 1980.
- [166] A.R. Adamantidis, C. Gutierrez-Herrera, and T.C. Gent. Oscillating circuitries in the sleeping brain. *Nat. Rev. Neurosci.*, 20(12):746–762, 2019.
- [167] S. Jogo, S.D Glasgow, C. Gutierrez-Herrera, M. Ekstrand, S.J. Reed, R. Boyce, J. Friedman, D. Burdakov, and A.R. Adamantidis. Optogenetic identification of a rapid eye movement sleep modulatory circuit in the hypothalamus. *Nat. Neurosci.*, 16(11):1637–1643, 2013.
- [168] R.G. Yamada and H.R. Ueda. Molecular mechanisms of rem sleep. *Front. Neurosci.*, 13:1402, 2020.
- [169] M. El Mansari, K. Sakai, and M. Jouvet. Unitary characteristics of presumptive cholinergic tegmental neurons during the sleep-waking cycle in freely moving cats. *Exp. Brain Res.*, 76(3):519–529, 1989.
- [170] M. Steriade, S. Datta, D. Pare, G. Oakson, and R.C. Dossi. Neuronal activities in brain-stem cholinergic nuclei related to tonic activation processes in thalamocortical systems. *J. Neurosci.*, 10(8):2541–2559, 1990.

- [171] S. Singh and B.N. Mallick. Mild electrical stimulation of pontine tegmentum around locus coeruleus reduces rapid eye movement sleep in rats. *Neurosci. Res.*, 24(3):227–235, 1996.
- [172] C. Cirelli, G. Tononi, M. Pompeiano, O. Pompeiano, and A. Gennari. Modulation of desynchronized sleep through microinjection of α 1-adrenergic agonists and antagonists in the dorsal pontine tegmentum of the cat. *Pflügers Arch.*, 422(3):273–279, 1992.
- [173] O. Clément, S. Valencia Garcia, P-A. Libourel, S. Arthaud, P. Fort, and P. Luppi. The inhibition of the dorsal paragigantocellular reticular nucleus induces waking and the activation of all adrenergic and noradrenergic neurons: a combined pharmacological and functional neuroanatomical study. *PLoS One*, 9(5):e96851, 2014.
- [174] S. Park and F. Weber. Neural and homeostatic regulation of rem sleep. *Front. Psychol.*, 11:1662, 2020.
- [175] S. Park, J. Baik, J. Hong, H. Antila, B. Kurland, S. Chung, and F. Weber. A probabilistic model for the ultradian timing of rem sleep in mice. *PLoS Comp. Biol.*, 17(8):e1009316, 2021.
- [176] F. Weber, J.P.H. Do, S. Chung, K.T. Beier, M. Bikov, and Y. Doost, M.S. and Dan. Regulation of rem and non-rem sleep by periaqueductal gabaergic neurons. *Nat. Comm.*, 9(1):1–13, 2018.
- [177] M.E. Carter, O. Yizhar, S. Chikahisa, H. Nguyen, A. Adamantidis, S. Nishino, K. Deisseroth, and L. De Lecea. Tuning arousal with optogenetic modulation of locus coeruleus neurons. *Nat. Neurosci.*, 13(12):1526–1533, 2010.
- [178] H. Yamaguchi, F.W. Hopf, S. Li, and L. de Lecea. In vivo cell type-specific crispr knockdown of dopamine beta hydroxylase reduces locus coeruleus evoked wakefulness. *Nat. Comm.*, 9(1):1–8, 2018.
- [179] G. Oikonomou, M. Altermatt, R. Zhang, G.M Coughlin, C. Montz, V. Gradinaru, and D.A. Prober. The serotonergic raphe promote sleep in zebrafish and mice. *Neuron*, 103(4):686–701, 2019.
- [180] J.M. Monti and D. Monti. The involvement of dopamine in the modulation of sleep and waking. *Sleep Med. Rev*, 11(2):113–133, 2007.

- [181] Y. Oishi and M. Lazarus. The control of sleep and wakefulness by mesolimbic dopamine systems. *Neurosci. Res.*, 118:66–73, 2017.
- [182] J.M. Monti, L. D’Angelo, H. Jantos, L. Barbeito, and V. Abo. Effect of dsp-4, a noradrenergic neurotoxin, on sleep and wakefulness and sensitivity to drugs acting on adrenergic receptors in the rat. *Sleep*, 11(4):370–377, 1988.
- [183] W. Wan, J. Peng, X. Li, T. Qian, K. Song, J. Zeng, F. Deng, S. Hao, J. Feng, P. Zhang, et al. A genetically encoded sensor for measuring serotonin dynamics. *Nat. Neurosci.*, 24(5):746–752, 2021.
- [184] M.A. Kim, H.S. Lee, B.Y. Lee, and B.D. Waterhouse. Reciprocal connections between subdivisions of the dorsal raphe and the nuclear core of the locus coeruleus in the rat. *Brain Res.*, 1026(1):56–67, 2004.
- [185] F. Sun, J. Zeng, M. Jing, J. Zhou, J. Feng, S.F. Owen, Y. Luo, F. Li, H. Wang, and T. Yamaguchi. A genetically encoded fluorescent sensor enables rapid and specific detection of dopamine in flies, fish, and mice. *Cell*, 174(2):481–496, 2018.
- [186] M. Jing, Y. Li, J. Zeng, P. Huang, M. Skirzewski, O. Kljakic, W. Peng, T. Qian, K. Tan, J. Zou, et al. An optimized acetylcholine sensor for monitoring in vivo cholinergic activity. *Nat. Meth.*, 17(11):1139–1146, 2020.
- [187] L. Duffet, S. Kosar, M. Panniello, B. Viberti, E. Bracey, A.D. Zych, A. Radoux-Mergault, X. Zhou, J. Dernic, L. Ravotto, et al. A genetically encoded sensor for in vivo imaging of orexin neuropeptides. *Nat. Meth.*, 19(2):231–241, 2022.
- [188] E. Hasegawa, A. Miyasaka, K. Sakurai, Y. Cherasse, Y. Li, and T. Sakurai. Rapid eye movement sleep is initiated by basolateral amygdala dopamine signaling in mice. *Science*, 375(6584):994–1000, 2022.
- [189] M. Bandarabadi, C. Gutierrez-Herrera, T.C. Gent, C. Bassetti, K. Schindler, and A.R. Adamantidis. A role for spindles in the onset of rapid eye movement sleep. *Nat. Commun.*, 11(1):1–12, 2020.
- [190] M. Takigawa and G.J. Mogenson. A study of inputs to antidromically identified neurons of the locus coeruleus. *Brain Res.*, 135(2):217–230, 1977.
- [191] D.A. Groves, E.M. Bowman, and V.J. Brown. Recordings from the rat locus coeruleus during acute vagal nerve stimulation in the anaesthetised rat. *Neurosci. Lett.*, 379(3):174–179, 2005.

- [192] R.W. Roosevelt, D.C. Smith, R.W. Clough, R.A. Jensen, and R.A. Browning. Increased extracellular concentrations of norepinephrine in cortex and hippocampus following vagus nerve stimulation in the rat. *Brain Res.*, 1119(1):124–132, 2006.
- [193] D.A. Nita, S. Vanhatalo, F.D. Lafortune, J. Voipio, K. Kaila, and F. Amzica. Nonneuronal origin of co₂-related dc eeg shifts: an in vivo study in the cat. *J. Neurophysiol.*, 92(2):1011–1022, 2004.
- [194] L.H. Gargaglioni, L.K. Hartzler, and R.W. Putnam. The locus coeruleus and central chemosensitivity. *Respir. Physiol. Neurobiol.*, 173(3):264–273, 2010.
- [195] J.A. Filosa, J.B. Dean, and R.W. Putnam. Role of intracellular and extracellular ph in the chemosensitive response of rat locus coeruleus neurones. *Physiol. J.*, 541(2):493–509, 2002.
- [196] V. Biancardi, K.C. Bicego, M.C. Almeida, and L.H. Gargaglioni. Locus coeruleus noradrenergic neurons and co₂ drive to breathing. *Pflugers Arch.*, 455(6):1119–1128, 2008.
- [197] Magor L.L. Hughes, S.W. and, H.R. Parri, and V. Crunelli. Intraslow (\approx 0.1 hz) oscillations in thalamic relay nuclei: basic mechanisms and significance to health and disease states. *Prog. Brain Res.*, 193:145–162, 2011.
- [198] M.L. Lőrincz, F. Geall, Y. Bao, V. Crunelli, and S.W. Hughes. Atp-dependent infra-slow (\approx 0.1 hz) oscillations in thalamic networks. *PLoS one*, 4(2):e4447, 2009.
- [199] H.R. Parri and V. Crunelli. Pacemaker calcium oscillations in thalamic astrocytes in situ. *Neuroreport*, 12(18):3897–3900, 2001.
- [200] Z. Cohen, G. Molinatti, and E. Hamel. Astroglial and vascular interactions of noradrenaline terminals in the rat cereb. cortex . *J. Cerebr. Blood Flow & Metab.*, 17(8):894–904, 1997.
- [201] M. Ennis and G. Aston-Jones. Evidence for self-and neighbor-mediated postactivation inhibition of locus coeruleus neurons. *Brain Res.*, 374(2):299–305, 1986.
- [202] B. Rasch and J. Born. About sleep’s role in memory. *Physiol. Rev.*, 2013.
- [203] J.M. Krueger, M.G. Frank, J.P. Wisor, and S. Roy. Sleep function: Toward elucidating an enigma. *Sleep Med. Rev.*, 28:46–54, 2016.

- [204] J.M. Siegel. Sleep viewed as a state of adaptive inactivity. *Nat. Rev. Neurosci.*, 10 (10):747–753, 2009.
- [205] K. Takahashi, Y Kayama, J.S. Lin, and K. Sakai. Locus coeruleus neuronal activity during the sleep-waking cycle in mice. *Neuroscience*, 169(3):1115–1126, 2010.
- [206] J. Seibt, C.J. Richard, J. Sigl-Glöckner, N. Takahashi, D.I. Kaplan, G. Doron, D. De Limoges, C. Bocklisch, and M.E. Larkum. Cortical dendritic activity correlates with spindle-rich oscillations during sleep in rodents. *Nat. Commun.*, 8(1):1–13, 2017.
- [207] Y. Sela, A. Joseph. Krom, L. Bergman, N. Regev, and Y. Nir. Sleep differentially affects early and late neuronal responses to sounds in auditory and perirhinal cortices. *J. Neurosci. Res.*, 40(14):2895–2905, 2020.
- [208] T. Takeuchi, A.J. Duzkiewicz, A. Sonneborn, P.A. Spooner, M. Yamasaki, M. Watanabe, C.C. Smith, G. Fernández, K. Deisseroth, R.W. Greene, et al. Locus coeruleus and dopaminergic consolidation of everyday memory. *Nature*, 537(7620): 357–362, 2016.
- [209] K.A. Kempadoo, E.V. Mosharov, S.J. Choi, D. Sulzer, and E.R. Kandel. Dopamine release from the locus coeruleus to the dorsal hippocampus promotes spatial learning and memory. *Proc. Natl. Acad. Sci. USA*, 113(51):14835–14840, 2016.
- [210] A. Wagatsuma, T. Okuyama, C. Sun, L.M. Smith, K. Abe, and S. Tonegawa. Locus coeruleus input to hippocampal ca3 drives single-trial learning of a novel context. *Proc. Natl. Acad. Sci. USA*, 115(2):E310–E316, 2018.
- [211] A.M. Kaufman, T. Geiller, and A. Losonczy. A role for the locus coeruleus in hippocampal ca1 place cell reorganization during spatial reward learning. *Neuron*, 105(6):1018–1026, 2020.
- [212] B. Yang, J. Sanches-Padilla, J. Kondapalli, S.L. Morison, E. Delpire, R. Awatramani, and D.J. Surmeier. Locus coeruleus anchors a trisynaptic circuit controlling fear-induced suppression of feeding. *Neuron*, 109(5):823–838, 2021.
- [213] Y. Novitskaya and N.K. and Eschenko O. Sara, S.J. and Logothetis. Ripple-triggered stimulation of the locus coeruleus during post-learning sleep disrupts ripple/spindle coupling and impairs memory consolidation. *Learn. & Mem.*, 23(5):238–248, 2016.
- [214] F.S. Giorgi, A. Galgani, S. Puglisi-Allegra, F. Limanaqi, and F. Busceti, C.L. and Fornai. Locus coeruleus and neurovascular unit: From its role in physiology

- to its potential role in alzheimer’s disease pathogenesis. *J. Neurosci. Res.*, 98(12): 2406–2434, 2020.
- [215] J. O’Donnell, D. Zeppenfeld, E. McConnell, S. Pena, and M. Nedergaard. Norepinephrine: a neuromodulator that boosts the function of multiple cell types to optimize cns performance. *Neurochem. Res.*, 37(11):2496–2512, 2012.
- [216] M.K. Rasmussen, H. Mestre, and M. Nedergaard. Fluid transport in the brain. *Physiol. Rev.*, 2021.
- [217] N.E. Fultz, G. Bonmassar, K. Setsompop, R.A. Stickgold, B.R. Rosen, J.R. Polimeni, and L.D. Lewis. Coupled electrophysiological, hemodynamic, and cerebrospinal fluid oscillations in human sleep. *Science*, 366(6465):628–631, 2019.
- [218] C. Wang and D.M. Holtzman. Bidirectional relationship between sleep and alzheimer’s disease: role of amyloid, tau, and other factors. *Neuropsychopharmacol.*, 45(1):104–120, 2020.
- [219] M. Van Egroo, E. Koshmanova, G. Vandewalle, and H.I.L. Jacobs. Importance of the locus coeruleus-norepinephrine system in sleep-wake regulation: implications for aging and alzheimer’s disease. *Sleep Med. Rev.*, page 101592, 2022.
- [220] H. Braak, D.R. Thal, E. Ghebremedhin, and K. Del Tredici. Stages of the pathologic process in alzheimer disease: age categories from 1 to 100 years. *J. Neuropathol. Exp. Neurol.*, 70(11):960–969, 2011.
- [221] C.H. Lew, C. Petersen, T.C. Neylan, and L.T. Grinberg. Tau-driven degeneration of sleep-and wake-regulating neurons in alzheimer’s disease. *Sleep Med. Rev.*, 60: 101541, 2021.
- [222] J.M. Rorabaugh, T. Chalermphanupap, C.A. Botz-Zapp, V.M. Fu, N.A. Lembeck, R.M. Cohen, and D. Weinshenker. Chemogenetic locus coeruleus activation restores reversal learning in a rat model of alzheimer’s disease. *Brain*, 140(11):3023–3038, 2017.
- [223] B. E Jones. Arousal systems. *Front. Biosci.*, 8(5):438–51, 2003.
- [224] G. Moruzzi and H. Winchell Magoun. Brain stem reticular formation and activation of the eeg. *Electroencephalogr. clin. neurophysiol.*, 1(1-4):455–473, 1949.
- [225] G.V. Russel. The nucleus locus coeruleus (dorsolateralis tegmenti). *Tex. rep. biol. med.*, 13(4):939–988, 1955.

- [226] T. Maeda and N. Shimizu. Projections ascendantes du locus coeruleus et d'autres neurones aminergiques pontiques au niveau du prosencéphale du rat. *Brain Res.*, 36(1):19–35, 1972.
- [227] U. Ungerstedt. Stereotaxic mapping of the monoamine pathways in the rat brain. *Acta Physiol. Scand.*, 82(S367):1–48, 1971.
- [228] K. Fuxe, T. Hökfelt, and U. Ungerstedt. Morphological and functional aspects of central monoamine neurons. volume 13, pages 93–126. Elsevier, 1970.
- [229] J.M. Koolhaas, A. Bartolomucci, B. Buwalda, S.F de Boer, G. Flugge, S.M Korte, P. Meerlo, R. Murison, B. Olivier, P. Palanza, et al. Stress revisited: a critical evaluation of the stress concept. *Neurosci. Biobehav. Rev.*, 35(5):1291–1301, 2011.
- [230] W.M. Vanderheyden, G.R. Poe, and I. Liberzon. Trauma exposure and sleep: using a rodent model to understand sleep function in ptsd. *Exp. Brain Res.*, 232(5):1575–1584, 2014.
- [231] E.J.W Van Someren. Brain mechanisms of insomnia: new perspectives on causes and consequences. *Physiol. Rev.*, 101(3):995–1046, 2021.
- [232] B. Zhang and Y.K. Wing. Sex differences in insomnia: a meta-analysis. *Sleep*, 29(1):85–93, 2006.
- [233] G.W. Vogel, F. Vogel, R.S. McAbee, and A.J. Thurmond. Improvement of depression by rem sleep deprivation: new findings and a theory. *Arch. Gen. Psychiatry*, 37(3):247–253, 1980.
- [234] G.W. Vogel. A review of rem sleep deprivation. *Arch. Gen. Psychiatry*, 32(6):749–761, 1975.
- [235] Barbara E Jones. From waking to sleeping: neuronal and chemical substrates. *Sci. Trends. Pharmacol. Sci.*, 26(11):578–586, 2005.

F Article

Noradrenergic circuit control of non-REM sleep substates

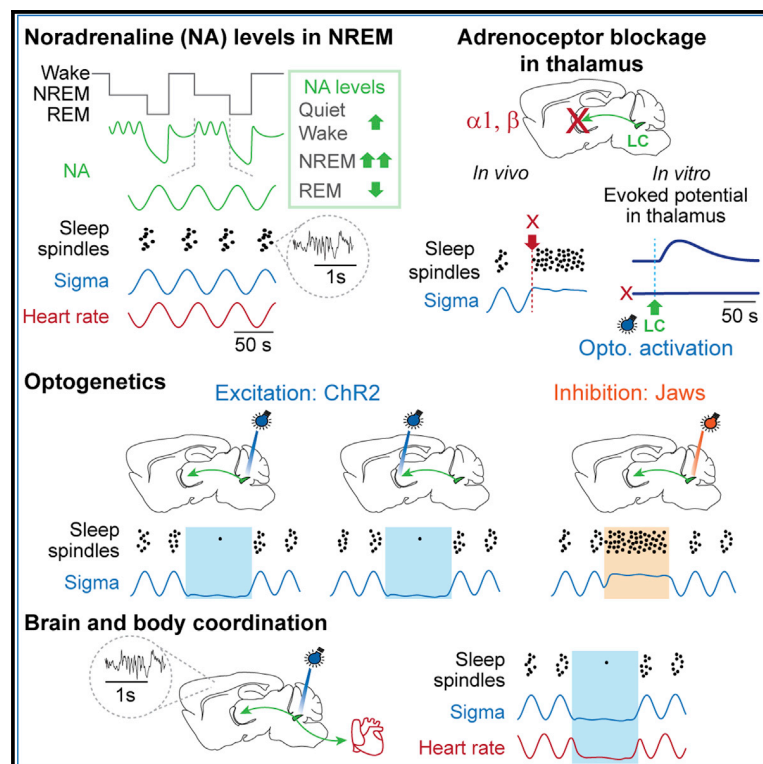
Alejandro Osorio-Forero, Romain Cardis, Gil Vantomme, Aurelie Guillaume-Gentil, Georgia Katsioudi, Christiane Devenoges, Laura M.J. Fernandez, and Anita Lüthi

<https://doi.org/10.1016/j.cub.2021.09.041>

Current Biology

Noradrenergic circuit control of non-REM sleep substates

Graphical abstract



Authors

Alejandro Osorio-Forero,
Romain Cardis, Gil Vantomme, ...,
Christiane Devenoges,
Laura M.J. Fernandez, Anita Lüthi

Correspondence

anita.luthi@unil.ch

In brief

Osorio-Forero et al. find that the neurotransmitter noradrenaline, known to be released in attentive wakefulness, is also released during non-REM sleep. Noradrenaline levels reached are even higher than in quiet wakefulness and fluctuate to coordinate forebrain and autonomic correlates of arousability on a 50-s timescale.

Highlights

- In NREMS, thalamic noradrenaline (NA) levels are higher than in quiet wakefulness
- Thalamic NA fluctuates over ~50 s and is anticorrelated to sleep spindles
- NA released from LC depolarizes thalamic neurons through $\alpha 1$ - and β -adrenoceptors
- Infralow LC activity coordinates heart-rate variations with spindles

Article

Noradrenergic circuit control of non-REM sleep substates

Alejandro Osorio-Forero,¹ Romain Cardis,¹ Gil Vantomme,^{1,2} Aurélie Guillaume-Gentil,¹ Georgia Katsioudi,^{1,3} Christiane Devenoges,¹ Laura M.J. Fernandez,¹ and Anita Lüthi^{1,4,5,*}

¹Department of Fundamental Neurosciences, University of Lausanne, Rue du Bugnon 9, 1005 Lausanne, Switzerland

²Present address: Department of Neurology, Wu Tsai Neurosciences Institute, Stanford University, 290 Jane Stanford Way, Stanford, CA 94305, USA

³Present address: Center for Integrative Genomics, University of Lausanne, Génopode, 1015 Lausanne, Switzerland

⁴Twitter: @LabLuthi

⁵Lead contact

*Correspondence: anita.luthi@unil.ch

<https://doi.org/10.1016/j.cub.2021.09.041>

SUMMARY

To understand what makes sleep vulnerable in disease, it is useful to look at how wake-promoting mechanisms affect healthy sleep. Wake-promoting neuronal activity is inhibited during non-rapid-eye-movement sleep (NREMS). However, sensory vigilance persists in NREMS in animals and humans, suggesting that wake promotion could remain functional. Here, we demonstrate that consolidated mouse NREMS is a brain state with recurrent fluctuations of the wake-promoting neurotransmitter noradrenaline on the ~50-s timescale in the thalamus. These fluctuations occurred around mean noradrenaline levels greater than the ones of quiet wakefulness, while noradrenaline (NA) levels declined steeply in REMS. They coincided with a clustering of sleep spindle rhythms in the forebrain and with heart-rate variations, both of which are correlates of sensory arousability. We addressed the origins of these fluctuations by using closed-loop optogenetic locus coeruleus (LC) activation or inhibition timed to moments of low and high spindle activity during NREMS. We could suppress, lock, or entrain sleep-spindle clustering and heart-rate variations, suggesting that both fore- and hindbrain-projecting LC neurons show coordinated infraslow activity variations in natural NREMS. Noradrenergic modulation of thalamic, but not cortical, circuits was required for sleep-spindle clustering and involved NA release into primary sensory and reticular thalamic nuclei that activated both α 1- and β -adrenergic receptors to cause slowly decaying membrane depolarizations. Noradrenergic signaling by LC constitutes a vigilance-promoting mechanism that renders mammalian NREMS vulnerable to disruption on the close-to-minute timescale through sustaining thalamocortical and autonomic sensory arousability.

INTRODUCTION

The restorative and beneficial effects of sleep arise from its continuity.¹ This requires that behavioral interactions with the sensory environment are suppressed. However, birds would crash and dolphins would drown if switching off from the sensory environment were not supplemented by vigilance.² Because natural dangers and predators pose a risk to all animals, irrespective of whether they are asleep or awake, it is natural to hypothesize that sleep evolution must have been tightly coupled to vigilance-promoting mechanisms. This may have placed natural healthy sleep dangerously close to vulnerability, such that minor shifts in the environment or in the organism's physiology easily disrupt sleep. Indeed, neurological and psychiatric conditions underlying sleep disorders are highly diverse, yet identifying their origins remains challenging.^{3–5} For these reasons, a better estimate of sleep's vulnerability in the healthy animal and of its neuronal basis is desirable.

During deep, restorative non-rapid-eye-movement sleep (NREMS), the activity of wake-promoting areas projecting into the forebrain is much reduced.⁶ However, already the first

recordings of neuronal electrical activity in the sleeping animal indicated that not all these areas were entirely silent.^{7–13} The locus coeruleus (LC), the most dorsal of ten noradrenergic nuclei located in the pontine brainstem,¹⁴ is strongly wake promoting,^{15,16} tonically active during wakefulness,^{7,17} and becomes even more active in response to unexpected sensory stimuli.^{17–19} The LC also remains active during NREMS, although at minor rates that do not cause awakening.^{10,16,20,21} This LC activity coincides with electroencephalogram (EEG) rhythms, such as sleep spindles^{10,21–23} and cortical slow waves,^{20,24} and is relevant for sleep-dependent memory consolidation.²⁵ Opto- or chemogenetic reinforcement of LC activity in rodents lowers auditory arousal thresholds in NREMS²³ and increases functional connectivity in resting-state salience networks,²⁶ which is a signature of enhanced vigilance. Therefore, natural variations of LC activity during NREMS could underlie sleep's vulnerability. To address this, we aimed to elucidate the dynamics of LC noradrenergic activity and its functional impact on brain and bodily substates during NREMS. We used closed-loop optogenetic manipulation of LC activity in combination with local and global sleep recordings in mouse, fiber

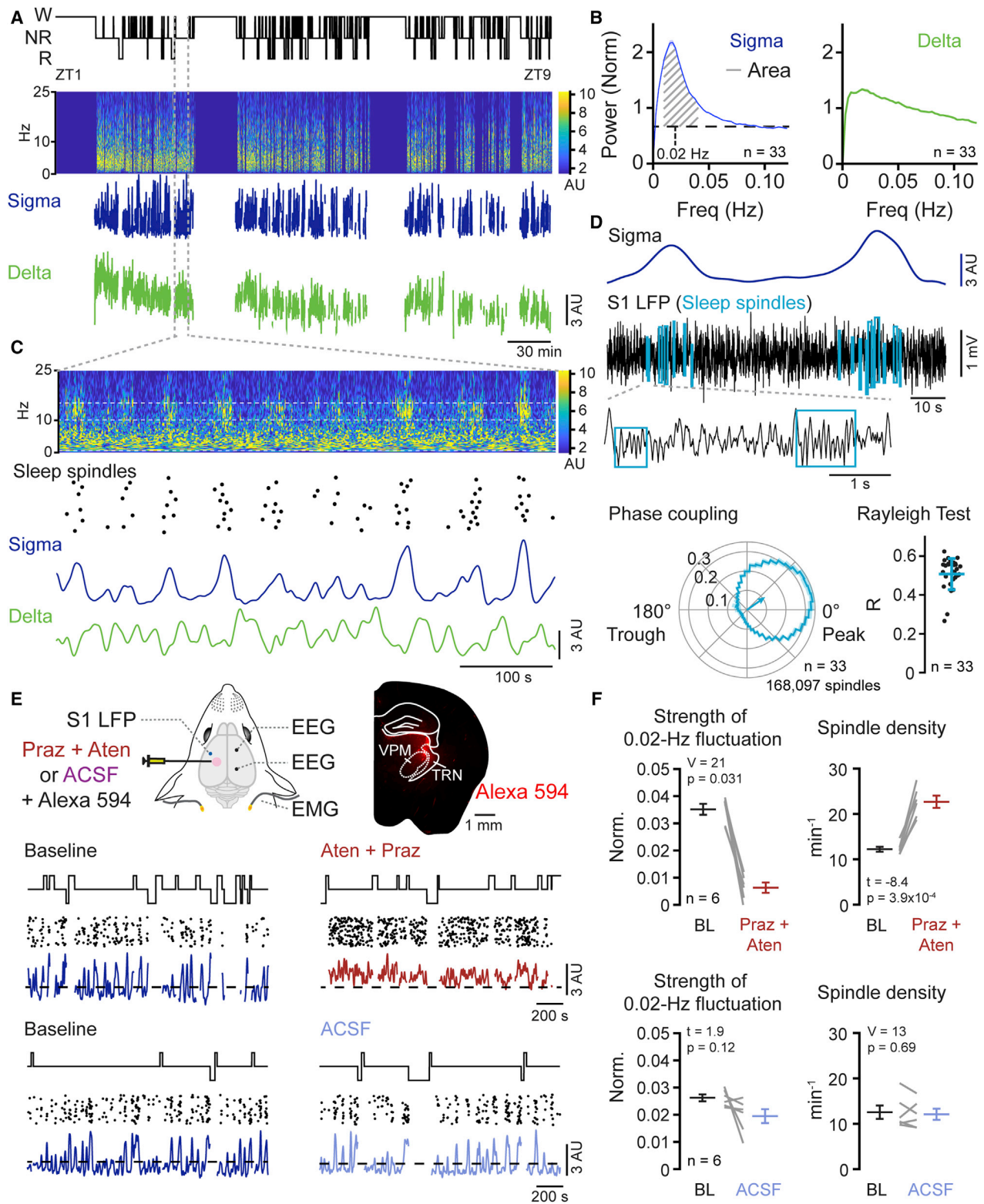


Figure 1. Noradrenergic signaling clusters sleep-spindle rhythms during NREMS

(A) Hypnogram showing wake (W), NREMS (NR), and REMS (R), with corresponding time-frequency distribution of S1 LFP signal. Power for NREMS in color code. Summed sigma (10–15 Hz) and delta (1.5–4 Hz) power dynamics were derived from the time-frequency distributions.

(legend continued on next page)

photometric assessment of noradrenaline (NA) levels, heart rate monitoring, and the analysis of synaptic potentials generated by LC afferents *in vitro*. We demonstrate that noradrenergic activity in thalamic sensory nuclei is unexpectedly high in NREMS and fluctuates on an infraslow timescale. Moreover, LC coordinates central and autonomic physiological correlates that make NREMS alternate between substates of low and high arousability.

RESULTS

Noradrenergic signaling during NREMS regulates the timing of sleep-spindle rhythms

Freely behaving mice sleep predominantly during the light period (ZT0–ZT12), which is their preferred resting phase. **Figure 1A** presents the sleep-wake behavior of a single mouse showing a hypnogram, obtained from polysomnography, and the corresponding time-frequency distribution derived from local field potential (LFP) recordings in the primary somatosensory cortex S1. We calculated power dynamics for two frequency bands characteristic for NREMS, the sigma (10–15 Hz) and the delta (1.5–4 Hz) frequency bands. As shown previously,^{27,28} sigma power fluctuates prominently in S1 on an infraslow timescale with a peak ~50 s (~0.02 Hz; **Figure 1B**). This fluctuation underlies infraslow variations in spontaneous and sensory arousability.^{27,28} Compared to sigma power, delta power in S1 fluctuates weakly ($n = 33$ mice; 12 C57BL/6J and 21 dopamine- β -hydroxylase [DBH]-Cre+/- mice recorded during the light phase; paired t test; $t = 16.03$; $p = 7.5 \times 10^{-15}$) and is anticorrelated to sigma in S1 due to shared neuronal mechanisms in local thalamocortical circuits.²⁹ The sigma frequency band is populated by sleep-spindle rhythms³⁰ that contribute to sensory decoupling during NREMS.^{30,31} To determine whether sleep-spindle density covaried over 0.02 Hz, we used a previously developed spindle detection algorithm²⁹ (**Figure S1A**) and analyzed the phase-locking between sigma power and sleep spindle density in the same group of 33 mice, recorded during the light phase. Sleep spindles clustered at the peak of the 0.02-Hz fluctuation in sigma power, whereas they were rare in the troughs (**Figures 1C and 1D**). Polar plots depicting the phase coupling of 168,097 spindles to the 0.02-Hz fluctuation demonstrate the non-uniformity of this distribution ($n = 33$ mice; R of Rayleigh 0.51 ± 0.07 ; **Figure 1D**). Sleep spindles thus cluster on the 50-s timescale during NREMS, consistent with other reports in rodent and human.^{32,33} This indicates that NREMS fluctuates between spindle-rich and spindle-poor substates that are now known to cause varying spontaneous and sensory arousability.^{27,28,34}

To elucidate the role of noradrenergic signaling for infraslow variations in spindle density, we pharmacologically blocked noradrenergic receptors in thalamus, where sleep spindles originate.³⁰ C57BL/6J mice were injected with a mix of α - and β -noradrenergic antagonists (0.1 mM prazosin hydrochloride and 5 mM (S)-(-)-atenolol; 150 nL) or control artificial cerebrospinal fluid (ACSF) (150 nL) locally into the somatosensory thalamus (**Figure 1E**). Exposure to these antagonists preserved the properties of individual spindles (**Figure S1B**). However, noradrenergic antagonist, but not ACSF injections, resulted in a rapid and reversible reduction of the strength of the 0.02-Hz fluctuation in sigma power in the ipsilateral S1 LFP, but not in the contralateral EEG (**Figures 1E, 1F, and S2**). Moreover, instead of being clustered, sleep spindles now appeared irregularly and at a mean density that was ~2-fold higher (**Figure 1F**). Noradrenergic signaling in thalamus appears thus necessary for the generation of spindle-free periods and their repeated clustering on the infraslow timescale.

Activity of the LC is necessary and sufficient for spindle clustering during NREMS

To optogenetically interfere with the activity of the noradrenergic LC during NREMS in a time-controlled manner, we virally infected LC neurons of DBH-Cre mice³⁵ to express excitatory (hChR2(H134R)_mCherry [ChR2_mCherry]) or inhibitory (Jaws_s_EGFP) opsins. Using immunohistochemistry for tyrosine hydroxylase (TH) in a subgroup of 4 animals, we found that ~80% of TH-positive cells expressed the viral transgene (**Figure S3**). We then implanted these animals with EEG/electromyogram (EMG), an S1 LFP electrode and an optic fiber positioned uni- (for ChR2-expressing animals) or bilaterally (for Jaws-expressing animals) over the LC (**Figures 2A and 2B**). Optimal fiber positioning was ensured through intra-surgical pupil diameter monitoring (**Figure S4**) and through post hoc anatomical verification (**Figure S3**). Using closed-loop monitoring of vigilance states, we first stimulated the LC specifically during NREMS at a low frequency (1 Hz; **Figure 2C**) and confirmed the successful expression of the opsins postmortem (**Figures 2D and S3**). The 1-Hz frequency is within the range of spontaneous LC unit activity during NREMS^{20,21,36} and does not cause arousal in optogenetic studies.^{16,21} Stimulation sessions took place in the first 20 min of each hour during 8 h of the light phase (ZT1–ZT9), with light or sham (light source turned off) stimulation alternating over successive recording days. Light stimulation in NREMS produced a rapid and almost complete suppression of sigma power and of sleep spindles. The effect lasted as long as light was present and instantly

(B) Fourier transform over sigma and delta power dynamics. Lines show means \pm standard error (shadowed). Diagonal lines, area underneath the Fourier transform used to quantify the strength of the 0.02-Hz fluctuation; horizontal dashed line, mean values from 0.08 to 0.12 Hz.

(C) Single NREMS bout indicated in (A). Vertically jittered dots, automatically detected spindle events. See also **Figure S1**.

(D) Example S1 LFP raw trace showing automatically identified sleep spindles (**Figure S1**). “Phase coupling,” sleep spindle occurrence along the 0.02-Hz fluctuation phases; arrow, mean Rayleigh vector; “Rayleigh test,” quantification of the non-uniform distribution via R values ($p < 1.0 \times 10^{-16}$). Means \pm standard errors are superimposed over individual datapoints. See also **Figure S2**.

(E) Scheme for intracranial local pharmacology and sleep recordings (**STAR Methods**). Prazosin hydrochloride (Praz) (0.1 mM) and (S)-(-)-atenolol (Aten) (5 mM) or artificial cerebrospinal fluid (ACSF) were co-injected with the red fluorescent dye Alexa Fluor 594 for post hoc verification. TRN, thalamic reticular nucleus; VPM, ventroposterior medial thalamus. Traces indicate hypnogram, sleep spindles, and sigma power for two representative mice injected either with Aten + Praz (top) or ACSF (bottom). Dashed horizontal line, mean sigma power in baseline.

(F) Strength of the 0.02-Hz oscillation (as explained in B) and of sleep-spindle densities for intracranial pharmacology experiments. Gray lines show individual animals; black, red, and blue lines show means \pm standard error.

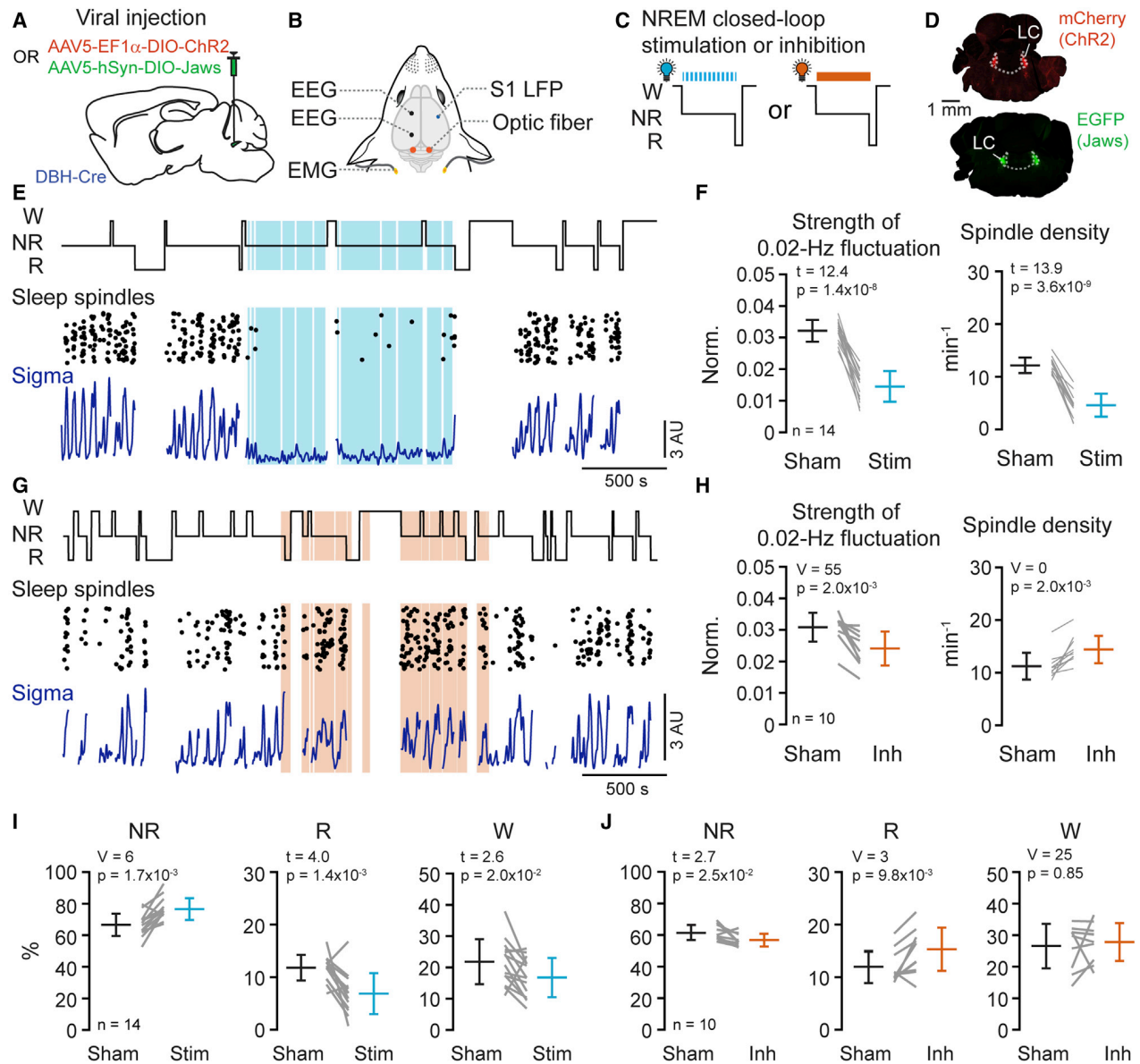


Figure 2. Optogenetic interrogation of the LC during NREMS

(A) Viral injection strategy for DBH-Cre mice.
 (B) Experimental schematic showing electrode and fiber positioning.
 (C) Schematic indicating closed-loop stimulation (blue) or inhibition (orange) of LC during NR.
 (D) Representative fluorescent micrographs for two mice included in the dataset. See also [Figure S3](#).
 (E) Representative recording for optogenetic LC stimulation (1 Hz; blue shading) during NR, arranged as in Figure 1E. See also [Figure S4](#).
 (F) Quantification of effects on 0.02-Hz fluctuation strength and on spindle density. Gray lines show individual animals; black and blue lines show means \pm standard error.
 (G and H) Same as (E) and (F) for optogenetic inhibition of LC. Note that optogenetic inhibition was carried out almost exclusively during online detection of NREMS.
 (I and J) Quantification of times spent in NR, R, or W during LC stimulation (I) or inhibition (J) and sham periods.

recovered once optogenetic stimulation stopped ([Figure 2E](#)), decreasing the strength of the 0.02-Hz fluctuation and sleep-spindle density ([Figure 2F](#)). These effects were not mediated directly by light or by light-induced heat propagation into LC, as verified via a computational model of heat propagation³⁷ and in control animals expressing mCherry alone ([Figure S4](#)).

Conversely, continuous optogenetic inhibition according to the same experimental protocol locked sigma power at high levels and disrupted its fluctuation, increasing spindle density ([Figures 2G and 2H](#)). These results demonstrate that LC activity is both necessary and sufficient for the 0.02-Hz fluctuation and the clustering of sleep spindles.

To explore whether LC stimulation or inhibition affected sleep architecture, we quantified total time spent in the different vigilance states. We found that LC stimulation prolonged total time spent in NREMS at the expense of REMS and wakefulness (Figure 2I), whereas LC inhibition had opposite effects (Figure 2J). These architectural alterations were not accompanied by significant changes in relative delta power in S1 (stimulation: increase by 7%, $t = -1.69$, $p = 0.11$; inhibition: decrease $<1\%$, $t = -1.33$, $p = 0.90$). Therefore, a low level of LC activity appears to consolidate NREMS. This could be explained by an inhibitory action of monoaminergic signaling to enter REMS, which would cause NREMS to continue while we stimulated LC.^{10,22,38}

LC signaling in thalamus, but not in cortex, underlies sleep-spindle clustering

From their thalamic site of origin, sleep-spindle activity propagates to cortical circuits.³⁰ As LC innervates both thalamic and cortical brain areas,^{18,39} we tested the involvement of both innervation sites in the effects observed by direct LC stimulation. We placed the optic fiber over somatosensory thalamus or S1. For S1, the optic fiber stub was glued to the S1 LFP electrode at a distance of 800–1,200 μm over the tip ($n = 5$ mice) or inserted into layers 2/3, with the S1 electrode implanted below at an angle of 40° ($n = 3$ mice; Figures 3A and 3B). Confocal imaging demonstrated the presence of ChR2-expressing noradrenergic fibers in both thalamus and cortex (Figure 3C). Light stimulation of thalamic LC fibers reproduced the suppressive effects observed with direct LC stimulation (Figures 3D and 3E). In contrast, cortical stimulation was ineffective, irrespective of whether the optic fiber was positioned over the cortex or inserted into layer 2/3 (Figures 3F and 3G). This finding suggests that LC fibers targeting upper or lower cortical layers did not play a major role in regulating LFP correlates of sigma activity in S1. Note that all 8 animals implanted with an optic fiber over the cortex responded to direct optogenetic LC stimulation and are included in the data in Figure 2F. Thus, synaptic noradrenergic activity within the thalamus, but not the cortex, appears to sensitively control the clustering of sleep spindles measured in S1, in agreement with the pharmacological results in Figure 1.

LC activity fluctuates on an infraslow timescale during NREMS

LC cells can discharge action potentials in both tonic and phasic modes during wakefulness, and both these modes have also been proposed to occur during NREMS.^{10,20,22,36} To address whether time variations in LC activity were relevant for the infraslow clustering of sleep spindles, we restricted the optogenetic manipulation of LC activity to distinct phases of the infraslow cycles. We detected these phases online through a machine-learning algorithm and triggered optogenetic activation based on whether sigma power started to rise or decline, thereby targeting preferentially high or low arousability periods (Figure 4).²⁸ When we optogenetically activated LC whenever sigma power started rising, the 0.02-Hz fluctuation was suppressed (Figures 4A and 4B). This indicates that sigma increases, and sleep-spindle generation, are not compatible with LC activity. Conversely, when we inhibited LC during sigma power decline, sleep-spindle density persisted at high levels (Figures 4C and 4D). The decline in sigma power thus required LC activity. These two results are

best compatible with LC activity increasing on infraslow timescales to suppress sleep spindles.

Based on this result, we predicted that the converse experiment, stimulating LC when sigma power declined or inhibiting it when sigma power rose, would not disrupt infraslow dynamics. Intriguingly, for the first condition, successive cycles of high sigma power kept appearing (Figure 4E). Close inspection revealed that cycles appeared at shorter time intervals (sham: 52.9 ± 0.7 s; stim: 44.6 ± 1.7 s; $n = 9$; $p = 5.0 \times 10^{-7}$; paired t test) and were more regular, as evident by the decreased peak-to-peak variability (Figure 4F). Strengthening LC activity when it was already naturally high thus entrained a regular and faster infraslow fluctuation. When we specifically inhibited LC activity during online detected periods of low sigma activity, an entrainment was again observed, with interpeak intervals shortened (sham: 53.7 ± 2.6 , inhibition: 50.8 ± 1.5 s, $n = 9$; paired t test, $p = 3.6 \times 10^{-3}$; Figure 4G) and regularized (Figure 4H). LC activity, already low at this moment, could thus be further inhibited by the light. This indicates that enforcing LC silence facilitates sigma level buildup and regularizes spindle clustering. Together, these results unravel a functionally relevant LC activity pattern during NREMS that interchanges between high and low activity at infraslow timescales.

Thalamic NA levels during NREMS are high and fluctuate on infraslow time intervals

LC activity is expected to increase NA within thalamus and to stimulate noradrenergic receptors. However, the time course of free NA is unknown, leaving open causal relationships to sleep-spindle dynamics. We used fiber photometry to measure free NA levels in somatosensory thalamus across the sleep-wake cycle by expressing the newly developed fluorescent NA biosensors GRAB_{NE1h} or GRAB_{NE1m} that have high and moderate affinity for NA, respectively.⁴⁰ Mice expressing one of the two biosensors in thalamus were implanted for sleep monitoring and fiber photometry. The fluorescence signals varied across the three vigilance states, declining in particular during REMS, similar to recent measures based on GRAB sensors in prefrontal cortex (Figure 5A).²² We were surprised to see that NA levels during NREMS overlapped with the ones of quiet wakefulness within the first hours of the light phase, overall yielding higher mean values (Figures 5B and S5). We further observed rapid increases in NA levels when we stimulated the awake mouse in its cage by approaching one of our hands (Figure S6), indicating that thalamic NA levels followed variations in arousal during wakefulness. Focusing on NREMS bouts only, NA signals fluctuated in a manner inversely correlated with sigma power (with a time lag <0.5 s; $t = -1.0$; $p = 0.35$) and displaying recurrent negative peaks at infraslow intervals (Figure 5C). To resolve the time course of noradrenergic signaling on a cycle-to-cycle basis, we detected all infraslow sigma power cycles taking place during NREMS (excluding transitional periods) and examined the corresponding dynamics of free NA (Figure 5D). NA levels rose rapidly before sigma power declined, consistent with the suppressant effects of LC activity. Conversely, NA levels declined as sigma power was rising. Across animals, NA had already declined when sigma levels started rising, producing a non-symmetrical U-shaped time course. A similar profile of NA dynamics and similarly higher mean NA levels for NREMS compared to quiet

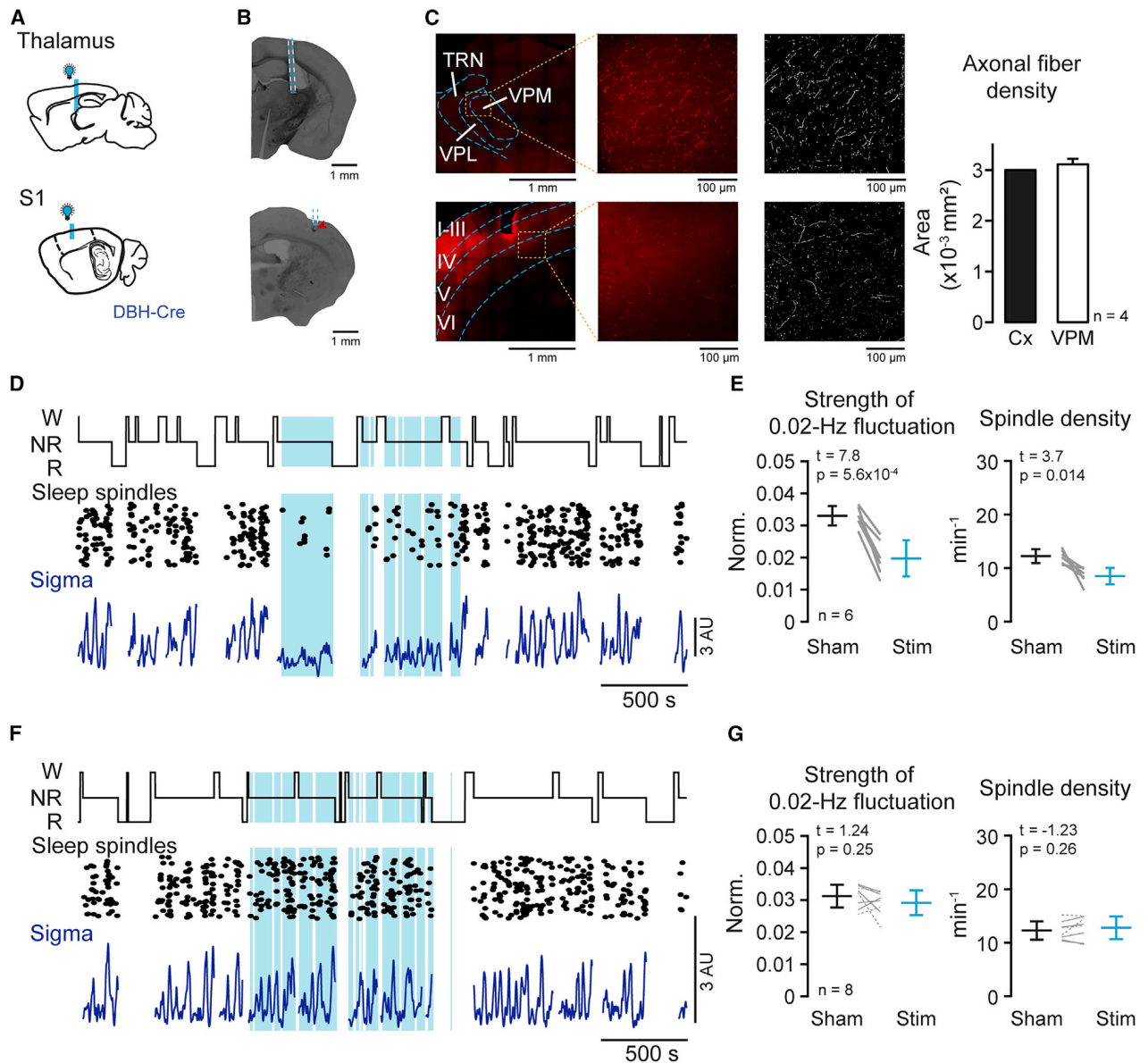


Figure 3. Optogenetic interrogation of LC afferents in thalamus or cortex during NREMS

(A) Experimental schematic indicating optic fiber positioning over somatosensory thalamus (VPM, top) or cortex (S1, bottom). (B) Example anatomical verification of optic fiber locations (dotted lines). Red arrowhead, tip of LFP electrode. See also Figure S3. (C) Representative images of noradrenergic LC fiber density within the thalamus (top) and S1 cortex (bottom). From left to right, full region of interest, selected area for quantification, and binary mask used for analysis (STAR Methods). Bar graphs, total area covered by bright pixels in a 0.13 mm² square. Data are means \pm standard error. (D) Representative traces for optogenetic stimulation of thalamic LC fiber terminals during NREMS; similar arrangement as in Figure 2E. See also Figure S4. (E) Corresponding quantification of effects on 0.02-Hz fluctuation strength and on spindle density. Data presented as in Figure 2F. (F and G) Same layout for experimental results in which the optogenetic fiber was positioned over cortex. Dotted lines, data from 3 animals with optic fiber positioned within layers 2/3.

wakefulness were observed for the medium-affinity biosensor GRAB_{NE1m} (Figure S6), indicating that the natural dynamics of NA across vigilance states were detectable even for a >10-fold lower sensor affinity.⁴⁰ Therefore, noradrenergic signaling in thalamic sensory nuclei is higher than in quiet wakefulness during the resting phase and tightly matches the infraslow dynamics of sleep spindles.

Ionic mechanisms underlying NA-induced membrane depolarizations

When exposed to NA, thalamic cells *in vitro* depolarize such that they no longer engage in spindle-like rhythms.⁴¹ However, the properties of LC-evoked postsynaptic potentials are unknown. We hence combined patch-clamp recordings with optogenetic LC fiber stimulation and studied evoked responses in

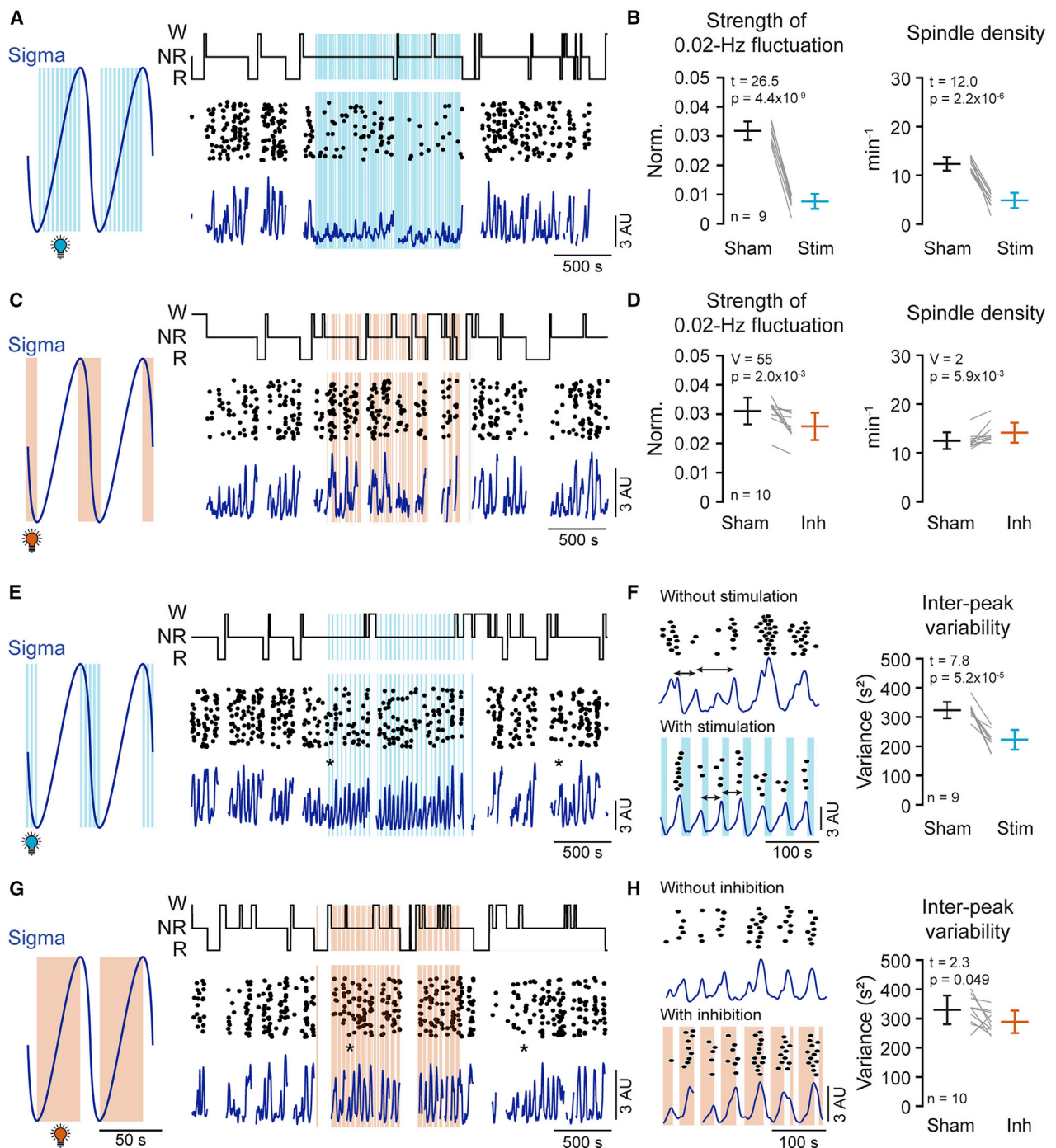


Figure 4. Optogenetic interrogation of LC during spindle-rich or poor periods of NREMS

(A) 1-Hz optogenetic stimulation of LC, restricted to NREMS periods with increasing sigma power. Blue waveform, schematic fluctuation to indicate the timing of the light stimuli. Representative traces are arranged as in Figure 2E.

(B) Quantification of effects on 0.02-Hz fluctuation strength and on spindle density, presented as in Figure 2F.

(C and D) Optogenetic inhibition of LC, restricted to NREMS periods with declining sigma power. Figure panels are analogous to (A) and (B). See also Figures S3 and S4.

(E) Optogenetic stimulation of LC when sigma power declined. Figure panels are analogous to (A) and (C).

(F) Expanded traces, from (*) in (E). Double-headed arrows denote interpeak intervals of the sigma power fluctuation. The regularization of the interpeak intervals in stimulation conditions is quantified through the variance (shown on the right). Note also the tighter temporal alignment between sleep spindles and sigma power. Gray lines show individual animals; black and blue lines show means \pm standard error.

(G and H) Optogenetic inhibition of LC when sigma power increased. Figure panels are analogous to (E) and (F).

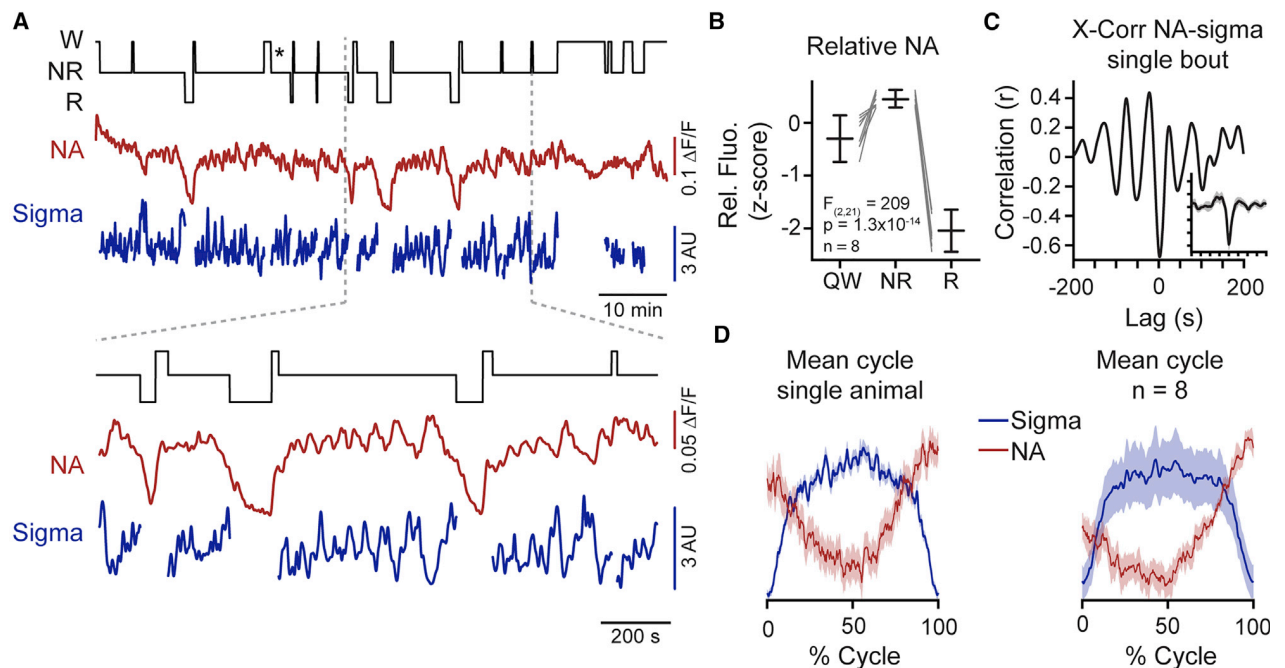


Figure 5. Free noradrenaline levels in thalamus are high and fluctuate during NREMS

(A) Representative recording showing (from top to bottom) hypnogram, relative fluorescence derived from the NA biosensor GRAB_{NE1th}, and sigma power dynamics. Expanded portion is shown below. *, bout selected for analysis in (C). See also Figures S5 and S6.

(B) Z-scored relative fluorescence derived from the NA biosensor GRAB_{NE1th} in quiet wakefulness (QW), NR, and R. One-way ANOVA followed by post hoc t tests is shown, which yielded: QW versus NR: $t = -4.56$, $p = 2.6 \times 10^{-3}$; QW versus R: $t = 9.27$, $p = 3.35 \times 10^{-5}$; and NR versus R: $t = 39.26$, $p = 1.81 \times 10^{-9}$. Gray lines show individual animals; black lines show means \pm standard error.

(C) Cross-correlation (X-Corr) between sigma power and the NA biosensor signal for a single NREMS bout. Inset: means \pm standard error for X-Corr across all bouts in the recording, with identical axis scaling.

(D) Left: overlay of mean \pm standard error for sigma power dynamics across all infraslow cycles with corresponding NA biosensor signal for one mouse. Right: mean \pm standard error across 8 animals.

thalamocortical and thalamic reticular neurons, both of which are involved in sleep-spindle generation.³⁰ From DBH-Cre mice expressing ChR2 in LC, we prepared coronal thalamic slices and recorded from cells in the ventrobasal complex, which contains the somatosensory thalamus. Thalamocortical and thalamic reticular neurons were distinguished based on location within the slice, membrane potential, and action potential discharge patterns (Figure S7). Optogenetic stimulation induced a slow membrane depolarization for stimulation frequencies at 1, 3, and 10 Hz (Figure 6A). Amplitudes of evoked potentials ranged between 0.8 and 4.5 mV with onset latencies of 1.25–6.9 s and decayed with a slow time course lasting 66–106 s (Figures 6B and S7). Only onset latency was modulated by stimulation frequency. The optogenetically evoked noradrenergic currents measured in cells voltage clamped at -70 mV were blocked by atenolol (10 μ M in bath), indicating involvement of β -adrenergic receptors (Figures 6C and 6D).⁴¹ Furthermore, the current response was eliminated by bath application of 1.5–3 mM Cs⁺ (Figures 6E and 6F), a blocker of hyperpolarization-activated cation channels.⁴² Both atenolol and Cs⁺ produced outward currents, indicating a standing receptor and current activation.

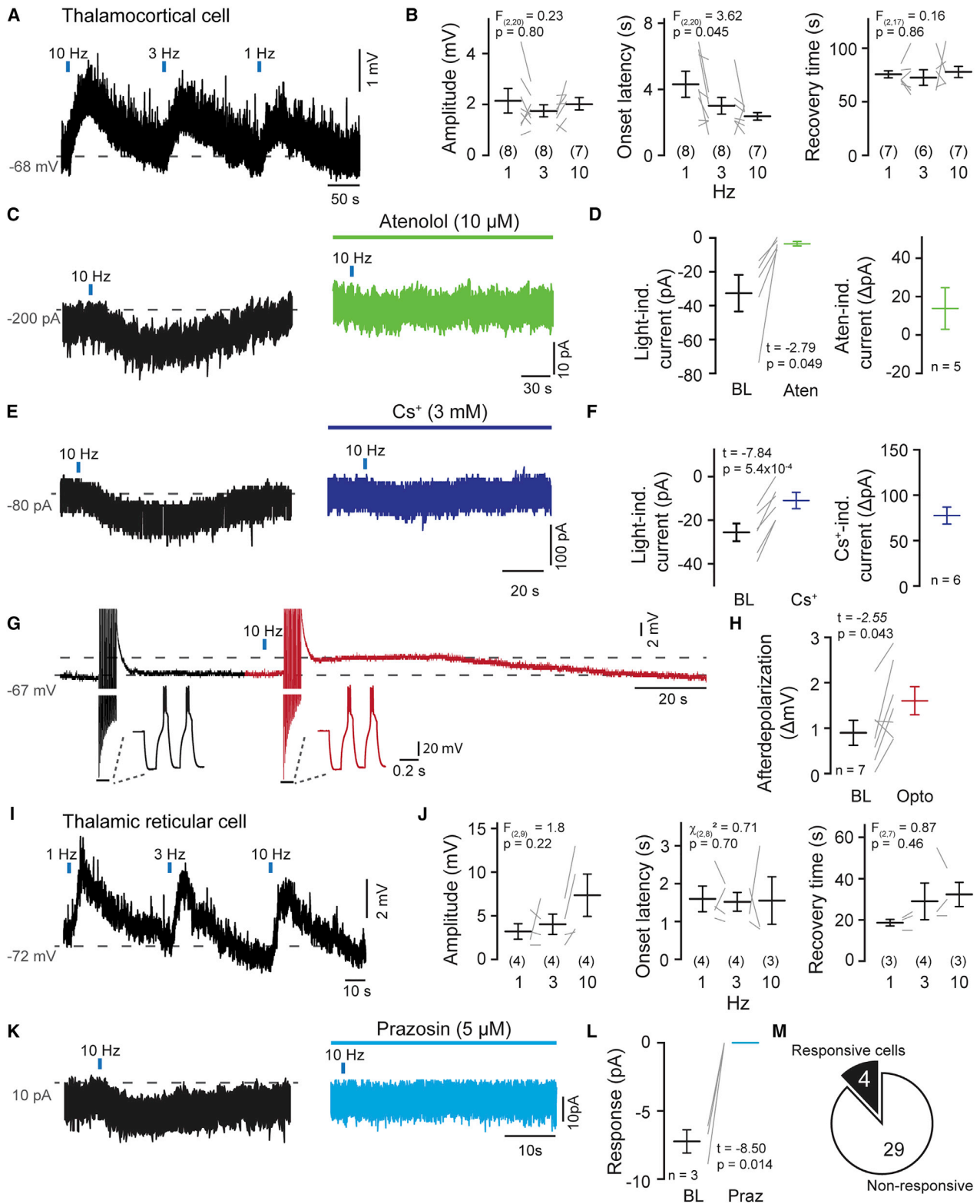
To estimate the time course of action of NA on spindle-related cellular activity, we combined optogenetic stimulation of LC fibers with negative current injections to generate repetitive low-threshold burst discharges,⁴³ known to occur during sleep

spindles (Figure 6G).³⁰ This resulted in a persistent afterdepolarization that was larger and longer than the one generated by cellular bursting alone (Figure 6H). The coincidence of sleep spindle activity with NA release thus generates a prolonged period of cellular depolarization, known to be sufficient to render thalamocortical cells refractory to synaptically driven burst discharge that is necessary to engage in a next sleep spindle.^{30,43}

Light-induced depolarizations were also observed in thalamic reticular cells recorded in the somatosensory sector of thalamic reticular nucleus (TRN) (Figures 6I and 6J). Corresponding currents were largely blocked by the α 1-adrenergic antagonist prazosin (5 μ M in bath; Figures 6K and 6L).⁴¹ However, <15% of TRN cells showed a detectable current response (Figure 6M), suggesting that TRN cells could be heterogeneous in terms of noradrenergic responsiveness. Thalamic reticular cells thus also respond with slowly decaying membrane depolarizations when exposed to NA release from LC fibers.

The LC coordinates heart-rate variations with infraslow brain rhythms

During mouse NREMS, the heart rate (HR) fluctuates on an infraslow timescale and is anticorrelated to sigma power.²⁷ We conjointly monitored HR and sigma power in freely sleeping C57BL/6J mice (Figures 7A and 7B) and used peripheral cardiac pharmacology to determine which branch of the autonomic



(legend on next page)

nervous system controlled the infraslow variations in HR. The HR variations were suppressed by the peripheral parasympathetic antagonist methylatropine (10 mg kg⁻¹; **Figures 7C and 7D**),⁴⁴ but not by the peripheral sympathetic antagonist atenolol (1 mg kg⁻¹; **Figures 7E and 7F**).⁴⁵

LC activity has been implied in parasympathetically driven HR variability in humans⁴⁶ and, in rodents, augments inhibitory input to preganglionic cardiac vagal neurons.⁴⁷ Therefore, we next tested whether optogenetic manipulation of LC affected variations in HR. Indeed, 1-Hz-LC stimulation during NREMS disrupted the infraslow HR variations (**Figure 7G**) and decreased their anticorrelation with sigma power (**Figure 7H**). To directly evaluate the capability of LC in entraining HR variations, we stimulated LC specifically when sigma power declined, as done before (see **Figure 4E**). This visibly augmented HR variations and imposed anticorrelations with sigma power with side peaks showing an infraslow periodicity (**Figures 7I and 7J**). These data show that the LC is a source of HR variability during NREMS on an infraslow timescale. Moreover, LC is capable of coordinating sigma power and HR in a manner that supports a critical role in the generation of arousability variations during NREMS.

DISCUSSION

Noradrenergic cell groups in the pontine brainstem are conserved across fish, amphibians, reptiles, birds, and mammals^{48–50} and play universal roles during wakefulness, attention, and stress.^{15,17–19} Here, we find that NA signaling remained high during NREMS, with mean NA levels exceeding the ones of quiet wakefulness in sensory thalamus, a major subcortical area critical for routing sensory information. Moreover, at intervals close to a minute (~50 s), NA levels fluctuated around this mean, dividing NREMS into two substates previously associated with high and low sensory arousability.^{27,28,34} Noradrenergic signaling is thus an integral part of mammalian NREMS. This reverses the conventional notion of NREMS as a state of overall low monoaminergic signaling compared to wakefulness.^{6,51} Finally, consistent with the original general hypothesis, mammalian NREMS has an innate and high vulnerability to disruption that arises from powerful wake-promoting circuit control of NREMS substates.

Infraslow LC activity during NREMS could be conserved across mammals

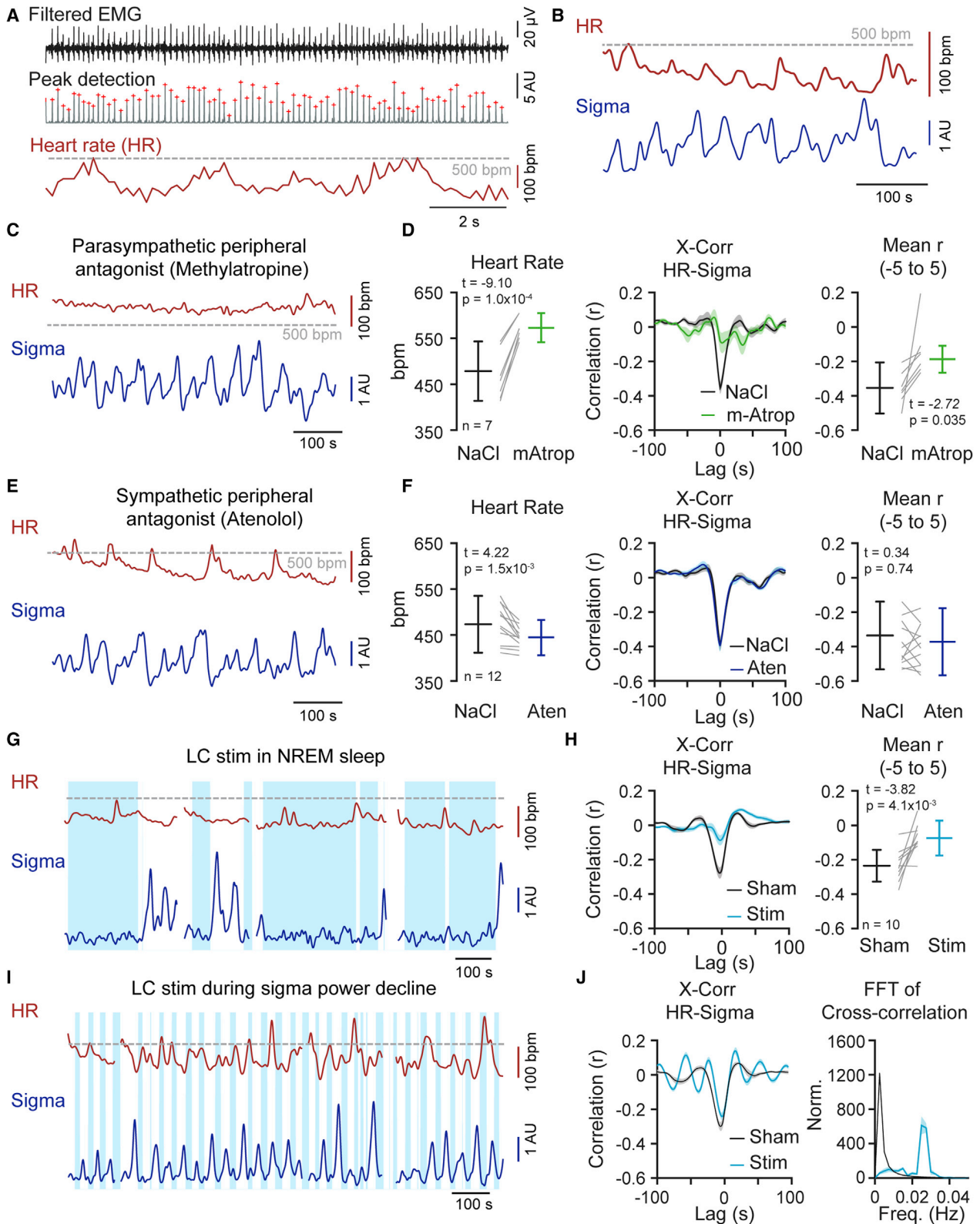
The infraslow timescale has been repeatedly observed in diverse dynamic measures of mammalian NREMS⁵² and also appears in reptile sleep,⁵³ suggesting that fluctuating noradrenergic signaling is phylogenetically preserved. Through timed optogenetic interference, we causally link LC activity to central and autonomic correlates of these fluctuations. In human functional imaging studies of deep NREMS (stage N3), the LC and surrounding areas increase activity in intervals of ~20 s.²⁴ Moreover, fast spindle activity appears clustered over tens of seconds, in particular during light NREMS (stage N2).^{27,32,33} These are timescales compatible with infraslow LC activity in human NREMS. Our study could renew efforts to identify the origins of the human-specific cyclic alternating patterns in the EEG. These events occur preferentially at the beginning and end of a NREMS period and lead to higher arousability every 20–40 s.⁵⁴ Intriguingly, the integrity of cyclic alternating patterns has been recently linked to the preservation of noradrenergic signaling in the LC and in forebrain.⁵⁵ The implication of LC in other electrical and hemodynamic correlates of infraslow fluctuations also remains to be assessed.⁵²

Infraslow noradrenergic fluctuations are found in thalamus and cortex during NREMS

The mean discharge rates of LC units during NREMS presented in pioneering studies from rodent^{8–10,20,21,23}, cat,^{7,11,56} and monkey^{8,9} are minor compared to wakefulness. However, subgroups of units showed activity levels remarkably similar for NREMS and quiet wakefulness.^{21,23,36} Moreover, some LC units tended to fire in bursts during NREMS,²⁰ which could increase the amount of NA released.^{57,58} Together, LC unit data from NREMS are scarce but seem compatible with the high free NA levels we monitored. Interestingly, free NA levels measured with the GRAB biosensors in mouse prefrontal cortex also overlap for NREMS and wakefulness. These authors overall found higher mean wake NA levels, consistent with strongly variable NA levels across substates of wakefulness and recording conditions.²² We focused on the early resting phase, when awake animals mostly sit undisturbed and poorly stimulated in their familiar environment. LC activity thus likely remained low in these moments, yet it is possible

Figure 6. Optogenetic LC fiber stimulation *in vitro* evoked slow noradrenergic membrane depolarizations in thalamic neurons

- (A) Representative recording from a whole-cell-patched thalamocortical cell exposed to three successive light stimuli (blue bars).
- (B) Quantification of evoked response amplitudes, onset latencies, and recovery times as explained in **Figure S7**. One-way ANOVA followed by post hoc t tests yielded 1 Hz versus 3 Hz: $t = 1.6$, $p = 0.13$; 1 Hz versus 10 Hz: $t = 2.7$, $p = 0.024$; and 3 Hz versus 10 Hz: $t = 1.1$, $p = 0.29$. In this and all panels, gray lines denote results from individual cells; black and colored lines show means \pm standard error. See also **Figure S7**.
- (C) Current response in a voltage-clamped thalamocortical neuron, held at -70 mV to 10 Hz light pulses before (left) and after (right) bath application of the β -adrenergic antagonist atenolol.
- (D) Left: quantification of light-induced currents in baseline (BL) and Aten. Right: Aten-induced positive holding current shift.
- (E and F) Same as (C) and (D) after bath application of Cs⁺.
- (G) Example recording from a thalamocortical neuron injected with repetitive negative current pulses to evoke low-threshold Ca²⁺ bursts, with hyperpolarizing voltage responses and action potentials truncated. Responses to two current pulses are expanded and untruncated in insets. Bursts were followed by an afterdepolarization that was prolonged when light pulses (10 Hz, 4 pulses, blue bar) preceded current injections. Dashed lines aligned to baseline membrane potential and peak of the afterdepolarization.
- (H) Quantification of afterdepolarizations in BL (without light exposure) and with light exposure (Opto).
- (I and J) As (A) and (B) for a representative recording from a thalamic reticular neuron.
- (K) Current response in a voltage-clamped thalamic reticular neuron, held at -70 mV to 10 Hz light pulses before (left) and after (right) bath application of the α_1 -adrenergic antagonist prazosin.
- (L) Quantification of current response amplitude in BL and during Praz.
- (M) Number of thalamic reticular neurons responding to LC optogenetic fiber stimulation.



(legend on next page)

that the NA profile could evolve differently during the dark active, and more attentive, phase of the light-dark cycle, as well as across brain regions.

Measures of intracellular Ca^{2+} levels at the mouse LC cell population level were recently found to peak about once a minute during NREMS,²² suggesting that numerous LC units are synchronously active on an infraslow timescale. These results combined with ours in sensory thalamus indicate that a fluctuating neuromodulatory tone of NA is an integral part of major thalamocortical circuits during NREMS. Further work is needed to determine the extent to which NA fluctuations generalize across functionally different thalamocortical circuits, as well as to other forebrain areas innervated by LC.

Besides LC, other neuromodulatory systems are known to be active during NREMS. An interesting case is the coincidence of noradrenergic and cholinergic activity that occurs for tens of seconds prior to NREM-REMS transitions^{6,12,13} and that gives rise to brief moments of high spindle activity, while hippocampus starts to generate REMS-related theta rhythmicity.⁵⁹ Infraslow activity variations during NREMS were recently also reported in REMS-regulating midbrain and medullar neurons^{60,61} that target the serotonin-releasing raphe nuclei.⁶² Therefore, not only NA but also levels of other neuromodulatory neurotransmitters, such as serotonin, are likely to fluctuate during NREMS.⁶³

LC-dependent control of sensory arousability during NREMS

LC activity is known to control sensory arousability through several mechanisms.^{17,18} First, LC responds to sensory stimuli;⁶⁴ therefore, if LC neurons depolarize and discharge more action potentials, sensory throughput will be facilitated.^{16,23} Second, sleep-spindle-related oscillatory electrical activity along the thalamocortical axis protects sleep from external perturbations.³⁰ These protective effects will be lost when LC activates. Third, sensory-evoked discharge of single or multiple thalamic and cortical units is strengthened by LC stimulation, with thalamic neurons increasing sensory responsiveness more robustly.^{18,65} The density of LC fiber varicosities is higher in somatosensory thalamus compared to cortical areas in rat,³⁹ and DBH immunoreactivity is overall highest in sensorimotor over other cortical areas in human.⁶⁶ These findings offer several entry points to further examine how noradrenergic modulation of thalamic circuits facilitates the processing of sensory stimuli during states of NREMS.

Noradrenergic signaling does not terminate spindles but regulates their clustering

Based on sleep spindles measured in EEG¹⁰ and in hippocampal LFPs,²¹ the LC is thought to terminate sleep spindles. We

establish here a mechanistic opposition between NA levels and spindle-generating circuit activity and can refine this widespread interpretation. Although we suppressed local sleep spindles in S1 via optogenetic LC activation, we could not observe major alterations in sleep-spindle properties when we pharmacologically antagonized noradrenergic signaling in thalamus. Yet in previous work, our spindle-detection algorithm reliably discriminated between fine cortical area-specific sleep-spindle properties.²⁹ Furthermore, synaptic evoked potentials caused by NA release rose slowly over seconds and are thus unlikely to shortcut individual spindle events. Based on these combined cellular and *in vivo* data, we propose that noradrenergic signaling is tailored to generate prolonged relatively spindle-free periods through depolarizing thalamic neurons, but it does not act rapidly enough to terminate individual spindles.

The cellular and ionic mechanisms underlying noradrenergic control of sleep-spindle clustering

Although infraslow cellular and glial mechanisms have been reported,^{43,67} their roles in sleep are open. Through combining *in vivo* and *in vitro* approaches, we identify an infraslow time course of action for NA released from LC terminals that likely underlies sleep-spindle variations. NA induces a slowly decaying membrane depolarization through activation of both $\alpha 1$ or β receptors in thalamocortical and thalamic reticular neurons, which retards the re-engagement of these cells in sleep-spindle generation. Furthermore, we could entrain rhythmically the infraslow fluctuations when we reinforced or attenuated LC activity at appropriate moments. The reinforcement of LC activity most likely triggered membrane depolarizations more sequentially across large cell populations. Conversely, the attenuation of LC activity likely removed spurious LC activity and allowed a more synchronous entry and exit of thalamic circuits within the infraslow cycles. While LC activity thus regulates spindle clustering at the population level, other processes could preferentially terminate spindle activity in individual cells (reviewed in Fernandez and Lüthi³⁰). Furthermore, we cannot exclude that the optogenetic interference with LC activity modified cortical and/or brainstem feedback afferents onto LC that could have accelerated its infraslow activity.

The slow membrane depolarizations elicited by low-frequency LC stimulation in the thalamus add to growing evidence that even minor levels of LC activity are functionally efficient in the forebrain.^{68,69} Thalamic LC-fiber-elicited responses were present and relatively uniform in amplitude and time course over the 1–10 Hz frequency range. The stability of the response across stimulation frequencies ensures that thalamic membrane potentials are homogeneously depolarized across many

Figure 7. The LC coordinates heart rate and infraslow brain rhythms

- (A) Extraction of heart rate (HR) from EMG traces. Raw high-pass-filtered EMG (top), used for peak detection (middle) and HR (bottom) calculation, are shown.
- (B) Representative NREMS traces showing sigma power dynamics and corresponding HR after an intraperitoneal (i.p.) injection of NaCl.
- (C) Example traces illustrating the effects of the parasympathetic antagonist methylatropine (mAtrop) (10 mg kg^{-1}) on HR and sigma power dynamics.
- (D) Left: quantification of mean HR following NaCl or mAtrop injections; middle: corresponding X-Corr; right: values of the X-Corr between -5 and $+5$ s. Black and colored lines denote means \pm standard error in this and all following panels.
- (E and F) As (C) and (D) for injection of a sympathetic peripheral antagonist (Aten; 1 mg kg^{-1}).
- (G) Example traces illustrating the effects of LC stimulation (stim) in NREMS on HR and sigma power dynamics. See also [Figures S3](#) and [S4](#).
- (H) Corresponding X-Corrs quantified as in (D) and (F).
- (I) As (G), for LC stimulation restricted to periods of declining sigma power.
- (J) Corresponding X-Corr and its Fourier transform highlight the appearance of an infraslow peak.

neurons. Ultrastructural studies indeed suggest that noradrenergic terminals in the rodent ventrobasal thalamic complex do not form well-defined synaptic contacts,⁷⁰ suggesting that released NA may diffuse from the site of release into the extracellular medium. In support of such a signaling scheme, we find that noradrenergic receptors activated by optogenetic LC fiber stimulation are the same as the ones targeted by bath-applied NA.⁴¹

Noradrenergic signaling is a source of HR variations during NREMS

We identified the parasympathetic system to underlie the infraslow variations in HR, as was also observed for infraslow pupil diameter variations.³⁴ The LC increases HR through several pathways, in part through a suppression of activity in the parasympathetic preganglionic vagal nuclei.⁴⁷ Our data suggest that this pathway could play a role in HR regulation during NREMS. Furthermore, 1-Hz stimulation during NREMS abolished infraslow HR variations, demonstrating that LC coordinates the infraslow activity patterns in brain and heart. Such coordinated fluctuations suggest that LC units become synchronized across dorsal and ventral regions of the LC, in which forebrain- and hindbrain-projecting cells preferentially reside, respectively.⁷¹ Appropriate timing of LC stimulation also increased the fluctuations of the HR and strengthened central and peripheral coordination on the infraslow timescale. The direct demonstration of LC's role in HR variability will renew interest in the varied autonomic and central manifestations of arousal-like events during NREMS.⁷²

We find that mammalian sleep harnesses on wake promotion to enable sensory vigilance. This insight requires a renewal of current models of sleep-wake control in which reciprocal and exclusive antagonism is prevalent between sleep- and wake-promoting brain areas, including the LC.⁶ Still, the origins of how LC becomes periodically activated and overcomes this antagonism during NREMS remain to be addressed. On the one hand, the LC is engaged in multiple and recurrent input-output loops across fore-, mid-, and hindbrain that could induce infraslow rhythms through the summed actions of slow synaptic inputs.⁷¹ Of particular interest are recent studies identifying infraslow fluctuations of neuronal activity in midbrain and dorsomedullary areas involved in the regulation of NREM-REMS cycle that innervate LC.^{60,61} Alternatively, it is important to consider that the majority of LC neurons respond sensitively to CO₂ and pH changes.⁷³ Such chemosensation may activate LC during NREMS, for example, in response to pulsatile brain fluid exchange that, intriguingly, is anticorrelated to infraslow hemodynamic signals.⁷⁴ Based on such mechanistic insights, it will be interesting to probe whether the enhanced appearance of cyclic alternating patterns in cases of sleep-related breathing disorders, such as sleep apnea, can be controlled with noradrenergic antagonists.⁵⁴ Furthermore, there is strong evidence that LC and sleep disruptions could be linked in post-traumatic stress disorders;¹⁸ in neurodegenerative diseases, such as Alzheimer's and Parkinson's disease;⁷⁵ and in insomnia.⁵ We are now able to concretize questions into possible noradrenergic origins of a large variety of primary and secondary sleep disorders, in which hyperarousals, autonomic arousals, and movement-related arousals prominently feature.

STAR★METHODS

Detailed methods are provided in the online version of this paper and include the following:

- KEY RESOURCES TABLE
- RESOURCE AVAILABILITY
 - Lead contact
 - Materials availability
 - Data and code availability
- EXPERIMENTAL MODEL AND SUBJECT DETAILS
 - Subjects
- METHOD DETAILS
 - Viral injections
 - Other surgical procedures
 - *In vivo* electrophysiological recordings
 - Procedures for intracranial pharmacology
 - Procedures for *in vivo* optogenetics
 - Procedures for *in vivo* fiber photometry
 - *In vitro* electrophysiological recordings
 - Pharmacological manipulation of heart rate
 - Histology
- QUANTIFICATION AND STATISTICAL ANALYSIS
 - *In vivo* data analysis
 - Statistical analysis

SUPPLEMENTAL INFORMATION

Supplemental information can be found online at <https://doi.org/10.1016/j.cub.2021.09.041>.

ACKNOWLEDGMENTS

We thank Paul Steffan and Dr. David McCormick for providing us with the original DBH-Cre breeders. We greatly appreciate the time-efficient support provided to us from Drs. Yulong Li and Jessie Feng regarding the NA sniffers. Particular thanks go to the animal caretaking team headed by Michelle Blom and to Titouan Tromme, who took so good care of our animal lines. Expert veterinary advice was given by Drs. Delphine Perret and Laure Sériot. We thank Dr. Jean Pierre Hornung for support in histological analysis. We appreciate the helpful exchange regarding optogenetic LC manipulation and NA sniffer experimentation with Drs. Simone Astori, Antoine Adamantidis, Ernesto Durán, Oxana Eschenko, Jessie Feng, Paul Franken, Celia Kjaerby, Maiken Nedergaard, Niels Niethard, Patricia Bonnavion, and Andrea Volterra. We are indebted to Francesca Siclari, Christoph Michel, and Francesco Petrelli for insightful discussions on the human noradrenergic system. Simone Astori, Francesca Siclari, and Freddy Weber provided valuable input on preliminary versions of the manuscript. All lab members provided constructive input to this study throughout the experimental period and to preliminary versions of the manuscript. This study was funded by The Swiss National Science Foundation (no. 310030-184759 to A.L.), Etat de Vaud, and a FBM UNIL PhD Fellowship to A.O.-F.

AUTHOR CONTRIBUTIONS

Conceptualization, A.L., A.O.-F., R.C., and L.M.J.F.; methodology, A.L. and A.O.-F.; software, A.O.-F. and R.C.; validation, A.L., A.O.-F., R.C., and L.M.J.F.; formal analysis, A.O.-F.; investigation, A.O.-F., R.C., G.V., A.G.-G., and G.K.; resources, A.L. and A.O.-F.; data curation, A.O.-F. and L.M.J.F.; writing – original draft, A.L. and A.O.-F.; writing – review & editing, L.M.J.F., R.C., G.V., A.G.-G., G.K., A.O.-F., and A.L.; visualization, A.O.-F. and L.M.J.F.; supervision, A.L.; project administration, A.L.; funding acquisition, A.L. and A.O.-F.

DECLARATION OF INTERESTS

The authors declare no competing interests. A.L. is a member of the journal's advisory board.

Received: May 11, 2021

Revised: August 9, 2021

Accepted: September 15, 2021

Published: October 13, 2021

REFERENCES

1. Van Someren, E.J., Cirelli, C., Dijk, D.J., Van Cauter, E., Schwartz, S., and Chee, M.W. (2015). Disrupted sleep: from molecules to cognition. *J. Neurosci.* **35**, 13889–13895.
2. Mascetti, G.G. (2021). Adaptation and survival: hypotheses about the neural mechanisms of unihemispheric sleep. *Laterality* **26**, 71–93.
3. Mander, B.A., Winer, J.R., and Walker, M.P. (2017). Sleep and human aging. *Neuron* **94**, 19–36.
4. Siclari, F., Valli, K., and Arnulf, I. (2020). Dreams and nightmares in healthy adults and in patients with sleep and neurological disorders. *Lancet Neurol.* **19**, 849–859.
5. Van Someren, E.J.W. (2021). Brain mechanisms of insomnia: new perspectives on causes and consequences. *Physiol. Rev.* **101**, 995–1046.
6. Saper, C.B., Fuller, P.M., Pedersen, N.P., Lu, J., and Scammell, T.E. (2010). Sleep state switching. *Neuron* **68**, 1023–1042.
7. Chu, N.S., and Bloom, F.E. (1974). Activity patterns of catecholamine-containing pontine neurons in the dorso-lateral tegmentum of unrestrained cats. *J. Neurobiol.* **5**, 527–544.
8. Foote, S.L., Aston-Jones, G., and Bloom, F.E. (1980). Impulse activity of locus coeruleus neurons in awake rats and monkeys is a function of sensory stimulation and arousal. *Proc. Natl. Acad. Sci. USA* **77**, 3033–3037.
9. Rajkowski, J., Kubiak, P., and Aston-Jones, G. (1994). Locus coeruleus activity in monkey: phasic and tonic changes are associated with altered vigilance. *Brain Res. Bull.* **35**, 607–616.
10. Aston-Jones, G., and Bloom, F.E. (1981). Activity of norepinephrine-containing locus coeruleus neurons in behaving rats anticipates fluctuations in the sleep-waking cycle. *J. Neurosci.* **1**, 876–886.
11. Hobson, J.A., McCarley, R.W., and Wyzinski, P.W. (1975). Sleep cycle oscillation: reciprocal discharge by two brainstem neuronal groups. *Science* **189**, 55–58.
12. el Mansari, M., Sakai, K., and Jouvet, M. (1989). Unitary characteristics of presumptive cholinergic tegmental neurons during the sleep-waking cycle in freely moving cats. *Exp. Brain Res.* **76**, 519–529.
13. Kayama, Y., Ohta, M., and Jodo, E. (1992). Firing of 'possibly' cholinergic neurons in the rat laterodorsal tegmental nucleus during sleep and wakefulness. *Brain Res.* **569**, 210–220.
14. Dahlstroem, A., and Fuxe, K. (1964). Evidence for the existence of monoamine-containing neurons in the central nervous system. I. Demonstration of monoamines in the cell bodies of brain stem neurons. *Acta Physiol. Scand. Suppl.* **232**, 1–55.
15. Berridge, C.W. (2008). Noradrenergic modulation of arousal. *Brain Res. Brain Res. Rev.* **58**, 1–17.
16. Carter, M.E., Yizhar, O., Chikahisa, S., Nguyen, H., Adamantidis, A., Nishino, S., Deisseroth, K., and de Lecea, L. (2010). Tuning arousal with optogenetic modulation of locus coeruleus neurons. *Nat. Neurosci.* **13**, 1526–1533.
17. Aston-Jones, G., and Cohen, J.D. (2005). An integrative theory of locus coeruleus-norepinephrine function: adaptive gain and optimal performance. *Annu. Rev. Neurosci.* **28**, 403–450.
18. Poe, G.R., Foote, S., Eschenko, O., Johansen, J.P., Bouret, S., Aston-Jones, G., Harley, C.W., Manahan-Vaughan, D., Weinschenker, D., Valentino, R., et al. (2020). Locus coeruleus: a new look at the blue spot. *Nat. Rev. Neurosci.* **21**, 644–659.
19. Sara, S.J., and Bouret, S. (2012). Orienting and reorienting: the locus coeruleus mediates cognition through arousal. *Neuron* **76**, 130–141.
20. Eschenko, O., Magri, C., Panzeri, S., and Sara, S.J. (2012). Noradrenergic neurons of the locus coeruleus are phase locked to cortical up-down states during sleep. *Cereb. Cortex* **22**, 426–435.
21. Swift, K.M., Gross, B.A., Frazer, M.A., Bauer, D.S., Clark, K.J.D., Vazey, E.M., Aston-Jones, G., Li, Y., Pickering, A.E., Sara, S.J., and Poe, G.R. (2018). Abnormal locus coeruleus sleep activity alters sleep signatures of memory consolidation and impairs place cell stability and spatial memory. *Curr. Biol.* **28**, 3599–3609.e4.
22. Kjaerby, C., Andersen, M., Hauglund, N., Ding, F., Wang, W., Xu, Q., Deng, S., Kang, N., Peng, S., Sun, Q., et al. (2020). Dynamic fluctuations of the locus coeruleus-norepinephrine system underlie sleep state transitions. *bioRxiv*. <https://doi.org/10.1101/2020.09.01.274977>.
23. Hayat, H., Regev, N., Matosevich, N., Sales, A., Paredes-Rodriguez, E., Krom, A.J., Bergman, L., Li, Y., Lavigne, M., Kremer, E.J., et al. (2020). Locus coeruleus norepinephrine activity mediates sensory-evoked awakenings from sleep. *Sci. Adv.* **6**, eaaz4232.
24. Dang-Vu, T.T., Schabus, M., Desseilles, M., Albouy, G., Boly, M., Darsaud, A., Gais, S., Rauchs, G., Sterpenich, V., Vandewalle, G., et al. (2008). Spontaneous neural activity during human slow wave sleep. *Proc. Natl. Acad. Sci. USA* **105**, 15160–15165.
25. Gais, S., Rasch, B., Dahmen, J.C., Sara, S., and Born, J. (2011). The memory function of noradrenergic activity in non-REM sleep. *J. Cogn. Neurosci.* **23**, 2582–2592.
26. Zerbi, V., Floriou-Servou, A., Markicevic, M., Vermeiren, Y., Sturman, O., Privitera, M., von Ziegler, L., Ferrari, K.D., Weber, B., De Deyn, P.P., et al. (2019). Rapid reconfiguration of the functional connectome after chemo-genetic locus coeruleus activation. *Neuron* **103**, 702–718.e5.
27. Lecci, S., Fernandez, L.M.J., Weber, F.D., Cardis, R., Chatton, J.-Y., Born, J., and Lüthi, A. (2017). Coordinated infraslow neural and cardiac oscillations mark fragility and offline periods in mammalian sleep. *Sci. Adv.* **3**, e1602026.
28. Cardis, R., Lecci, S., Fernandez, L.M., Osorio-Forero, A., Chu Sin Chung, P., Fulda, S., Decosterd, I., and Lüthi, A. (2021). Cortico-autonomic local arousals and heightened somatosensory arousability during NREMS of mice in neuropathic pain. *eLife* **10**, e65835.
29. Fernandez, L.M., Vantomme, G., Osorio-Forero, A., Cardis, R., Béard, E., and Lüthi, A. (2018). Thalamic reticular control of local sleep in mouse sensory cortex. *eLife* **7**, e39111.
30. Fernandez, L.M.J., and Lüthi, A. (2020). Sleep spindles: mechanisms and functions. *Physiol. Rev.* **100**, 805–868.
31. Andriillon, T., and Kouider, S. (2020). The vigilant sleeper: neural mechanisms of sensory (de)coupling during sleep. *Curr. Opin. Physiol.* **15**, 47–59.
32. Lázár, Z.I., Dijk, D.J., and Lázár, A.S. (2019). Infraslow oscillations in human sleep spindle activity. *J. Neurosci. Methods* **316**, 22–34.
33. Antony, J.W., Piloto, L., Wang, M., Pacheco, P., Norman, K.A., and Paller, K.A. (2018). Sleep spindle refractoriness segregates periods of memory reactivation. *Curr. Biol.* **28**, 1736–1743.e4.
34. Yüzgeç, Ö., Prsa, M., Zimmermann, R., and Huber, D. (2018). Pupil size coupling to cortical states protects the stability of deep sleep via parasympathetic modulation. *Curr. Biol.* **28**, 392–400.e3.
35. Harris, J.A., Hirokawa, K.E., Sorensen, S.A., Gu, H., Mills, M., Ng, L.L., Bohn, P., Mortrud, M., Ouellette, B., Kidney, J., et al. (2014). Anatomical characterization of Cre driver mice for neural circuit mapping and manipulation. *Front. Neural Circuits* **8**, 76.
36. Eschenko, O., and Sara, S.J. (2008). Learning-dependent, transient increase of activity in noradrenergic neurons of locus coeruleus during slow wave sleep in the rat: brain stem-cortex interplay for memory consolidation? *Cereb. Cortex* **18**, 2596–2603.
37. Stujenske, J.M., Spellman, T., and Gordon, J.A. (2015). Modeling the spatiotemporal dynamics of light and heat propagation for in vivo optogenetics. *Cell Rep.* **12**, 525–534.

38. Wyatt, R.J., Chase, T.N., Kupfer, D.J., Scott, J., and Snyder, F. (1971). Brain catecholamines and human sleep. *Nature* 233, 63–65.
39. Agster, K.L., Mejias-Aponte, C.A., Clark, B.D., and Waterhouse, B.D. (2013). Evidence for a regional specificity in the density and distribution of noradrenergic varicosities in rat cortex. *J. Comp. Neurol.* 521, 2195–2207.
40. Feng, J., Zhang, C., Lischinsky, J.E., Jing, M., Zhou, J., Wang, H., Zhang, Y., Dong, A., Wu, Z., Wu, H., et al. (2019). A genetically encoded fluorescent sensor for rapid and specific *in vivo* detection of norepinephrine. *Neuron* 102, 745–761.e8.
41. Lee, K.H., and McCormick, D.A. (1996). Abolition of spindle oscillations by serotonin and norepinephrine in the ferret lateral geniculate and perigeniculate nuclei *in vitro*. *Neuron* 17, 309–321.
42. Lüthi, A., and McCormick, D.A. (1998). H-current: properties of a neuronal and network pacemaker. *Neuron* 21, 9–12.
43. Lüthi, A., and McCormick, D.A. (1998). Periodicity of thalamic synchronized oscillations: the role of Ca²⁺-mediated upregulation of I_h. *Neuron* 20, 553–563.
44. Smith, R.D., Grzelak, M.E., and Coffin, V.L. (1994). Methylatropine blocks the central effects of cholinergic antagonists. *Behav. Pharmacol.* 5, 167–175.
45. Neil-Dwyer, G., Bartlett, J., McAinsh, J., and Cruickshank, J.M. (1981). β -adrenoceptor blockers and the blood-brain barrier. *Br. J. Clin. Pharmacol.* 11, 549–553.
46. Mather, M., Joo Yoo, H., Clewett, D.V., Lee, T.H., Greening, S.G., Ponzio, A., Min, J., and Thayer, J.F. (2017). Higher locus coeruleus MRI contrast is associated with lower parasympathetic influence over heart rate variability. *Neuroimage* 150, 329–335.
47. Wang, X., Piñol, R.A., Byrne, P., and Mendelowitz, D. (2014). Optogenetic stimulation of locus coeruleus neurons augments inhibitory transmission to parasympathetic cardiac vagal neurons via activation of brainstem α 1 and β 1 receptors. *J. Neurosci.* 34, 6182–6189.
48. Noronha-de-Souza, C.R., Bícago, K.C., Michel, G., Glass, M.L., Branco, L.G., and Gargaglioni, L.H. (2006). Locus coeruleus is a central chemoreceptive site in toads. *Am. J. Physiol. Regul. Integr. Comp. Physiol.* 291, R997–R1006.
49. Smeets, W.J., and González, A. (2000). Catecholamine systems in the brain of vertebrates: new perspectives through a comparative approach. *Brain Res. Brain Res. Rev.* 33, 308–379.
50. Totah, N.K.B., Logothetis, N.K., and Eschenko, O. (2019). Noradrenergic ensemble-based modulation of cognition over multiple timescales. *Brain Res.* 1709, 50–66.
51. Jones, B.E. (2020). Arousal and sleep circuits. *Neuropsychopharmacology* 45, 6–20.
52. Watson, B.O. (2018). Cognitive and physiologic impacts of the infraslow oscillation. *Front. Syst. Neurosci.* 12, 44.
53. Libourel, P.A., Barrillot, B., Arthaud, S., Massot, B., Morel, A.L., Beuf, O., Herrel, A., and Luppi, P.H. (2018). Partial homologies between sleep states in lizards, mammals, and birds suggest a complex evolution of sleep states in amniotes. *PLoS Biol.* 16, e2005982.
54. Parrino, L., Ferri, R., Bruni, O., and Terzano, M.G. (2012). Cyclic alternating pattern (CAP): the marker of sleep instability. *Sleep Med. Rev.* 16, 27–45.
55. Doppler, C.E.J., Smit, J.A.M., Hommelsen, M., Seger, A., Horsager, J., Kinnerup, M.B., Hansen, A.K., Fedorova, T.D., Knudsen, K., Otto, M., et al. (2021). Microsleep disturbances are associated with noradrenergic dysfunction in Parkinson's disease. *Sleep* 44, zsab040.
56. Rasmussen, K., Morilak, D.A., and Jacobs, B.L. (1986). Single unit activity of locus coeruleus neurons in the freely moving cat. I. During naturalistic behaviors and in response to simple and complex stimuli. *Brain Res.* 371, 324–334.
57. Florin-Lechner, S.M., Druhan, J.P., Aston-Jones, G., and Valentino, R.J. (1996). Enhanced norepinephrine release in prefrontal cortex with burst stimulation of the locus coeruleus. *Brain Res.* 742, 89–97.
58. Dugast, C., Cespeglio, R., and Suaud-Chagny, M.F. (2002). *In vivo* monitoring of evoked noradrenaline release in the rat anteroventral thalamic nucleus by continuous amperometry. *J. Neurochem.* 82, 529–537.
59. Durán, E., Oyanedel, C.N., Niethard, N., Inostroza, M., and Born, J. (2018). Sleep stage dynamics in neocortex and hippocampus. *Sleep (Basel)* 41, zsy060.
60. Stucynski, J.A., Schott, A.L., Baik, J., Chung, S., and Weber, F. (2021). Regulation of REM sleep by inhibitory neurons in the dorsomedial medulla. *bioRxiv*. <https://doi.org/10.1101/2020.11.30.405530>.
61. Weber, F., Hoang Do, J.P., Chung, S., Beier, K.T., Bikov, M., Saffari Doost, M., and Dan, Y. (2018). Regulation of REM and non-REM sleep by periaqueductal GABAergic neurons. *Nat. Commun.* 9, 354.
62. Gervasoni, D., Peyron, C., Rampon, C., Barbagli, B., Chouvet, G., Urbain, N., Fort, P., and Luppi, P.H. (2000). Role and origin of the GABAergic innervation of dorsal raphe serotonergic neurons. *J. Neurosci.* 20, 4217–4225.
63. Wan, J., Peng, W., Li, X., Qian, T., Song, K., Zheng, J., et al. (2021). A genetically encoded sensor for measuring serotonin dynamics. *Nat. Neurosci.* 24, 746–752.
64. Takahashi, K., Kayama, Y., Lin, J.S., and Sakai, K. (2010). Locus coeruleus neuronal activity during the sleep-waking cycle in mice. *Neuroscience* 169, 1115–1126.
65. Devilbiss, D.M., and Waterhouse, B.D. (2004). The effects of tonic locus coeruleus output on sensory-evoked responses of ventral posterior medial thalamic and barrel field cortical neurons in the awake rat. *J. Neurosci.* 24, 10773–10785.
66. Gaspar, P., Berger, B., Febvret, A., Vigny, A., and Henry, J.P. (1989). Catecholamine innervation of the human cerebral cortex as revealed by comparative immunohistochemistry of tyrosine hydroxylase and dopamine- β -hydroxylase. *J. Comp. Neurol.* 279, 249–271.
67. Hughes, S.W., Lörincz, M.L., Parri, H.R., and Crunelli, V. (2011). Infraslow (<0.1 Hz) oscillations in thalamic relay nuclei basic mechanisms and significance to health and disease states. *Prog. Brain Res.* 193, 145–162.
68. Bacon, T.J., Pickering, A.E., and Mellor, J.R. (2020). Noradrenaline release from locus coeruleus terminals in the hippocampus enhances excitation-spike coupling in CA1 pyramidal neurons via β -adrenoceptors. *Cereb. Cortex* 30, 6135–6151.
69. Liang, Y., Shi, W., Xiang, A., Hu, D., Wang, L., and Zhang, L. (2021). The NAergic locus coeruleus-ventrolateral preoptic area neural circuit mediates rapid arousal from sleep. *Curr. Biol.* 31, 3729–3742.e5.
70. Nothias, F., Onteniente, B., Roudier, F., and Peschanski, M. (1988). Immunocytochemical study of serotonergic and noradrenergic innervation of the ventrobasal complex of the rat thalamus. *Neurosci. Lett.* 95, 59–63.
71. Schwarz, L.A., and Luo, L. (2015). Organization of the locus coeruleus-norepinephrine system. *Curr. Biol.* 25, R1051–R1056.
72. Parrino, L., Halasz, P., Tassinari, C.A., and Terzano, M.G. (2006). CAP, epilepsy and motor events during sleep: the unifying role of arousal. *Sleep Med. Rev.* 10, 267–285.
73. Madan, V., and Jha, S.K. (2012). A moderate increase of physiological CO(2) in a critical range during stable NREM sleep episode: a potential gateway to REM sleep. *Front. Neurol.* 3, 19.
74. Fultz, N.E., Bonmassar, G., Setsompop, K., Stickgold, R.A., Rosen, B.R., Polimeni, J.R., and Lewis, L.D. (2019). Coupled electrophysiological, hemodynamic, and cerebrospinal fluid oscillations in human sleep. *Science* 366, 628–631.
75. Kelberman, M., Keilholz, S., and Weinshenker, D. (2020). What's that (blue) spot on my MRI? Multimodal neuroimaging of the locus coeruleus in neurodegenerative disease. *Front. Neurosci.* 14, 583421.
76. Vantomme, G., Rovó, Z., Cardis, R., Béard, E., Katsioudi, G., Guadagno, A., Perrenoud, V., Fernandez, L.M.J., and Lüthi, A. (2020). A thalamic reticular circuit for head direction cell tuning and spatial navigation. *Cell Rep.* 31, 107747.

STAR★METHODS

KEY RESOURCES TABLE

REAGENT or RESOURCE	SOURCE	IDENTIFIER
Antibodies		
Goat anti-mouse Alexa Fluor 488	Invitrogen	Cat# A32723; RRID: AB_2633275
Mouse anti-TH	Immunostar	Cat# 22941; RRID:AB_572268
Rabbit polyclonal Anti-mCherry	abcam	Cat# Ab183628; RRID:AB_2650480
Donkey anti-Rabbit Alexa Fluor 594	Invitrogen	Cat# R37119; RRID: AB_2556547
Bacterial and virus strains		
ssAAV5/2-hEF1 α -dlox-hChR2(H134R) mCherry(rev)-dlox-WPRE-hGHp(A)	VVF Zurich	v80-5
pAAV5-CAG-FLEX-rc [Jaws-KGC-GFP-ER2]	Addgene	84445-AAV5
AAV8-hSyn-FLEX-Jaws- KGC-GFP-ER2	UNC Vector Core	N/A
ssAAV5/2-hSyn1-dlox- Jaws_KGC_EGFP_ERES(rev)- dlox-WPRE-bGHp(A)-SV40p(A)	VVF Zurich	v508-5
ssAAV5/2-hEF1 α -dlox-mCherry(rev)-dlox- WPRE-hGHp(A)	VVF Zurich	V218-5
ssAAV9/2-hSyn1-GRAB_NEh-WPRE- hGHp(A)	VVF Zurich	v472-9
ssAAV9/2-hSyn1-GRAB_NEm-WPRE- hGHp(A)	VVF Zurich	v471-9
Chemicals, peptides, and recombinant proteins		
(S)-(-)-atenolol	Sigma-Aldrich	A7655
Prazosin hydrochloride	Sigma-Aldrich	P7791
Methylatropine bromide	Sigma-Aldrich	M1300000
Cesium chloride	Sigma-Aldrich	C3032-25G
Deposited data		
Raw and analyzed data	This paper	https://doi.org/10.5281/zenodo.5520888
MATLAB code	This paper	available from lead contact on request, see also https://github.com/Romain2-5/IntanLuthiLab .
Experimental models: Organisms/strains		
M. musculus, C57BL/6J	Jackson Laboratory	Jax: 000664
M. musculus, B6.FVB(Cg)-Tg(Dbh-cre) KH212Gsat/Mmucd	MMRRC, University of California, Davis	MMRRC_036778-UCD
Software and algorithms		
NIS-Elements 4.5	Nikon	N/A
Zen lite 2012	Zeiss	N/A
Adobe Photoshop 2020	Adobe Creative Cloud	N/A
Adobe Illustrator 2020, 2021	Adobe Creative Cloud	N/A
Clampex10.2	Molecular Devices	N/A
Clampfit v2.2	Molecular Devices	N/A
R 3.5.1	R Core Team	N/A
MATLAB 2015b, 2018a	MathWorks	N/A
Excel	Microsoft	N/A

RESOURCE AVAILABILITY

Lead contact

For information and request for resources should be directed to the lead contact, Anita Lüthi (anita.luthi@unil.ch)

Materials availability

The study did not produce any new materials or reagents.

Data and code availability

All data included in this publication will be stored on one of the servers of the University of Lausanne and will be made available by the lead contact upon request (<https://doi.org/10.5281/zenodo.5520888>). All Customized MATLAB scripts for analysis are available from the corresponding author upon reasonable request. For data acquisition and scoring, MATLAB scripts are available in the following GitHub repository: <https://github.com/Romain2-5/IntanLuthiLab>.

EXPERIMENTAL MODEL AND SUBJECT DETAILS

Subjects

Mice from the C57BL/6J line and from the B6.FVB(Cg)-Tg(Dbh-cre)KH212Gsat/Mmucd (MMRRC Stock#036778-UCD) line,³⁵ referred to here as DBH-Cre line, were bred on a C57BL/6J background and housed in a humidity- and temperature-controlled animal house with a 12 h / 12 h light-dark cycle (lights on at 9 am). Food and water were available *ad libitum* throughout all the experimental procedures. For viral injections, 2- to 7-week-old mice of either sex were transferred to a P2 safety level housing room with identical conditions 1 d prior to injection. For *in vivo* experimentation, animals were transferred to the recording room 3 d after viral injection and left to recover for at least 1 week prior to the implantation surgery, after which they were singly housed in standard-sized cages. The grids on top of the cage were removed and replaced by 30 cm-high Plexiglass walls. Fresh food was regularly placed on the litter and the water bottle inserted through a hole in the cage wall. Objects (tissues, paper rolls, ping-pong balls) were given for enrichment. For *in vitro* experimentation, animals were transferred 3 d after viral injection to a housing room with identical conditions and were used 3 – 6 weeks after injection. In total, 12 male C57BL/6J mice were used for intracranial pharmacological experiments, 19 male C57BL/6J mice for cardiac pharmacology experiments and 10 C57BL/6J (8 males and 2 females) mice for the fiber photometry experiments. From the DBH-Cre line, 27 (12 males and 15 females) heterozygous Cre ± animals were used for optogenetic experiments, and 14 (2 males and 12 females) for *in vitro* experiments. All experiments were conducted in accordance with the Swiss National Institutional Guidelines on Animal Experimentation and were approved by the Swiss Cantonal Veterinary Office Committee for Animal Experimentation.

METHOD DETAILS

Viral injections

Optogenetics *in vivo* and *in vitro*

Animals were anaesthetized with ketamine (83 mg kg⁻¹)/xylazine (3.5 mg kg⁻¹), kept on a thermal blanket to maintain body temperature around 37°C, and injected i.p. with carprofen (5 mg kg⁻¹) for analgesia. Mice were then head-fixed on a stereotaxic frame equipped with a head adaptor for young animals (Stoelting 51925). The scalp was disinfected, injected with a mix of lidocaine (6 mg kg⁻¹)/bupivacaine (2.5 mg kg⁻¹) for local anesthesia and opened with scissors exposing the desired region of the skull. For the injections, we used a thin glass pipette (5-000-1001-X, Drummond Scientific) pulled on a vertical puller (Narishige), initially filled with mineral oil, and backfilled with the virus-containing solution just prior to injection. Injections took place at an injection rate of 100 – 200 nL min⁻¹. For optogenetic stimulation experiments, 1 animal was injected with a ssAAV5/2-hEF1α-dlox-hChR2(H134R)-mCherry(rev)-dlox-WPRE-hGHp(A) (titer: 9.1x10¹² vg / ml, 0.8 – 1 μL; Zurich VVF) virus unilaterally in a region close to the LC. The stereotaxic coordinates were (relative to Bregma, given in mm here and throughout the rest of the [STAR Methods](#)): lateral (L) ± 1.28; antero-posterior (AP) –5.45, depth (D) –3.65, as done previously.¹⁶ Additionally, 10 animals were injected bilaterally with the same virus (0.3 – 0.6 μL) directly into the LC (L ± 1.05; AP –5.45; D –3.06) and 4 animals were injected unilaterally in the right LC. These viral injections yielded comparable results and data were pooled. For optogenetic inhibition, all animals were injected bilaterally into the LC (0.2 – 0.35 μL) with either pAAV5-CAG-FLEX-rc[Jaws-KGC-GFP-ER2] (7x10¹² vg / ml; n = 2, Addgene), AAV8-hSyn-FLEX-Jaws-KGC-GFP-ER2 (3.2x10¹² vg / ml; n = 3, UNC Vector Core) or ssAAV-5/2-hSyn1-dlox-Jaws_KGC_EGFP_ERES(rev)-dlox-WPRE-bGHp(A)-SV40p(A) (titer: 6.4x10¹² vg / ml; n = 5, VVF Zürich). For control experiments, 3 animals were injected with ssAAV5/2-hEF1α-dlox-mCherry(rev)-dlox-WPRE-hGHp(A) (titer: 7.3x10¹² vg / ml, 300 nL; Zurich VVF) unilaterally in the right LC.

Fiber photometry

For the assessment of NA dynamics in the thalamus, AAV viruses (ssAAV9/2-hSyn1-GRAB_NE1h-WPRE-hGHp(A), titer: 7.2x10¹² vg / ml, or ssAAV9/2-hSyn1-GRAB_NE1m-WPRE-hGHp(A), titer: 5.5x10¹² vg / ml, both from VVF Zürich) containing the plasmid encoding a NA sensor (pAAV-hSyn-GRAB_NE1h, Addgene Plasmid #123309, 8 animals, or pAAV-hSyn-GRAB_NE1m, Addgene Plasmid #123308, 2 animals, respectively)⁴⁰ were injected into the thalamus (500 nL; L 2.0; AP –1.6; D –3.0). After the injections,

the incision was sutured, and the area disinfected. Animals were carefully monitored and returned to the home cage once awake and moving around. Recovery time after injections took place for a minimum of 1 week before the next surgeries. Paracetamol was given in the water for the 4 postoperative days at a concentration of 2 mg ml⁻¹.

Other surgical procedures

For *in vivo* EEG/EMG combined with local field potential (LFP) recordings, electrode implantation was as previously described.^{27–29} In short, animals were anesthetized with isoflurane (1.5–2.5%) in a mixture of O₂ and N₂O. After analgesia (i.p. carprofen 5 mg kg⁻¹) and disinfection, animals were fixed in a Kopf stereotax and injected into the scalp with a mix of lidocaine (6 mg kg⁻¹)/bupivacaine (2.5 mg kg⁻¹) and a piece of the scalp was removed after 3–5 min, the skull exposed and the bone scratched to improve adhesion of the head implant. Then, we drilled small craniotomies (0.3–0.5 mm) over left frontal and parietal bones and positioned two conventional gold-coated wire electrodes in contact with the dura mater for EEG recordings. On the contralateral (right) side, a high-impedance tungsten LFP microelectrode (10–12 MΩ, 75 μm shaft diameter, FHC) was implanted in the primary somatosensory cortex (L 3; AP –0.7; D –0.85). Additionally, as a neutral reference, a silver wire (Harvard Apparatus) was inserted into the occipital bone over the cerebellum and two gold pellets were inserted into the neck muscles for EMG recordings. All electrodes were fixed using Loctite Schnellkleber 401 glue and soldered to a multisite connector (Barrettes Connectors 1.27 mm, male connectors, Conrad).

For intracranial injection of noradrenergic antagonists, we additionally made a craniotomy over the thalamus (L 2; AP –1.60) and covered it with a silicone-based sealant (Kwik-Cast Silicone Sealant, WPI). Additionally, we glued and cemented a light-weight metal head-post (Bourgeois Mécanique SAS, Lyon, France) onto the midline skull to perform painless head-fixation during injection of noradrenergic antagonists.

For optogenetic experiments, DBH-Cre animals were implanted with custom-made optic fibers.⁷⁶ A multimode fiber (225 μm outer diameter, Thorlabs, BFL37-2000/FT200EMT) was inserted and glued (heat-curable epoxy, Precision Fiber Products, ET-353ND-16OZ) to a multimode ceramic zirconia ferrule (Precision Fiber Products, MM-FER2007C-2300). The penetrating end was cut at the desired length with a carbide-tip fiber optic scribe (Precision Fiber Products, M1-46124). The outside end was then polished using fiber-polishing films (Thorlabs). For optogenetic stimulation of the LC cell bodies (n = 14 animals) a single 3-mm-long fiber stub was implanted directly over the LC (L 1.0; AP –5.4; D –2.3). Out of the 14 animals, 6 animals were also implanted with a 3 mm-optic fiber stub over the somatosensory thalamus (L 2.0; AP –1.7; D –2.5). For 5 additional animals, we implanted a custom-made optrode in S1 built with a high-impedance fine tungsten LFP microelectrodes (10–12 MΩ, 75 μm shaft diameter, FHC) glued to the stub of a 2 mm-optic fiber at a distance of 800–1,200 μm. The optrode was then inserted into S1 (L 3.0; AP –0.7; D –0.8). In the 3 additional animals, the optic fiber was not glued to the electrode but instead inserted into S1 (L 2.8; AP –0.7; D –0.3 to –0.4), while the LFP electrode was positioned at an angle of 40° below the optic fiber (L 3.0; AP –0.7; D –0.5 to –0.6). In this way, we ensured more intense illumination of the deep-layer LC fibers surrounding the LFP electrode. For optogenetic inhibition of the LC bodies (n = 10), bilateral optic fibers were implanted at a 20° lateral angle targeting the LC (L ± 1.84; AP –5.4; D –2.47). To establish the final coordinates of the optic fibers, pupil diameter changes were monitored in a subgroup of 5 animals while lowering the optic fiber and applying light stimuli (Figure S4; 10–30 pulses at 10 Hz). A custom-made software developed in MATLAB was used for image acquisition and data analysis (See [In vivo data analysis](#)).

For fiber photometry experiments, in addition to the recording electrodes, we implanted C57BL/6J animals (n = 10) with a premade 400 μm-thick optic fiber coupled to a cannula (MFC_400/430-0.66_3.5mm_ZF1 25(G)_FLT, Doris Lenses) over the dorsal and reticular thalamus (L 1.8; AP –1.7; D –2.5) at a speed of 1 mm min⁻¹.

Finally, a dental cement structure was built to fix the implant in place. After disinfection with iodine-based cream, animals were returned to their home cage and kept in careful monitoring. Animals were provided with paracetamol (2 mg mL⁻¹) in the drinking water for at least 4 days after the procedure.

In vivo electrophysiological recordings

Once recovered from the surgery, animals were habituated to the cabling for 5–7 days, followed by a baseline recording to ascertain the quality of the signals. We acquired the EEG, EMG and LFP signals at a 1 kHz sampling frequency using an Intan digital RHD2132 amplifier board and a RHD2000 USB Interface board (Intan Technologies) connected via SPI cables (RHD recording system, Intan Technologies). Homemade adapters containing an Omnetics - A79022-001 connector (Omnetics Connector) linked to a female Barrettes Connector (Conrad) were used as an intermediate between the head implant of the animal and the headstage. We acquired the data with MATLAB using the RHD2000 MATLAB toolbox and a customized software in the same environment.^{27,28}

Procedures for intracranial pharmacology

We gently and gradually habituated mice to being head-fixed by increasing the amount of time spent in head fixation daily from 5 min to 45 min over a period of 4–5 days. The rest of the time, the animals spent being tethered to the recording system in their home cage. On the first experimental day, we removed the silicone cover of the craniotomy in head-fixed conditions and positioned a glass pipette (5-000-1001-X, Drummond Scientific, pulled on a vertical Narishige PP-830 puller, tip size of 15–25 μm) over the craniotomy and waited for 30 min while gently touching the side of the craniotomy to simulate an injection. Then, we covered the craniotomy again with the silicone-based sealant and returned the animals to the home cage for an 8 h-baseline polysomnographic recording. The next day, we removed the silicone again and injected 150 nL of noradrenergic antagonists or ACSF at two different depths within the thalamus (D: –3.2 and –2.8 mm). For the experimental group, we infused a mixture of 0.1 mM prazosin hydrochloride (prazosin)

and 5 mM (S)-(-)-atenolol (atenolol), diluted in ACSF together with a red fluorescent dye (5 mM Alexa 594) for later confirmation of the injection site. For the control group, we injected ACSF together with Alexa 594. Per animal, only one injection was done (either blockers or ACSF) and the animal sacrificed after completion of the recording.

Procedures for *in vivo* optogenetics

All optogenetic manipulation took place during the first 20 min of each hour between ZT1 and ZT9. A custom-made close-loop detection of NREMS²⁸ was used for state specificity. In short, NREMS was detected whenever the delta (1–4 Hz) to theta (5–10 Hz) power ratio derived from the differential frontal-parietal EEG channels crossed a threshold for 2 out of 5 s and the EMG absolute values went below a threshold during at least 3 s. This led to reliable stimulation during NREMS (Figure 2), with the exception of a few brief interruptions that occurred during artifacts (e.g., muscle twitches). Stimulation sessions took place in the first 20 min of each hour during 8 h of the light phase (ZT1–9), with light or sham (light source turned off) stimulation alternating over successive recording days. Optogenetic stimulation of the LC cell bodies was carried out using a PlexBright Optogenetic Stimulation System (Plexon) coupled to a PlexBright Table-top blue LED Module (Wavelength 465 nm) at 1 Hz (light intensity of 2.8–3.2 mW at the tip). Stimulation of LC terminals in the thalamus or cortex was delivered at 2 Hz (Figure 3). Optogenetic inhibition of LC cell bodies was performed using a continuous stimulation with a PlexBright Table-top orange LED Module (Wavelength 620 nm, light intensity 1.55–1.7 mW at the tip) (Figure 2). Optogenetic stimulation (1 Hz) or inhibition (continuous) was also carried out specifically when sigma power declined or rose. This was achieved via a machine-learning-based closed-loop procedure²⁷ built with a multilayer perceptron model neural network of 10 neurons in the hidden layer and 3 output neurons (for rising or decreasing sigma power during NREM or to no stimulation, in the case of epochs outside this sleep state). The network was fed with the last 200 s of a 9th-order polynomial fit of the sigma activity (10–15 Hz) calculated for each s. The neural network was then trained, validated, and tested using the sleep scoring from 13 C57BL/6J animals (642,000 epochs) that were otherwise not included in this study. Online, the same data stretches obtained from the mouse in recording were used.

For each animal, multiple recording sessions took place with a random allocation of the stimulation protocol: i.e., optogenetic stimulation during NREMS in the LC bodies, its terminals (thalamus for 6 animals or cortex 8 animals), or stimulation of the LC bodies during spindle-enriched or -poor substates (in a subgroup of 9 mice). Similarly, for optogenetic inhibition of LC bodies, random allocation of inhibition protocols took place during NREMS (10 animals) or NREMS substates (10 animals).

Procedures for *in vivo* fiber photometry

After the recovery (> 7 d) and habituation to the cabling procedure (> 4 d), we performed two recordings per animal with at least one day between sessions. All recordings were limited to the first 3–4 h from ZT1 to minimize possible photobleaching. For fluorescent measurements, we used a pulse-width-modulated sinusoidal signal of 400 Hz using a Raspberry Pi3 (Raspberry Pi Foundation) to modulate a LEDD_2 driver (Doric Lenses) connected to a blue LED (CLED 465 nm; Doric Lenses). The power of the driver was set to 200 mA. The blue LED was coupled to a fluorescence MiniCube (iFMC4_IE(400-410)_E(E460-490)_F(500-550)_S, Doric Lenses) that redirected the light to the animal via a low autofluorescence 400- μ m-thick fiberoptic patchcord (MFP_400/430/1100-0.57_1m_FMC-ZF1.25_LAF, Doric Lenses). The cord was connected to the Optic fiberoptic Cannula (MFC_400/430-0.57_3mm_ZF1.25(G)_FLT) implanted in the head of the mouse. A photodetector integrated into the MiniCube head turned the emitted light from the fluorescent NA sensor into a current signal that was fed into an analog signal of the Intan RHD2132 amplifier board. To ensure that data collected were within the dynamic range of the biosensors, awake animals were exposed to the experimenter's hand held within the cage for 1 min moving gently but without touching the animal (Figure S6).

In vitro electrophysiological recordings

Thalamic brain slice recordings were performed as previously described in detail.^{29,76} Briefly, 3–6 weeks after viral injection, DBH-Cre mice aged 8–16 weeks were subjected to isoflurane anesthesia, after which they were decapitated, brains extracted and quickly immersed in ice-cold oxygenated sucrose solution (which contained in mM): NaCl 66, KCl 2.5, NaH₂PO₄ 1.25, NaHCO₃ 26, D-saccharose 105, D-glucose 27, L(+)-ascorbic acid 1.7, CaCl₂ 0.5 and MgCl₂ 7, using a sliding vibratome (Histocom). Brains were trimmed at the level of the brainstem, glued on the trimmed surface on an ice-cold metal blade and apposed to a supporting agar block on their ventral side. Acute 300- μ m-thick coronal brain slices were prepared in the same ice-cold oxygenated sucrose solution and kept for 30 min in a recovery solution at 35°C (in mM: NaCl 131, KCl 2.5, NaH₂PO₄ 1.25, NaHCO₃ 26, D-glucose 20, L(+)-ascorbic acid 1.7, CaCl₂ 2, MgCl₂ 1.2, myo-inositol 3, pyruvate 2) before being transferred to room temperature for at least 30 min. All recordings were done at room temperature.

Recording glass pipettes were pulled from borosilicate glass (TW150F-4) (WPI) with a DMZ horizontal puller (Zeitz Instr.) to a final resistance of 2–4 M Ω . Pipettes were filled with a K⁺-based intracellular solution that contained in mM: KGluconate 140, HEPES 10, KCl 10, EGTA 0.1, phosphocreatine 10, Mg-ATP 4, Na-GTP 0.4, pH 7.3, 290–305 mOsm. Slices were placed in the recording chamber of an upright microscope (Olympus BX50WI) and continuously superfused with oxygenated ACSF containing in mM: NaCl 131, KCl 2.5, NaH₂PO₄ 1.25, NaHCO₃ 26, D-glucose 20, L(+)-ascorbic acid 1.7, CaCl₂ 2 and MgCl₂ 1.2. Cells were visualized with differential interference contrast optics and 10X and 40X immersion objectives, and their location within the thalamic ventroposterior medial nucleus or within the somatosensory reticular thalamus could be verified based on previous studies in the lab.^{29,76} Infrared images were acquired with an iXon Camera X2481 (Andor). Prior to recording, pipette offset was zeroed, and the stability of the offset verified by monitoring pipette potential in the bath for 10 min. Drifts were < 0.5 mV / 10 min. Signals were amplified using a Multiclamp

700B amplifier, digitized via a Digidata1322A and sampled at 10 kHz with Clampex10.2 (Molecular Devices). Immediately after gaining whole-cell access, cellular membrane potential and access resistance were measured. Cells included had a resting membrane potential < -55 mV and access resistances < 15 M Ω . The cell types were identified based on their rebound bursting properties (Figure S7). Whole-field blue LED (Cairn Res) stimulation (455 or 470 nm, duration: 0.1 – 1 ms, maximal light intensity 0.16 and 0.75 mW/mm² for the two LEDs, respectively). Per slice, only one cell was recorded and exposed to light stimulation. For characterization of LC fiber-evoked membrane depolarizations, cells were held between -65 to -70 mV and exposed to 1 Hz, 3 Hz or 10 Hz stimulation (4 pulses each, of 100 μ s). Stimulation at different frequencies were applied in random order, with each frequency used maximally twice to avoid run-down of the evoked response. When light-induced depolarizations did not return to the original membrane potential, they were not included in the analysis. For the study of LC-dependent effects on prolonged afterdepolarizations, thalamocortical cells were first injected with series of repetitive negative current injections (100 – 300 pA, 20 pulses, each 120 ms) known to evoke rebound low-threshold Ca²⁺ bursts. Such protocols have been used previously to characterize the cell-intrinsic mechanisms accompanying sleep-spindle-related arrival of barrages of inhibitory synaptic potentials.⁴³ Following 1 – 2 such repetitive current injections (each followed by 3 – 5 min of recovery time), the current injections were preceded by LC fiber stimulation (10 Hz, 4 pulses) by 5 s, such that the maximum of the LC-evoked membrane depolarization coincided with the end of the negative current injections. For characterization of LC fiber-evoked membrane currents, cells were held in voltage-clamp at -70 mV. Baseline light-evoked currents were evoked maximally 1 – 2 times, followed by bath application of cesium chloride or noradrenergic antagonists ((S)-(-)-atenolol (Abcam) for thalamocortical cells or prazosin hydrochloride (Abcam) for thalamic reticular cells) for 5 – 10 min before the next optogenetic stimulation. The *in vitro* data were manually analyzed using Clampfit v2.2 and as illustrated in Figure S7.

Pharmacological manipulation of heart rate

After the recovery period of the electrode implantation (> 7 d), mice were habituated to the recording conditions for one week. Mice were injected intraperitoneally with NaCl, (S)-(-)-atenolol (1 mg kg⁻¹) (Abcam), a sympathetic antagonist or methylatropine bromide (10 mg kg⁻¹) (Sigma-Aldrich), a parasympathetic antagonist, both known to poorly permeate the blood-brain barrier.^{44,45} Injections were done at 9 am and followed by polysomnographic recording for 100 min. Two recording sessions per drug took place in an intercalated manner. Experimenters were blind to the drug injected.

Histology

After all recording sessions were completed, animals were injected intraperitoneally with a lethal dose of pentobarbital. For animals implanted with electrodes for LFP recording, the position of the electrode was marked via electro-coagulation (50 μ A, 8 – 10 s) of the region. Subsequently, ~ 45 mL of paraformaldehyde (PFA) 4% were perfused intracardially at a rate of ~ 2.5 mL min⁻¹. Brains were post-fixed for at least 24 h in PFA 4% cooled to 4°C. Brains were then sliced in 100 μ m-thick sections with a vibratome (Microtome Leica VT1000 S; speed: 0.25 – 0.5 mm s⁻¹ and knife sectioning frequency: 65 Hz) or a freezing microtome (Microm). Brain sections were directly mounted on slides or kept in well plates filled with 0.1 M PB for later processing. Then, we confirmed the position of LFP electrodes and optic fibers and the fluorescent expression of the injected viruses or local pharmacology injections with a Nikon SMZ25 Stereomicroscope equipped with a Nikon DS-Ri2 16 Mpx color camera. When needed, higher magnification images were acquired using an Axiovision Imager Z1 (Zeiss) microscope equipped with an AxioCam MRc5 camera (objectives used EC-Plan Neofluar 2.5x/0.075 ∞ /0.17, 5x/0.16 ∞ /0.17, 10x/0.3 ∞ /- or 20x/0.5 ∞ /0.17).

For quantification of TH-expressing neurons and the fraction of ChR2_mCherry neurons, 50- μ m slices (coronal, ~ 5.3 mm from bregma) were washed 3 times in PBS and 0.3% Triton, followed by a 1-h incubation in a blocking solution of PBS 0.3% Triton and 2% normal goat serum. Next, overnight incubation of the sections in the primary antibody was performed at 4°C on a shaking platform with a dilution of 1:2000 mouse anti-TH antibody (Immunostar, 22941) as primary antibody in the same blocking solution. After at least 12 h, slices were washed 3 times in PBS and 0.3% Triton, followed by a 1 – 1.5 h incubation with 1:150 goat anti-mouse antibody coupled to Alexa Fluor 488 (Invitrogen, A32723) as secondary antibody (in a PBS and 0.3% Triton, at room temperature) on a shaking platform. After immunostaining, slices were rinsed with PB 0.1 M and mounted on slides with Moviol as mounting medium. For visualization of ChR2_mCherry-expressing fibers in thalamus and cortex, an immunostaining enhancement of the mCherry fluorophore was performed using a procedure similar to the one for staining LC cell bodies, using 1:500 Rabbit polyclonal Anti-mCherry antibody (abcam, Ab183628) and 1:300 donkey anti-rabbit Alexa Fluor 594 antibody (Invitrogen, R37119) as primary and secondary antibodies respectively.

QUANTIFICATION AND STATISTICAL ANALYSIS

In vivo data analysis

Scoring of vigilance states

Using EEG/EMG data, we detected sleep and wake episodes following previous standard procedures in a manner blinded to the treatment. For this purpose, we used a custom-made software developed in MATLAB (MathWorks) that allows semiautomatic scoring of sleep stages.^{27,28} Shortly, we defined three distinct stages as follows: wakefulness, periods containing large muscle tonus or phasic activity in the EMG signal, together with low-voltage EEG exhibiting fast oscillatory components. NREMS was defined as periods containing low EMG activity together with high amplitude EEG activity showing slow oscillatory components such as slow oscillations (< 1.5 Hz), delta (1.5 – 4 Hz) or sleep spindles (10 – 15 Hz). REMS episodes were defined as periods with low EMG activity

with prominent Theta (5 – 10 Hz) activity in the EEG. Microarousals were defined as short (< 12 s) periods of wakefulness contained between the epochs of the same sleep stage. Quiet wakefulness (QW) studied in Figure 5 was distinguished from active wakefulness based on EMG, as illustrated in Figure S5 and as published.²⁸ For the intracranial pharmacology experiments, analysis was done for the first 2 h of recording and comparisons were made in a paired manner between the baseline and drug conditions. For all optogenetic experiments, scored data for the first 20 min of each hour (during which light stimulation was done) were compared with the same periods in sham conditions (*ceteris paribus* with the LED turned off). For the fiber photometry experiments, analysis included the complete 3 – 4 h of recordings. For the pharmacological manipulation of the HR, analysis took place for the first 100 min after the i.p. injections.

Analysis of sigma and delta dynamics

Throughout the study, all analyses of spectral dynamics, in particular within the sigma (10 – 15 Hz) and delta (1.5 – 4 Hz) bands, were quantified from either the S1 LFP or EEG signal using a wavelet transform with a Mother Gabor-Morlet wavelet with 4 cycles of standard deviation for the Gaussian envelope (Figures 1A and 1C). The frequency dimensions were then collapsed to the two frequency bands of interest, the 10 – 15 Hz sigma band and the 1.5 – 4 Hz delta band. The mean signals were then resampled at 10 Hz and filtered using a 100th order filter with a 0.025 Hz cutoff frequency for further analysis. For NREMS bouts of ≥ 96 s, a Fast Fourier transform was calculated (Figure 1B) to measure the strength of the 0.02 Hz oscillatory patterns defined here as the area underneath the Fourier transform from 0.01 – 0.04 Hz, subtracting the mean activity between 0.08 to 0.12 Hz (as depicted in Figure 1B). For the example depicted in Figure 1B, the sigma and delta grand averages were calculated from the long bouts (> 96 s) of NREMS of baseline recordings contained within ZT1-7 (local pharmacology experiment) or ZT1-9 (optogenetic experiments).

Sleep spindle detection, phase coupling analysis and feature extraction

Sleep spindles were detected from the S1 LFP signal for all the experiments. Spindle detection was done using a previously described algorithm²⁹ that is illustrated in Figure S1. Briefly, we filtered (FIR filter of order 2000) the raw S1 LFP signal in a wide sigma band (9 – 16 Hz). Then, we squared the signal and applied a threshold of 1.5 the standard deviation above the mean values in NREMS. We then detected all the peaks crossing this threshold and marked as a putative spindle all events containing at least 3 cycles. The starting and ending point of the events were extended to the closest cycle at 0 crossing before and after the threshold, respectively. Events separated by < 50 ms were merged as a single event. For display purposes, we positioned a black dot for each individual spindle event at the center of the spindle in time and a random jittered vertical position.

After spindle detection, we extracted the following features: *Amplitude*, the maximum value of the absolute filtered signal within the event. *Frequency*, mean intra-peak frequency within the detected spindle event. *Number of cycles* in the spindle. *Duration*, time span between the beginning and end of the event.

For the analysis of the phase coupling of the spindle events to the sigma activity we first centered the sigma activity at zero by subtracting the mean of the sigma activity in NREMS. Then we constructed a distribution using the phase of the sigma dynamics (calculated as described in [Analysis of sigma and delta dynamics](#)) at the center of each spindle event (half point between the beginning and the end of the spindle). By using the CircStat toolbox for MATLAB (MathWorks),⁷¹ we then confirmed the non-uniformity of the distribution by using the Rayleigh test.

Detection of infraslow cycles

We detected individual cycles of sigma within NREMS using a custom-made MATLAB routine. We used the sigma dynamics as described in [Analysis of sigma and delta dynamics](#) and eliminated the regions containing artifacts. Then, we identified the peaks and troughs in the signal with a minimum distance of 25 and 20 s, respectively. Finally, we arranged the positions of successive troughs and kept the starting and ending point for each individual cycle. Next, the marked locations were used to normalize the time in 1000 points for each individual cycle and to interpolate the sigma activity to generate a mean dynamics normalized in time. The same positions were used to normalize the dynamics of NA-related fluorescent signals from the fiber photometry measurements. Only those cycles that within NREMS periods were included in the mean.

Pupil diameter measurements

To standardize the correct location of the optic fibers in the LC cell bodies stimulation or inhibition, we performed pupil diameter measurements in a subset of animals. In short, we set a Basler GigE infrared camera (Basler acA800-510 um, SVGA, 1/3.6", 510 fps, USB3 Vision) close to one eye of the animal and used a custom-made infrared LED-based lantern directed to the recorded eye to increase the contrast between the pupil and the surrounded area. We built a custom-made software in MATLAB (MathWorks) for online or offline pupil detection (using the videos recorded from online trials). First, the user manually selects both the area of interest for the analysis and the initial location of the pupil. Then, for each frame (recorded at 10 fps), a binary image was created using an Otsu's method adaptive threshold with the function `imbinarize` from MATLAB (MathWorks). The threshold was set manually to adapt to the conditions of the image and the angles of the infrared light source and the camera. The size of the binary object closest to the marked pupil was then measured. The dynamics of the pupil diameter was then tracked and z-scored for comparison (Figure S4).

Fiber Photometry

Changes in bioluminescence were recorded via a photodetector connected to an analog channel in the Intan RHD2000 USB Interface board (Intan Technologies) as described before. The recorded signal fluctuated between 0 – 3.3 V with peaks at 400 Hz as the sinusoidal waveform created to modulate the excitation of the biosensors. The fluorescent dynamics signal was then created using an RMS envelope of 1 s. The changes in biofluorescence $\Delta F * F^{-1}$ were computed by dividing the enveloped signal by its fitted exponential decrease calculated from the dynamics at NREMS. We computed the relative fluorescence across different sleep states using the z-scored data per recording session; using the mean values across all vigilance states for the z-scoring. The values presented in

Figure 5B and in Figure S5 show the mean values of multiple sessions per animal for quiet wakefulness (QW), NREM (NR) and REM (R) sleep. In every case, only epochs flanked by epochs of the same vigilance state were included.

Cross correlation analysis

To study the similarity of the dynamics between the sigma activity and the NA changes or changes in HR, we performed cross correlation analysis between these two pairs of signals in MATLAB (MathWorks). For each long bout (≥ 96 s) of NREMS within the time of analysis (see [Scoring of vigilance states](#)), we z-scored each signal individually and normalized it to the length of the bout. Then, the cross-correlation was calculated using the function `xcorr` of MATLAB and normalized to the length of the bout. Mean cross correlation values were computed for each animal and across animals. Mean correlation coefficient (r) was computed between -5 to 5 s lags.

Heart rate analysis

Changes in HR were computed as previously described.²⁷ Shortly, EMG signal was filtered using a Chebyshev type 2 high-pass filter. We then differentiated (using the function `diff` from MATLAB) and squared the signal to highlight the R peaks. The resulting signal was z-scored to normalize across animals and recording sessions. Then, the R peaks were identified using the MATLAB function `findpeaks` with a heuristically found threshold of 0.3 and an interpeak distance of at least 0.08 ms. Peaks with a z-score higher than 10 were considered as artifacts and eliminated. Finally, the HR signal was constructed by measuring the inter-peak time distance and divided by 60 (1 min). An interpolation of the values was performed using the function `interp1` of MATLAB and resampled at 10 Hz.

Histological analysis

The efficiency and specificity of expression of viral transgenes was done by quantifying the overlap between TH- and mCherry-expressing neurons. Total cell counts were obtained from two 50- μm -thick sections per mouse containing LC around Bregma -5.3 using spinning disk confocal microscopy (Nikon Ti2, CrEST Optics X-Light V3). Per mouse, 100 – 279 TH-expressing and 100 – 214 mCherry-expressing cells were counted in separate green and red fluorescent channels. For quantifying the overlay, single-focal-plane pictures were used to count separately the green-only, red-only and the yellow cell bodies. Percentages were calculated with respect to the total cell count. Per animal, 67 – 190 cells were counted.

To assess the fiber density within the stimulation areas within the thalamus and the somatosensory cortex we performed an immunostaining enhancement of the mCherry fluorophore from the ChR2 expressing terminals as described before (Histology). From 100 μm -thick sections containing the VPM or the S1 cortex (-1.7 mm and -0.7 mm from bregma, respectively), we took Multi-layer Z stack pictures using a tile scan of 5x5 with a magnification of 40x (CFI Plan Apochromat Lambda 40XC N.A. 0.95, W.D. 0.21 mm, Spring-loaded, Cover glass correction: 0.11 – 0.23 mm). For latter analysis we used ImageJ (<https://imagej.nih.gov/ij/>). An area of 0.13 mm^2 was then randomly selected within the VPM and S1 around the stimulation optic fiber. Then a background subtraction with a 3 pixel-rolling radius was performed, then we performed a contrast enhancement with a saturation of 0.35 and a mask was created with a median radius of 2 pixels. From the resultant binary image, we quantified the area of the positive (bright) pixels within the window (Figure 3C).

Statistical analysis

For the statistical tests, we used R statistical language version 3.6.1. and MATLAB (MathWorks). First, we tested for normality of the datasets using the Shapiro-Wilk normality test. For comparisons of two parametric datasets, we used a paired Student's t test and the equivalent Wilcoxon signed rank test for non-parametric datasets. For comparisons on multiple (> 2) groups of data (as in the case of the amplitude, onset latency and recovery time in the in-vitro experiments), a one-way ANOVA or a Kruskal-Wallis test was used for parametric and non-parametric datasets, respectively. F and χ^2 indicated in the figures are derived from ANOVA and Kruskal-Wallis tests, respectively. In case of no significance, no further post hoc analysis was performed. In all figures, gray lines denote paired datasets from two conditions (e.g., baseline, opto). Mean values are given by large horizontal lines, error bars indicate standard errors of the mean. Throughout the figures, V , t and p values were derived from Wilcoxon signed rank or paired t tests, respectively.